THE DECOMPOSITION OF METALLIC OXALATES

by

Arthur Finch B.Sc., A.R.C.S.

A thesis

submitted in partial fulfilment of the requirements for the award of the Degree of Doctor of Philosophy in the University of London.

Royal College of Science,
Imperial College,
South Kensington,
London, S.W.7.

August 1953.

ACKNOWLEDGEMENTS

This research was carried out in the laboratories of the Department of Inorganic and Physical Chemistry of Imperial College; thanks are due to the Director, Professor H.V.A. Briscoe, for provision of laboratory accommodation and facilities.

It is a pleasure to express sincere gratitude to Assistant Professor F.C. Tompkins, who supervised the work, for his constant interest, criticism and many helpful discussions. Thanks are also due to Dr. P.W.M. Jacobs for much practical advice and continued interest. Acknowledgement is made of those friends engaged in cognate studies, whose cooperation and assistance were greatly appreciated.

Finally, the author wishes to acknowledge receipt of a scholarship, during the tenure of which this work was carried out, by the Education Department, South Shields.

Arthur Finch.

August 1953

CONTENTS

		Page
INTRODUCTION:		
A.	Ionic Conductance	
	Lattice Defects in Crystals	1
	Measurement of Ionic Conductance	5
B.	Decomposition of Solids	
	Effect of Irradiation on Solids	18
	Thermal Decomposition of Solids	20
	Photolysis of Solids	25
	Thermal Decomposition of Silver Oxalate	37
	Photolysis of Silver Oxalate	44
	Decomposition of Mercuric Oxalate	47
	Decomposition of Lead Oxalate	49
EXPERIMENTAL:		
	Measurement of Conductance	50
	Measurement of Photolysis	69
	Measurement of Thermal Decomposition	72
RESULTS:		
	Ionic Conductance of Oxalates	78
	Photolysis of Silver Oxalate	87
	Photolysis of Mercuric Oxalate	96
	Photolysis of Lead Oxalate	102

Page

Thermal Decomposition of Silver Oxalate 106.

DISCUSSION:

The Conductance of Metallic Oxalates 127

The Photolysis of Silver Oxalate 132

The Photolysis of Mercuric and Lead Oxalates 152

The Thermal Decomposition of Silver Oxalate 160

Abstract 175

Bibliography 179

INTRODUCTION

IONIC CONDUCTANCE

Lattice Defects in Crystals

It is generally recognised that all ionic crystals contain lattice defects. In a crystal the (thermal) lattice vibrations will result in a displacement of any ion from its mean position at any moment. Such displacements, however, are not regarded as defects. Two main types, Frenkel and Schottky defects, have been postulated.

In the former, an ion has left its normal lattice position, and occupies an interstitial position at some point in the lattice sufficiently remote for there to be no interaction between the interstitial atom and the ions surrounding the vacancy. Thus the Frenkel defect consists of one interstitial ion and one vacant site. In a Schottky defect, two ions of opposite sign have left their normal positions, and taken up new lattice positions on the surface of the crystal. Thus the volume of the crystal has increased, although the lattice constants may be unaffected. This defect consists of two vacant sites.

The concept of lattice defects haw proved of great

value in interpreting many phenomena shown by solids, notably ionic conductance and solid decomposition. The success of the model of the conduction process is perhaps the best evidence for the existence of the defects. This is considered in the next section. Various experimental tests have been applied to solids in order to obtain additional evidence for the existence of defects.

Mott and Gurney (2) have calculated the fractional number of interstitial ions in silver bromide, obtaining the figures shown below:-

Table I

Temperature °C	x, Concentration of Interstitial Ions
- 180	$1. \; 10^{-22}$
20	$8.3. \; 10^{-6}$
210	$7.6. \; 10^{-4}$
250	$1.8. \; 10^{-3}$
300	$4.0. \; 10^{-3}$
426	$2.0. \; 10^{-2}$

The very high value of x at 426°, the melting point of silver bromide, led them to predict an anomalous rise in the specific heat at this point, since 400 cals./mole. are required to form this number of interstitial ions. This effect has been verified by Kanzoki (4).

It has been noted that the presence of Schottky defects should lead to an increase in the volume of the crystal. If a crystal is rapidly cooled from a high temperature, then it is to be expected that the number of defects present would be in excess of the equilibrium number, due to the low mobility of defects at room temperature. Accurate density-determination experiments (1) on such crystals have, however, revealed no anomalous effect which can be ascribed to the presence of defects. This, however, cannot be taken as evidence of the non-existence of defects, since the limits of accuracy of the experiment are too small to detect the number of vacancies. Calculations have shown that at 1,000°K, the fractional number of vacant sites in potassium chloride is ca. 5.10^{-5}; the limits of accuracy of the experimental density determinations are given as one part in 10^4.

Evidence for the existence of defects has also been obtained from dielectric-loss measurements. The dielectric constant of a perfect crystal is the sum of two quantities: 1. an electronic contribution due to the distortion of the electron clouds of the individual ions relative to their nuclei; and 2. an atomic contribution due to the displacement of positive and negative

ions relative to one another. The resonance frequencies of 1. and 2. lie in the ultra-violet and infra-red regions respectively. Both these regions being far removed from the range of ordinary electric measurements, a dielectric constant independent of frequency and accompanied by very small losses should be observed.

In a crystal containing vacant sites there should be an anomalous dielectric effect due to the motion of vacancies in an alternating field. This effect has been experimentally observed by Breckenbridge, (5), with quenched crystals of alkali halides and silver chlorides. Breckenbridge attributes the effect to the jumping of positive ions into vacant lattice sites, and has calculated the number of lattice defects present in his crystals, and the activation energy for diffusion, U, of the positive ion in the crystal. For Ag Cl, U was found to be 0.21 e.v. in good agreement with the value obtained from conductivity measurements, (0.26), by Koch and Wagner (3).

Measurement of Conductance

The first published work on the measurement of conductance in crystals consisted in placing a slice of crystal between two electrodes connected to a high voltage supply, in series with a fibre electrometer. If the potential measured by the electrometer after isolation from earth for a time t, was V, then

$$i = C \frac{V}{t}$$

i = current flowing through the crystal

C = Total capacity of system

If Vo = applied voltage, then the specific conductance is given by

$$\sigma = \frac{il}{Voa}$$

l = thickness of cyrstal slice

a = Area of crystal slice.

Polarisation

It was noticed that i was a function of time, decreasing to a constant value, sometimes over a period of days. Jaffé and Rontgen (6) showed that this was due to a polarisation voltage, P, acting in opposition to the applied voltage.

i.e. $$\sigma = \frac{il}{(V_o - P)\, a}$$

The polarisation voltage was measured by application of a voltage of opposite sign and of magnitude just sufficient to prevent the flow of secondary current.

An obvious step to obviate danger of polarisation is to use an A.C. bridge for measurement of conductance. This method was used by Phipps and co-workers in the measurement of the conductance of alkali-metals halides. The disadvantages of A.C. Bridges is their restriction to low resistances. Phipps and Partridge (7) used a simple A.C. net for resistances of from 0- 5 MW., and a D.C. Bridge for resistances greater than this figure. They found polarization difficulties in this region, and attributed to this the irreproducible results obtained at high resistances. By using a very sensitive galvonometer they attempted rapid measurements, when P was very small. This principle was also applied by Phipps and Ginnings (8) using a sensitive galvonometer, and small currents. ($\sim 10^{-8}$ amp.).

Nature of Crystal

In contrast to metals, it was found that the specific conductance of ionic solids was often markedly sensitive to the thermal history and physical form of the sample (9). After repeated crystallisations

under controlled conditions it was possible to obtain reproducible values of σ for crystals, individual values for which had previously varied by a factor of $\sigma \pm 1$. The dependence of σ on crystal form is of importance, since many substances, such as those used in the present investigation, cannot be prepared in single-crystal form, and hence compressed pellets are used. The effect of compression appears to vary with the substance considered. Thus, Göthals (10) reported identical values of σ for pellet and single crystal modifications of potassium nitrate. Conversely, von Hevesy, (11), stated that the specific conductance of a single crystal of sodium nitrate at 210°C was 10^{-8} ohm/cm.$^{-3}$, whilst that of a pellet at the same temperature was 4×10^{-7} ohm.Cm^{-3}. The problem has been thoroughly investigated by Tamman and Veszi (12) and Phipps, Lansing and Cooke (13). The results of the latter indicate that at high compressions, of the order of 5 tons/sq.inch, differences between pellet and individual crystal are reduced to the limits of reproducibility shown by individual crystals.

The effect of field strength on conductivity has been investigated (14,15) and it has been shown

that for field strengths less than 10 kv./cm.^{2}, Ohm's Law is operative.

Transport Numbers and Validity of Faraday's Laws

Quantitative studies of the migration of ions in solids have been carried out by Tubandt and his school (16,17,18). The method used is analogous to those employed in aqueous solutions. Frequently the metal constituent is not deposited on the surface of the crystal, but forms dendritic growths within the crystal. This may be prevented by inclusion of a pellet of "protective electrolyte", such as α-A_g Cl or $BaCl_2$, between the crystal and cathode. The choice of protective electrolyte is limited by the temperature range throughout which the crystal phase is stable. A typical experimental set-up used by Tubandt is shown:-



The work established that alkaline and alkaline earth halides were pure ionic conductors and some oxides and sulphides showed electronic conductivity. Some compounds, e.g. Cuprous chloride and β-silver sulphide, showed mixed conductivity. Generally,

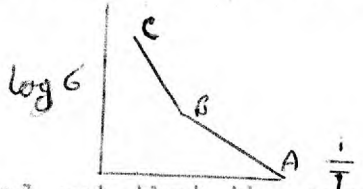
uni-bivalent salts, e.g. B_aCl_2, show anionic conduction, whilst in uni-univalent salts, e.g. A_g Cl, cationic conduction is operative. As the temperature is raised, the anion transport number becomes significant in uni-univalent salts.

Variation of Conductance with Temperature

The equation relating the variation of conductance with temperature, first formulated by Rasch and Hendrikson (19), has been repeatedly verified.

i.e. $\log\sigma = \log A - \frac{B}{T}$

The graph of $\log\sigma \sim \frac{1}{T}$ frequently shows two distinct parts, as shown in the diagram, corresponding to different values of the constants A and B.



Smekal pointed out that the curve could be represented throughout the entire range by the expression

$$= A_1 e^{\frac{-B1}{T}} + A_2 e^{\frac{-B_2}{T}}$$

The exponential constant is usually written $\frac{E}{R}$, where E is the activation energy associated with the conduction process.

If precautions are taken to prevent dendritic

metal growth, the upper portion of the curve, BC, is found to be reproducible. The region represented by this portion of the graph is hence known as the region of "permanent conductance". The lower portion of the curve, however, (AB), is found to be sensitive to the history of the crystal, and is referred to as the "structure sensitive" region.

Smekal (20) suggested that E2 referred to the energy necessary to move an ion from the 'perfect' lattice to the electrode. The first term in the conductance equation was due to the cracks and internal surfaces present in real crystals, at which the energy needed to move an ion is less than that required to move an ion in a perfect crystal lattice. Thus $E_1 < E_2$, and $A_2 >> A_1$, as is found experimentally, and the nature of the structive sensitive region is qualitatively explained. Joffé and Zechnowitzer (21) showed that when a single crystal was caused to become microcrystalline by plastic deformation the conductance remained unchanged. Jost (22) showed that if the number of ions conducting was proportional to the $e^{-E/RT}$, and if E1, E_2, were the activation energies necessary to liberate ions from 'surface' and lattice position respectively, these absurdly high values of

mability must be assumed to account for the measured conductance.

An alternative explanation, (23,24) based on the migration of lattice defects under an electric field has been developed: This accounts for the two activation energies, and the structive sensitive region. This will now be discussed:

That ionic movement takes place near lattice defects is indicated by a consideration of the energetics of the process. In a "perfect" ionic lattice i.e. a lattice wherein each lattice-point is occupied, ionic migration is only possible if ions interchange positions by "squeezing" past one another. This would necessitate an extremely high energy, of the order of the cohesive energy of the crystal (25).

A Schottky defect will consist of two separate vacant lattice points; if W is the work necessary to remove an anion and a cation from the interior to the surface of the crystal, then the number of (double) Schottky defects is given by:-

$$n = N\gamma e^{-\frac{W}{2kT}}$$

$\gamma = \left(\frac{\nu}{\nu'}\right)^S$ where ν = vibrational frequency of the crystal, and ν' = vibrational frequency of an ion adjacent to a vacant site (29).

Let $n(s)$ = number of Schottky defects at equilibrium, and suppose that in jumping from a lattice-point into the defect a potential barrier Es is surmounted. The jump frequency $\bar{\nu}$ is given by:

$$\bar{\nu} = S \frac{kT}{h} \frac{Q^*}{Q} e^{-\frac{Es}{kT}}$$

Q^* = partition function of the ion in its transition state

Q = " " " " " " " " normal "

S = symmetry factor, since there are S equivalent energy barriers round the defect.

$$\frac{Q^*}{Q} = 1 - e^{-\frac{h\nu'}{kT}} \approx \frac{h\nu'}{kT}$$

$$\therefore \bar{\nu} = s \nu' e^{-\frac{Es}{kT}}$$

When an electrostatic field of intensity F is applied the net jump frequency in the direction of the field is given by

$$\bar{\nu} = \nu' e^{-\frac{Es - \frac{1}{2} eFa}{kT}} - \nu' e^{-\frac{Es + \frac{1}{2} Fea}{kT}}$$

a = distance between two successive equilibrium positions of the saddle-point.

if F is small, $eFa \ll kT$

$$\therefore \bar{v} = v e^{-\frac{Es}{kT}} \; eFa/kT$$

The average velocity in the direction of the field is $\bar{v} - v_a$, hence the mobility, U, is given by

$$U = \frac{v_a}{F} e^{-\frac{Es}{kT}}$$

$$= \frac{v e a^2}{kT} e^{-\frac{Es}{kT}}$$

Hence the specific conductance, σ, is given by

$$\sigma = \frac{ne^2a^2\nu}{kT} e^{-\frac{Es}{kT}}$$

Generally, n = sum of n(s) and the impurity defects Y

I $$\therefore \sigma = \frac{Ve^2a^2\nu}{kT} e^{-\frac{Es}{kT}} + \gamma\frac{Nc^2a^2\nu}{kT} e^{-\frac{Es+\frac{1}{2}Ws}{kT}}$$

Suppose that Es, Ws, are linear functions of temperature (3)

$$\therefore Ws = Wo + (V - V_o)\, dWs/dV = Wo + \alpha VoT \frac{dWs}{dV}$$

α = Coefficient of thermal expansion of the crystal and Wo, Vo, are energies of formation of a Schottky defect and the volume of the crystal at $T = 0^\circ K$

Also, $Es = Eo + \alpha VoT\left(\frac{dEs}{dV}\right)$

$$\text{II} \quad \therefore \sigma = \frac{\gamma C c^2 a^2 \nu}{kT} e^{-\frac{Eo}{kT}} + \frac{\gamma BCNc^2 a^2 \nu}{kT} e^{-\frac{Eo + \frac{1}{2}Wo}{kT}}$$

where $B = e^{-\alpha Vo \frac{dWs}{dV} / 2k}$ and $C = \exp. -\alpha o \, Vo \frac{dEs}{dV}$

As independent values of γ, B, and C, are not available, a direct check of the equation (II) is not possible. It is, however, possible to calculate values of γB and C, assuming the validity of the equation.

Suppose to a uni-univalent salt a mole-fraction x of bivalent cation impurity is added. The number of impurity defects, xN, is greater than Ns, the equilibrium number of defects at any temperature, and hence the conductivity is given by the first term in II, viz:-

$$\sigma \text{ calc.} = \frac{xNe^2 a^2 \nu}{kT} e^{-\frac{Eo}{kT}}$$

which may be compared with the experimental value of σ. Wagner and Hantlemann, (32), measured the conductance of potassium chloride with added strontium chloride and Etzel and co-workers performed similar work on sodium chloride.

Subst.	B	C	Author	T°K.
KCl.	10-10.3	36.4	W. and H.	923-998
NaCl.	5.1	188	E. and M.	730-800

Experimental values of the conductance of the salt containing a known amount of impurity are used to calculate the molibity U from the equation:

$$\sigma = xNeU = xFpu/M$$

F = Faraday ρ = Density M = Molar. wt.

xs = Fractional number of cation vacancies in the pure salt,

$$xs = t_k M/p FU$$

tk = transference number of the cation.

It is expected that $\gamma B > C$ since for Schottky defects it is expected that $\gamma > 1$. γ is defined by $\left(\frac{\nu}{\nu_1}\right)^s$, or putting s = 6, and $\nu_1 = 0.8\nu$, $\gamma = 64$. If $\nu_1 = 0.5\nu$, $\therefore \gamma = 64$. It is concluded that for a value of γB of the order of 10, $B \approx 1$.

The only other information relating to the determination of γ, B, C, has been due to Jost and Nehlep (34) who measured the variation of σ with pressure.

Differentiation of Equation I at constant temperature gives:

$$\frac{d}{dP} (\log \sigma)\, T = \frac{d}{dP} \log a^2 \nu_1 - \frac{1}{kT} \frac{d}{dP} (Es + \tfrac{1}{2} Ws)$$

The first term may be neglected in comparison with the second

$$\text{hence } \frac{d}{dp} \log \sigma = \frac{V\gamma}{kT} \frac{d}{dV} \left(\tfrac{1}{2} Ws + Es\right)$$

where γ = Compressibility of the crystal.

Substituting for B,C, this reduces to:

$$\frac{d}{dp} \log \sigma = \frac{-}{\lambda T} \gamma \log BC$$

And hence (BC) may be found. The results of Jost and Nehlep on the conductance of silver chloride at 300 atmospheres at 300°C. showed an increase in resistance of 7%. Similar experiments on silver bromide showed an increase of 10%. Some of their results are tabulated below.

	Ag Cl	Ag Br
$-\frac{d}{dp} \log \sigma$ (cm^3/kg)	$2.5.10^{-4}$	3.5^{-4}
γ (cm^3/kg)	$8.0.10^{-7}$	9.10^{-7}
α	$3.3.10^{-5}$	$3.5.10^{-5}$

From these results, the value of BC for silver chloride was estimated to be ~350.

Throughout the foregoing discussion it has been assumed that each defect is capable of contributing

to the conductivity. Evidence for association of cation vacancies has, however, been obtained by Breckenbridge (5). Further, the failure of the Einstein relationship between specific conductance and the coefficient of diffusion has been ascribed by Mapother, Crooks and Maurer (27) to the association of divalent impurity ions and cation vacancies.

INTRODUCTION

DECOMPOSITION OF SOLIDS

Effect of Irradiation on Ionic Crystals

Before considering specific examples of solid thermal and photochemical decompositions, some relevant work on the action of light on crystals will be summarised.

If an alkali-halide crystal is exposed to ultra-violet irradiation, or to an electron beam, a characteristic colour, which can be thermally bleached is produced (28). A similar effect is produced by heating the crystal in the vapour of its metallic constituent. In this case, the coloration is stable to heat, and the presence of a stoicheiometric excess of metal may be demonstrated by chemical analysis. Such colorations are attributed to the existence of F-centres, which consist of an electron trapped at a vacant anion site. It is presumed that the excess metal atoms diffuse into the crystal as surface lattice cations. The electrons simultaneously released wander through the conduction band of the crystal. The surface cation is stabilised by an anion, which migrates to the surface, leaving behind a vacant site, which by trapping an electron can form an F-centre. The production of F-centres by

irradiation is explained by the presence of vacant anion sites in the original crystal, which trap photo-excited electrons from the lattice anions. Each F-centre produced leaves a free positive-hole in the full band of the crystal. These holes are mobile and may be trapped at vacant cation sites, forming V-centres. Evidence for this is provided by the close resemblance between the (V) band and the band produced by heating potassium bromide in bromine vapour (29).

Irradiation of potassium chloride by X-Rays leads to the production of a third band, the M-band, at 8200 A. If the crystal is subsequently irradiated in either the F- or M- bands, the bands are transformed, one into the other, with a loss in intensity. A new band, the R-band appears at this stage. Seitz (30) has suggested that an M-centre is a F-centre plus a (coupled) pair of anion and cation sites. R centres consist of pairs of vacant anion sites with one or two trapped electrons, i.e. F_2^+ or F_2-centres. Capture of a second electron by an F_2^+ centre or by an M- centre leads to an F_2^- centre. F_2^+- and F_2^- centres can revert to negative ion vacancies by capturing positive holes, but do not liberate photo-electrons when irradiated.

The mobility of F-centres has been discussed by

Mitchell (31). An electron can transfer from an F-centre to a neighbouring anion vacancy, by the tunnel effect. This represents a net movement of the F-centre. If two F-centres diffuse together, then resonance of the two electrons between the two sites will lead to a lower ground state than in a single F-centre. Further aggregation can occur, and thus an F- centre aggregate can be formed, the depth of the trap increasing at first with the size of the aggregate.

Irradiation of a crystal by a quantum of light of insufficient energy to produce a free positive hole and a free electron, may result in the production of an 'exciton'. This is regarded as a positive hole and an electron coupled together, in such a manner that movement as a whole through the crystal is possible. An exciton level lies between the ground state and the conduction band. Irradiation of a crystal may, therefore, produce either electrons in the conduction band, which will be reflected in photoconductance, or excitons, when no photo-conductance will occur.

Thermal Decomposition of Solids

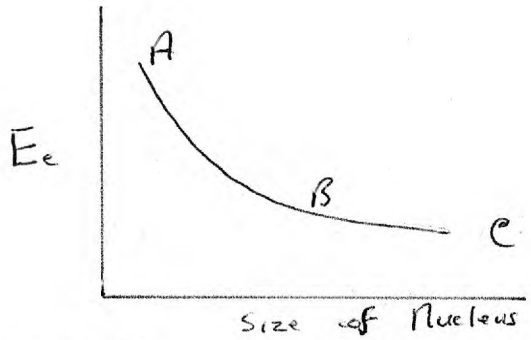
The term "solid decomposition" is here restricted to reactions which can be represented by the following equation: $A_s \rightarrow B_s + C_g$ I

Such reactions may be endothermic or exothermic; the latter class may further be subdivided into reactions the course of which is markedly affected by pre-irradiation with ultra-violet light, e.g. silver oxalate, barium azide, and those which are relatively unaffected by such pre-treatment. e.g. potassium, silver, permanganate.

In general, solid reactions are observed to start from specific points ("nuclei") in the solid, and proceed at the interface between reactant and reaction product. The elucidation of the mechanism of such reactions is concerned, therefore, with a), the origin and nature of the nucleus, and b), the rate of growth of reaction product round the nucleus. As the reaction proceeds, the number and size of nuclei increase, and after a certain fraction of solid has decomposed, the growing nuclei 'interfere' with one another. Thus the rate of reaction, after reaching a maximum, decreases. It is on the initial, acceleratory, period, that most attention is focussed. Nuclei may be visible as discrete particles, e.g. in barium azide, or optically non-observable as in silver oxalate. In the latter case, it is assumed that the nuclei are either very small or grow in one or two dimensions. No nuclei

are visible in silver oxalate at any stage in the decomposition, but as has been pointed out by Tompkins (32), individual centres containing 10^{10} Ag atoms would remain microscopically indetectable. Generally, nucleus formation is favoured at cracks and discontinuities in the crystal lattice. That nucleus formation is structure-sensitive is shown by different reaction rates in samples of silver oxalate which have been prepared under different experimental conditions (33). Thus silver oxalate prepared in the presence of excess oxalate ions is of the "unstable acceleratory" type; that produced with excess nitrate ions is considerably more stable. Direct observation of the rate of growth of nuclei are difficult, and few experimental observations have been reported. Two general conclusions may, however, be drawn. 1) In the early stages of growth, nuclei grow slowly, and, 2), After a critical size is reached, the rate of growth is constant. If the nucleus in the early stage is an F - centre aggregate (31), then, as has been pointed out by Mitchell, the larger the aggregate, the deeper the trap, and hence the increased later rate of growth is explained. These considerations may be expressed diagrammatically, as shown. The shape of the portion of the curve A-B is

hypothetical.



A - B Slow, variable, growth of nucleus.

B - C Constant rate of growth of nucleus.

Thomas has obtained an activation energy of 29 kcal. for growth in the early stages of reaction of barium azide, whilst that for "visible" growth is 23.5 kcal.

Solid decompositions of the type represented by eqn. I have been studied experimentally by measuring the pressure-time ($p \sim t$) curves obtained during reaction. These curves are usually fitted by one of three general equations, the interpretation of such equations depending on the manner in which the nucleus is assumed to grow. A general examination of these equations will be given, followed by applications to some reactions for which considerable experimental data are available. Some views of the operative mechanisms will be discussed later.

A. The Power Law: This is usually written:

$$p = Ct^x \quad \text{where C is a constant.}$$

This equation has proved useful in systems where

discrete nuclei are visible, e.g. in barium azide.

A theoretical derivation of this equation is possible if it is assumed a), The number of nuclei increase as a power of the time, and b), the rates of linear growth of nuclei in each direction are constant.

Let the number of nuclei formed in time t be given by

$$n = Bt$$

Then the rate of nucleus formation at time τ is

$$\frac{dn}{d\tau} = B\beta\tau^{\beta-1}$$

If the rate of linear advancement in one dimension is $\bar{v}$ at time t, then the size, x, of a nucleus formed at time τ is:

$$x = \text{Constant } \bar{v}^{\delta}(t-\tau)^{\delta}$$

where δ = 1, 2, or 3, corresponding to growth in 1, 2, or 3 dimensions.

The total size of all nuclei, V, at time t is

$$V = \int_0^t x\, dn. \quad \ldots\ldots\ldots 1.$$

Assuming that the pressure, p, is proportional to the volume of all the nuclei

$$p = \text{Constant} \int_0^t \bar{v}^{\delta}(t-\tau)^{\delta}\tau^{\beta-1}\, d\tau$$

whence $p = Ct = Ct^{x}$,

corresponding to the Power Law equation. For nuclei visible as discrete particles $\delta = 3$. In barium azide Wischin, (34), has found that

the number of nuclei increases as the third power of the time, hence $\beta = 3$. Thus for barium azide the pressure is expected to increase as the sixth power of the time. For ground azide Thomas (35) found a power varying from 6.5 to 6.8. By making a correction for slow growth this figure was reduced by ca. 0.5, and hence a good approximation to the predicted result was obtained.

Benton and Cunningham also obtained a power law for the thermal decomposition of silver oxalate. They assumed three-dimensional linear growth of nuclei as above, but treated the problem of nucleus formation differently. They assumed that $dn = k(N - n)\, d\tau$ where n is the number of nuclei formed at time τ, and N is the number of centres where nuclei may form. This leads to

$dn = k(N - no)\, e^{-k\tau} d\tau$ where no = number of molecules present at the start. Hence by substituting in equation 1.

$$V = \int^{t} \text{Constant } V^3 (t-\tau)^3 k(N-no) e^{-kt}\, d\tau$$

$$= k^{\prime}(N-no)\, t^4 \left(1 - \frac{kt}{5} + kt^2/5.6 \ldots\right.$$

i.e. $p = Kt^4$

These investigators found that their results were

described by an equation of this form, with a value of the power equal to 3.5 for early portions of the curve. Pretreatment with ultraviolet light caused a progressive decrease in the power of t. The smaller power of t may be explained by overlapping of growth, a general theory for which has been given by Avrami (36). If random formation of nuclei within the crystal is assumed, then the actual volume of nuclei produced may be expressed by $1 - e^{-Vu}$, where $Vu = V/1-V$. This correction has been applied by Tompkins to the Benton and Cunningham equation. Moreover, Tompkins considers each oxalate radical to be a potential nucleus-forming centre. i.e. N = total number of molecules. This once again leads to an equation of the form $p = Ct^4$ for small values of t. The smaller values of t actually found, viz. 3.9 to 3.27, are explained by coalescence of nuclei i.e. impinging nuclei continue to grow except at the area of mutual contact.

B. Branching-Chain Theory Garner and Hailes (37).

$$p = Ce^{kt}$$

This equation holds throughout 50% decomposition of lead azide, lead styphnate and ground mercury fulminate, reactions in which the power law in its

simplest form does not adequately represent the experimental results. It is assumed that nuclei are produced at a constant rate, and grow in the form of one-dimensional chains. It is further assumed that the chains may branch.

If B = number of nuclei produced in time t

$$\frac{dn}{dt} = B + kn$$

$$\log n = kt + \log \frac{B}{k}$$

since $\frac{dp}{dt}$ is proportional to n

$$\log p = Kt + \text{Constant}$$

$$\text{or } p = Ce^{kt}$$

The theory has been extended by Prout and Tompkins (38), who made allowance for interference between the chains as reaction proceeded.

C. Interfering-Chain Theory (38)

$$\frac{\log p}{(p - p)} = kt + \text{Constant}$$

The rate of increase of potentially-reactive molecules is given by

$$\frac{dn}{dt} = n_o + \frac{n}{dt}\alpha$$

α = probability of branching

n = number of molecules at time t

dt = average time between production and decomposition.

After reaction has proceeded for a given time there

exists a probability β, that the chains will interfere.

$$\frac{dn}{dt} = no + \frac{(\alpha-\beta)}{dt} n$$

Boundary relationships between α, β, are assumed as follows:

Put $\psi = \frac{\beta}{\alpha}$

i. When $t = 0$, $\beta = 0$ $\therefore \psi = 0$

ii. At t_i, the point of inflection of the p-t curve,

$\alpha = \beta$ $\therefore \psi = 1$

Let x = amount decomposed at any instant

x_i = amount decomposed at t_i

Assume $\psi = \frac{x}{x_i}$

$$\frac{dn}{dt} = \alpha(1 - x_i) \quad n = \alpha(x - \frac{x^2}{2x_i})$$

p is proportional to x, and for potassium permanganate Prout and Tompkins found that $p_i = \frac{Pf}{2}$

$$n\alpha\frac{dp}{dt} \quad \therefore \frac{dn}{dt} = kp\left(1 - \frac{p}{Pf}\right)$$

$$\frac{Pf\,dP}{p(Pf-P)} = kdt$$

$$\therefore \frac{\log P}{Pf-P} = kt + C$$

This equation has extended the usefulness of the chain theory of reaction to much later stages in the decomposition. The equation holds throughout the decomposition of potassium permanganate, and for 90% of the decomposition of mercury fulminate. It may be

noted that α is probably not constant, but may vary with time.

In the preceding sections it has been shown how application of the ideas of nucleus formation and growth could provide a basis for the experimentally-found p-t curves. The actual mechanisms governing such reactions will now be examined. In general, two main modes of reaction have been postulated:

A. A characteristic feature of reactions to which, an electronic mechanism has been successfully applied, is their sensitivity to pre-irradiation. In all cases the subsequent thermal rate is increased, and the effect of the irradiation is clearly to increase the number of nuclei or potential nucleus-forming centres. The first explanation of this type of reaction was given by Mott (39), in terms of lattice-defect theory, and applied to barium azide.

B. A mechanism which depends on the crystal structure of the decomposing solid, and A. An electronic mechanism, e.g. some kind of internal electrolysis. B. may be further subdivided into branching mechanisms and non-branching mechanisms.

Mott assumed that at room temperature barium azide is an ionic conductor, the conductance arising

from interstitial barium ions. An electron, produced thermally from an azide radical is released to the conduction band of the metallic nucleus. The negatively-charged nucleus attracts further interstitial barium ions. The positive holes are assumed to have sufficient mobility to diffuse to the surface, where two of them react to give three molecules of gaseous nitrogen. The formation of nuclei is explained by postulating a slow, uncatalysed, emission of nitrogen from the surface, the excess barium going into solution as interstitial Ba^{++}. The free electrons travel in the conduction band until two are trapped by a Ba^{++} ion, giving a metallic nucleus. Experimental measurements of the ionic conductivity of barium azide (40) have shown, however, that the conductance is too low by a factor of 10^6 to account for the measured rates of nucleus growth (34). The theory has consequently been modified by Thomas and Tompkins (41). An electron excited thermally from a surface azide anion is trapped, probably at a vacant anion site. If an azide ion adjacent to the first is sufficiently excited, the two positive holes react to form a nucleus. The aggregate can trap electrons thermally excited from adjacent azide ions. This is followed by reaction

of the azide radicals at the interface, leaving two anion sites, which become incorporated in the nucleus. As growth proceeds, the aggregate of F-centres and Ba ++ ions eventually reaches a critical size, at which it collapses away to form a metallic nucleus. The growth mechanism may be represented by the following equation, where $h^{\bullet}$ represents a positive hole, $\square$ a vacant anion site, F_n an F-centre aggregate, $e^{\ominus}$ an electron.

$$2N_3^- \rightarrow 2h^{\bullet} + 2e^{\ominus}$$

$$2e^{\ominus} + F_n \rightarrow F_n^{--}$$

$$2h^{\bullet} \rightarrow 3N_2 + 2\square$$

$$2\square + F_n^{--} \rightarrow F_{(n+2)}$$

In this mechanism, the existence of interstitial barium ions is not assumed.

B.i.) Another method of decomposition is that wherein the reaction spreads rapidly over the surface from a number of initial centres of reactivity, after which the rate is governed by the linear propogation of the reactant/product interface downwards. If N = number of radicals in the interface, the rate of reaction is given by the Polangi-Wigner eqn.,

$$\frac{dN}{dt} = N\nu e^{-\frac{E}{RT}}$$

an equation which adequately represents the dehydration kinetics of copper sulphate (42), but not, for example, the dehydration of calcium carbonate hexahydrate (43). Eyring and Stearn, (44) have suggested that the energy factor may be split into two terms, such that

$$\frac{dN}{dt} = N\nu e^{-\frac{\Delta H^*}{RT}} e^{+\frac{\Delta S^*}{R}}$$

For gases ΔS^* is small, but may be significantly large in solids. Garner (45) has suggested that the process of activation may involve blocks of "crystallites", with groups of radicals.

Colvin and Hume (46) have deduced equations for this type of mechanism, taking two special cases 1) Where the whole surface becomes rapidly covered with nuclei and 2) Where one nucleus is present on each crystal face at the outset. They assume that the rate of formation of nuclei is given by an expression of the form $\frac{dN}{dt} = k\,(no - n)$

no = number of centres where nuclei can form and therefore $n = no\,(1 - e^{-kt})$

The fractional decomposition at any time is then calculated from the locus of the movement of the interface across the crystal. Thus for the model of a contracting sphere, the fractional decomposition α at

a time t is given by:

$$\frac{u}{r} = 1 - (1-\alpha)^{\frac{1}{3}} / t \quad \text{---2.}$$

where u is the linear rate of penetration of the nucleus and r is the radius of a (spherical) nucleus. Equations representing other systems, e.g. a contracting parralelopæd, have been deduced. The thermal decomposition of mercuric oxalate has been shown by Prout and Tompkins (46) to be of the type expressed by eqn. 2. Since the initial number of nuclei may be increased by pre-irradiation, the initial rate of decomposition is increased. After a short while, however, the normal rate is re-established, and is maintained to the end of the reaction, indicating that the effect is confined to the surface. This is confirmed by the observation that there exists a saturation value, after which illumination has no further effect.

iii) In the group of reactions for which no electronic mechanism has been proposed, there is a further subdivision into decompositions which appear to be unaffected by pre-irradiation, e.g. silver, potassium, permanganate. Here nuclei are assumed to be molecules of reactant whose decomposition is favoured by virtue of their position in the lattice. It has been shown (48)

that the lattice constant of the surface of any heteropolar crystal is ca. 5% less than that in the interior of the crystal. Lateral strains, which may be relieved by the formation of Smekal cracks, are therefore set up. Further, the production of solid reaction product on the surface of the crystal will also be accompanied by such cracks, the larger the product molecule, the greater being the strain. Further reaction will lead to cracks spreading from the internal "parent" cracks, and thus there will occur "branching" in the crystal. This, then, is a physical interpretation of the 'branching-chain' theory of solid decomposition. The initial number of nuclei present will depend on the history of the crystal. Grinding and scratching of the surface, will favour the production of nuclei, and the initial rate of reaction will hence be increased. The acceleratory process, however, is not altered in type, and thus for potassium permanganate Prout and Tompkins (41) have reported the same acceleratory coefficients for ground and whole crystals.

PHOTOLYSIS OF SOLIDS

Few compounds have been investigated, detailed data being available only for the photolysis of silver bromide, silver oxalate, and barium and potassium azides. A characteristic feature of the photolysis of ionic compounds is the production of discrete particles of reaction product, despite uniform illumination. Most successful mechanisms for such photolytic decompositions are based on lattice-defect theory.

The formation of the latent image in silver bromide has been explained by Mott and Gurney (49), as follows: Photo-electrons are trapped at Ag_2S "sensitivity" specks. The charged speck then traps interstitial Ag^+ ions and electrons alternately, forming a metallic nucleus which grows by further trapping of ions and electrons. The positive holes are assumed to have sufficient mobility to allow bromine to escape, but insufficient to permit reaction with the negatively-charged nuclei. Mitchell (50) has suggested that in non-sensitised crystals of silver bromide, nuclei consist of F-centre aggregates. After a critical size is reached, the aggregate breaks

away from the lattice to form metallic silver. This can then grow in the manner suggested above.

The photolysis of barium azide has been investigated by Garner and Maggs (57) and by Thomas and Tompkins (35). Here the results show similarity to those obtained for silver bromide, but no evidence, via conductance measurements, (40), could be obtained for the existence of interstitial Ba^{++} ions, or for photo-conductance. The latter authors have suggested that irradiation results in the production of excitons, and not conduction electrons. It is assumed that excitons may be trapped at points in the lattice. Adjacent trapping of excitons may lead to decomposition, the energy deriving from the energy liberated during the trapping process. This theory has lead to a rate equation of the form:

$$R = I^2 \text{ constant } (b + e^{-\frac{E}{RT}}),$$

which has been shown to be in accord with experimental results obtained for the photolysis of barium and potassium azides.

THE DECOMPOSITION OF SILVER OXALATE

a) Thermal Decomposition

The first systematic investigation of the thermal decomposition of silver oxalate was due to MacDonald and Hinshelwood (33a), who followed the reaction by measurement of the gas evolved into a vacuum system. They showed that the reaction was quantitatively expressed by the equation

$$Ag_2C_2O_4 = 2Ag + 2CO_2$$

The course of the decomposition which is appreciable at temperatures above 70°C, is profoundly modified by a variety of factors. Oxygen, and excess of nitrate-ion decrease the rate of decomposition.

In a later paper (33c) MacDonald continued studies of the thermal rate, using several different specimens of silver oxalate, corresponding to samples prepared with an excess of nitrate or oxalate ions. As noted in his earlier paper, presence of oxalate ions increased the rate, whereas that of nitrate had the reverse effect. However, the general features of the curves obtained were similar for each preparation, in contrast to earlier work (33a), where differently-shaped curves appear to have been obtained. The decomposition of a gelatine emulsion followed the same pattern as powder-

decomposition, indicating that reaction did not spread from one crystal to another by infection. MacDonald carried out decompositions on single crystals, and on precipitated silver oxalate, under paraffin, and in vacuum. The rate of decomposition of the crystal was found to be the same in either environment; the rate of decomposition of the powder, however, was reduced by the paraffin. MacDonald considers that the unit of decomposition is a 'crystallite'. Macro-crystals are supposed to contain many, and micro-crystals of precipitated oxalate few, such crystallites. The essential difference between large crystals and precipitated powder is that the external surfaces of the microcrystals become internal surfaces of the macro-crystals. In large crystals these surfaces are not accessible to paraffin, hence decomposition proceeds as in a vacuum. Microscopic examination of silver oxalate during thermal decomposition showed uniform darkening with no observable nuclei.

Although in general each run was characteristic of the preparation used, it was found impossible to duplicate any experimental curve, variations in rates of up to 20% being found. Most of the preparations used by

MacDonald involved a high excess of one reactant in concentrated solution during precipitation, and Tompkins (32) has suggested that the lack of reproducibility may be attributed to the inhomogeneity of crystals produced under such conditions.

MacDonald has given the following analysis of his results: The decomposition is divided into four parts.

Process I. The first part, which amounts to some 3% decomposition, is controlled by nuclei which are present at the outset. The number of nuclei may be increased by grinding, or by irradiation with ultraviolet light, the fundamental equation being:

$$\frac{dp}{dt} = kt^x$$

Process II. The second process, which accounts for the main course of the reaction, is of an exponential form. This process may be suppressed by carrying out the decomposition in paraffin, or in air. MacDonald considers that this process is due to the production of nuclei which grow in two dimensions and which may branch, leading to an exponential law. That the points at which branching occurs are confined to "surfaces" is indicated by the sensitivity of the process to air,

paraffin and absorbed ions.

Process III. A third process is postulated to explain the reduced rate, and shape of the curve obtained by decompositions of the salt under paraffin wax. MacDonald assumes that nuclei are formed spontaneously at the edges of newly-formed crystal blocks. As the reaction proceeds, the blocks become smaller, and the length of edge correspondingly greater. This process is possible in reactions carried out under vacuum, but in this case is the rate-determining factor.

In general, then, the results of MacDonald may be summarised as follows: The reaction starts from a number of nuclei present in the crystal; the nuclei spread by two-dimensional growth in plates through individual crystal blocks, which are the units of decomposition. Branching of the plates leads to an exponential type of decomposition.

In a third paper MacDonald and Sandison (41) measured the electrical conductivity of the partially-decomposed salt. If the nuclei grow in plates, then the substance should conduct, due to crossing of the plates, at a much earlier stage in the decomposition [illegible], by [illegible] growth in

than if the nuclei grow in solid, discrete, form. Their results indicated that the nuclei are in the form of solid spots, and not of plates. The effect of various liquids on the decomposition was also studied. Although the rates of reaction were often profoundly altered, the shape of the curves remained the same. Generally, it was found that liquids with reactive groups caused acceleration of the reaction whilst non-polar liquids effected retardation.

Benton and Cunningham (52) conducted experiments on the thermal decomposition of silver oxalate which had been pre-irradiated with ultra-violet light. Their oxalate samples were prepared by slow mixing of dilute solutions of silver oxalate and sodium nitrate, in approximately stoicheiometrical proportions. The general effect of environment confirmed the results of MacDonald, but different p-t curves were obtained. It was found that the course of the reaction could be described by the equation $p = Ct^x$ where $x = 3.5$ for unirradiated samples, but decreased progressively for increasing exposure. They assumed that reaction started from a number of nuclei, the number of which could be increased by pre-irradiation. As has been shown, by assuming independent linear growth in three dimensions, an equation $P = Ct^3$ was derived for unexposed samples.

Tompkins (5) also investigated the thermal decomposition of silver oxalate, with and without irradiation, using samples prepared by slow mixing of dilute solutions of oxalic acid and silver nitrate in stoicheiometric proportions. The p-t plots obtained from two samples of the same preparation were indistinguishable after the first 5% of reaction, in distinction to MacDonald, who reported a deviation of up to 20%.

The first 5% of the reaction is described by $p = C(t-to)^{3.9}$, and afterwards to the end of the acceleratory period by $p = (t-to)^{3.27}$, where to =3 minutes. This is in substantial agreement with Benton and Cunningham, but not MacDonald. It is suggested, as before, that nuclei grow in three dimensions, each oxalate radical being a potential nucleus-forming centre. The volume of decomposed solid is corrected for the volume of "ghost" centres, i.e. those "produced" in decomposed volume. As had been mentioned, this leads to an equation $p = Ct^n$. The smaller values of the x actually obtained are attributed to two factors.

First, two nuclei may coalesce to form a larger, growing grain. Secondly, where there are many centres, growth may be sufficiently rapid along one dimension to become virtually two-dimensional. Thus the exponent is expected to decrease as the reaction proceeds, as is found.

The thermal reaction after irradiation is accelerated, but is still described by the Power law, $p = Ct^x$. The constant C is found to vary as $I^{3.25}t^{2.8}$, where I = intensity of incident irradiation. Tompkins suggests that as silver spots are formed, there is a tendency for a lattice more in conformity with the metal state to be set up by adjustment of the Ag-Ag distances. This results in distortion of the $Ag_2C_2O_4$ lattice, with preferred directions of growth, and of fragmentation, along cleavage planes.

Recently, Suchow and Hersh have investigated the "photo-thermal" decompositions of intimate mixtures of silver and mercurous oxalates. Their experimental technique was quite different from that employed by other workers in this field. The materials tested were suspended in gelatin, and the relative rates of decomposition determined by photographic sensitometric

methods. Thus the extent of darkening of the solid is taken as proportional to the amount of decomposition. They found that co-precipitated mixtures of the two salts containing 50-50 mole. per cent of mercurous oxalate exhibited much higher decomposition rates than did the separate components. X-Ray powder-diffraction patterns indicated that no compound or solid solution was formed. The results are attributed to the catalysis of the silver oxalate decomposition by Hg nuclei formed from photolysis of the mercurous salt. Since a close intimacy of mixing is required, decomposition does not spread to unexposed areas.

Finally, some evidence is available from X-ray powder diffraction photographs taken during reaction Griffiths (53). These indicate that the product is a pseudomorph of the original salt; the Ag atoms occupying substantially the same positions as in the original compound. There is no evidence for the existence of plates of silver.

Photolysis of Silver Oxalate

Although photolytic decomposition had been noticed by MacDonald and by Benton and Cunningham, the only quantitative investigation is due to Tompkins The

photolysis was measured at varying temperatures and intensities of irradiation. Gas evolution commenced immediately, and after about twenty minutes was almost constant. Evolution ceased immediately on cessation of illumination, and the constant rate was reproduced on subsequent irradiation. The variation of rate with temperature showed an activation energy of 850 cal. The rate varied as the 1.67 power of the intensity, the value increasing somewhat at high intensities. The following explanation of the photolysis has been given: Absorption of light is presumed to give free electrons and free positive holes. Some of the electrons may be trapped by silver atoms adjacent to the positive hole, and if the lifetime is short, the concentration of such "sites" will be proportional to $I^{\frac{1}{2}}$. Decomposition occurs when a free electron is trapped, giving COO^- Ag COOAg, which breaks up into silver atoms and one oxalate radical by transfer of the additional electron to a neighbouring silver ion. This process should lead to a rate proportional to the 1.5 power of the intensity. The power found, 1.67, is explained by additional trapping of electrons by Ag_2 atoms. If pl = the

probability that a site will react, and p2 = the probability that the trapped electron will be transferred to a positive hole, then the rate R is given by:

$$R = \frac{P1}{P1 + p2}$$

if $P2 > P1$ $\qquad R = \frac{p1}{p2}$

Put $P1 = C1e^{-\frac{E1}{RT}}$

$$P2 = C2e^{-\frac{E2}{RT}}$$

$$\therefore R = \frac{C1}{C2}\, e^{-\frac{(E2-E1)}{RT}}$$

Thus the small activation energy actually found, 850 cal., appears as the difference between E1 and E2.

Decomposition of Mercuric Oxalate

This has been studied by Prout and Tompkins, (38) who showed that the best representation for the overall reaction is:- $2Hg_2C_2O_4 \rightarrow Hg + HgO + 3CO_2 + Co$ the volume of gas being 92% of that calculated theoretically.

Neither the addition of the end-products of previous runs, nor allowing the reaction to proceed in presence of its gaseous or solid products had any effect on the decomposition. Pre-illumination with ultra-violet light increased the initial rate of decomposition. As has been mentioned before, this is a surface effect. Similarly, water-vapour was found to reduce the initial rate, the reaction proceeding afterwards as in normal "vacuum" decompositions. Direct observation of nuclei showed them to be spherical, with an average radius of $1.3.10^{-4}$ cm. The thermal reaction is a surface process, which spreads rapidly over the face of the crystal, after which the rate is controlled by the linear propagation of the face inwards. The activation energies for the two processes are 25.6 and 37.1 kcal. respectively. It is suggested that the increase in the initial rate by pre-treatment with ultra-violet light is due to the production of mercurous

oxalate. An electron is freed from a surface oxalate group. This is trapped by an Hg "ion" in the second layer of the crystal. The process thus corresponds to an electron transfer which, when followed by an intramolecular change, can result in the production of "mercurous" oxalate. This salt is known to be considerably less stable than the divalent compound. An extension of the process, i.e. capture of two electrons, leads to the production of metallic Hg.

The Thermal Decomposition of Lead Oxalate

Birchumshaw and Harris (57) showed that the endothermic reaction was best represented by the equation,

$$3\ Pb(CO_2)_2 \rightarrow 2\ PbO + Pb + 4\ CO_2 + 2\ CO,$$

and by conductivity and X-Ray measurements identified the solid product as an intimate mixture of lead and litharge, and not lead suboxide as had formerly been supposed.

In a later paper, the same authors investigated the kinetics of the reaction. Grinding reduced the induction period of the reaction, but the subsequent acceleratory period corresponded to that found with normal uncrushed samples. The p-t curves showed great similarity to those found for potassium permanganate, and were adequately fitted by the interfering-chain equation. The authors consider that the interfering-chain theory adequately explains their results, but owing to the assymetry of the p-t curve about the time of maximum decomposition, two constants were used in the equation. No direct evidence was reported of the effect of end-products on the reaction, but by analogy with potassium permanganate, positive catalysis is assumed. No work on the photolysis or effect of pre-irradiation, has been published.

EXPERIMENTAL

MEASUREMENT OF CONDUCTANCE

Since A.C. bridges are not practicable for the measurement of resistances greater than 10^8 ohm, and preliminary experiments had shown the order of resistance of the compounds investigated to be of the order of 10^{12} ohm, a D.C. circuit was used. As has been pointed out, this may involve complications due to polarization, and hence a low-frequency pulse circuit was used. The small currents obtained were amplified by a D.C. amphifier, using an electrometer valve having a grid current of 10^{-15} amp. Full details of the circuit and component parts are given elsewhere (55).

Amplifier Circuit

This is given in Figure I. The circuit is conventional, six 2-volt 120 A.H. accumulators being used to provide the power. The anode current is compensated by a current in the opposite direction by adjustment of R17, R18, the coarse and fine zero controls. R9, R13, are used to provide the recommended cathode and screen voltage of + 3 and + 7 volts respectively. By insertion of an Avo jack into J, the heating current

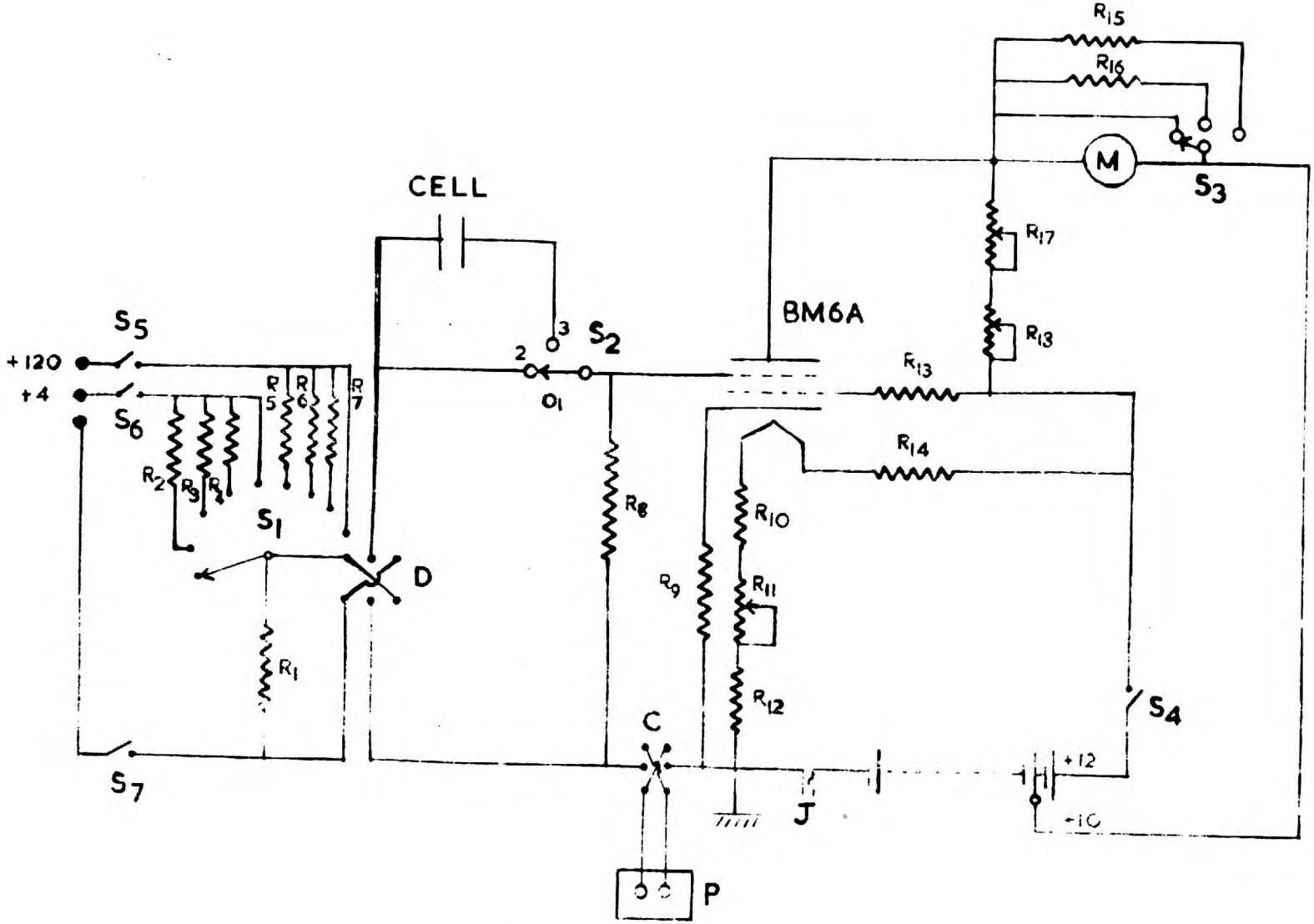

CELL
BM6A
M
S1
S2
S3
S4
S5
S6
S7
D
C
P
J
O1
+120
+4
+12
+10
R1
R2
R3
R4
R5
R6
R7
R8
R9
R10
R11
R12
R13
R14
R15
R16
R17

FIGURE I

can be set to 225 ma. by manipulation of the potentiometer R11. The accumulators were charged each night during runs, and were switched on thirty minutes before a measurement was made. Under these conditions the amplifier was quite stable. The electrometer valve, switch S2 and resistor R8, were mounted in a brass cylinder connected to the low-vacuum line via a phosphous pentoxide tube. All leads in the high-resistance part of the circuit were of shielded polyethylene-insulated cable, and connections were effected by direct soldering to the appropriate terminal. The polarity of the voltage of the potentiometer P, and of the potential divider circuit, is controlled by the relays C and D respectively. The potential divider circuit is discussed later.

The Counter Circuit

This is shown in Fig. II. The actual pulse recurrence frequency used was very low, the polarity being reversed every 25 or 50 seconds. In practice the latter time interval was employed, as it was found that the shorter time was insufficient for the attainment of a steady reading, due to the inertia of the

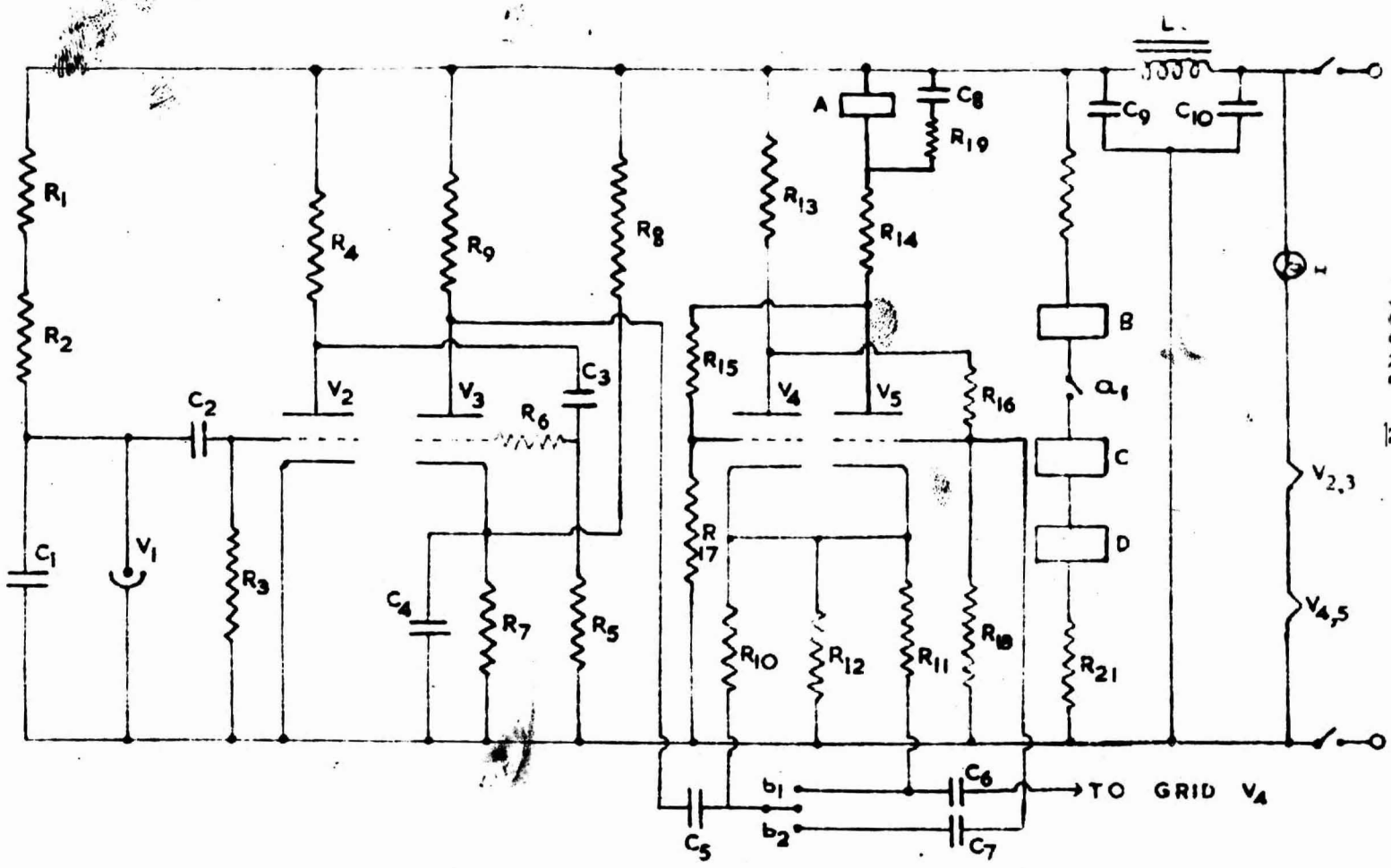

L
A
C8
R19
C9
C10
R1
R2
R4
R9
R8
R13
R14
I
B
R15
V4
V5
R16
a1
C2
V2
V3
C3
R6
C
V2,3
C1
V1
R3
R17
D
C4
R7
R5
R10
R12
R11
R18
R21
V4,5
C6
b1
TO GRID V4
b2
C5
C7

FIGURE II

measuring instrument. The circuit operated the relays C, D (Figure I), which reversed the applied voltage and that from the potentiometer every 50 seconds. V_4, V_5, are the two halves of a double triode connected so that a fraction of the voltage on each anode is applied to the grid of the opposite part of the (double) valve. Although the component parts in the valve circuit are identical, there is sufficient tolerance in valve characteristic and component valves for one valve to conduct first. (V5). The anode voltage of V5 falls to ca. 100 volts, and the grid of V_4 is held below cut-off by the potential divider circuit R15, R17, and the cathode bias generated by the valve current through R12. The anode voltage of V_4 is the supply voltages (ca.210 volts) and the fraction applied to the grid of V5 is sufficient to keep the tube conducting, the anode current being limited to ca. 10 ma. by the resistor R.12. The circuit remains in the above stable state until V5 receives a negative pulse of sufficient magnitude to cause it to cease conducting. This causes the anode voltage of V5 to rise, lifting the bias on V_4 which becomes conducting and immediately applies a negative bias to V5 via the potential divider R16, R18. The

circuit remains in this state until the next impulse is received.

The pulse generator consists of a high-resistance condenser C1, which is charged up to the firing potential of the mean tube V1 through the 100 MW resistar (R1 + Rs). When firing occurs, a negative pulse is applied to the grid of V2 through the coupling circuit C_2 R_3. The pulse is amplified and inverted in V2, passes through the circuit C3R5, and is applied to the grid of V3, which is biased to cut-off by R8 R7 R6 limits the grid current in V3. The negative pulse from the anode of V3 is passed to the appropriate grid via the contacts of relay B. When V5 is conducting, A operates, a. closes, and relays B, C, D operate so that V2 closes and the next pulse cuts off V5. The change-over contacts on C and D thus switch the applied voltage and that from the potentiometer each time the counter operates.

The Potential Divider Circuit

This is shown in Figure I.

In order to measure resistance greater than 10^{11} ohm, a supply voltage of more than one volt is necessary. The maximum voltage read on the potentiometer is 1.900 volt, hence suitable potential

dividers were constructed to calibrate voltages above this figure.

The two voltage sources, + 120 and + 4 volt, are calibrated with switch S1 in positions, 2, 8, respectively. In any other position, the applied voltage is equal to the product of the supply voltage and the resistance ratio = R1/R1+ Resistance.

All resistors, R1 - R7, were individually calibrated, on a D.C. Wheatstone bridge, and a table of values constructed.

The actual applied voltage used, is hence the calibration voltage multiplied by a factor dependent on the position of the switch S1. The method of calculation may be seen from the following example:-

Let s = voltage supplied by the potentiometer to zero the micrioammeter with switch S2 in position 2.

U = same quantity for position 3 of S2.

S = Actual voltage applied across the cell and standard resistor in series. This is the calibration voltage s multiplied by the factor, appropriate to the position of S1 in measuring U.

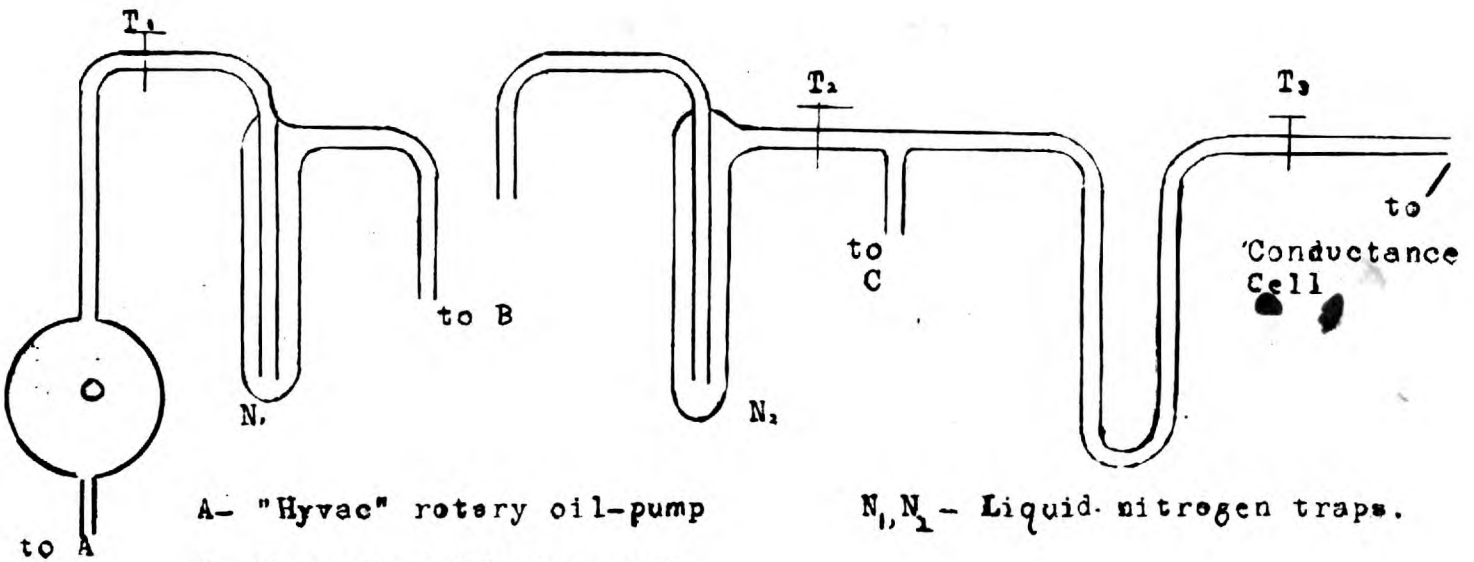
Hence the resistance R is given by:

$$R = \left(\frac{S - U}{U}\right) 1.02.10^{10} \text{ ohm.}$$

TABLE 1

Switch Position	Multiplying factor
1 app	0
2	1 Calibrate
3	1.406
4	2.341
5	3.504
6 vacant	
7 vacant	
8	1. Calibrate
9	7.722
10	25.14
11	100.10
12 app	0.

FIGURE 2.



A- "Hyvac" rotary oil-pump

B- Mercury-diffusion pump

C- Mc.Leod gauge

N_1, N_2 - Liquid nitrogen traps.

Vacuum Line

All measurements were carried out in hard vacuum to ensure complete absence of moisture from the compounds being investigated. A Pyrex vacuum line, shown diagrammatically in Figure 2, was constructed.

The pumping system consists of a two-stage mercury-diffusion pump, B, backed by a rotary-oil ('Hyvac') becking pump A. The usual liquid-nitrogen traps, N1, N2, and oil-trap O are included. Pressure was measured on a McLeod Gauge -C. Although pressure measurements were not needed for this section of the work, the apparatus was designed for later use in kinetic measurements, and the McLeod was calibrated in the usual manner. The pressure was given by the following formula:-

$$P = 2.36\ (hm - hc + 2.17)\ )ho-h).10^{-4}\ \text{MM./Hg.}$$

where hm = position of the mark on the closed capilliary

hc = height of meniscus in the closed capilliary

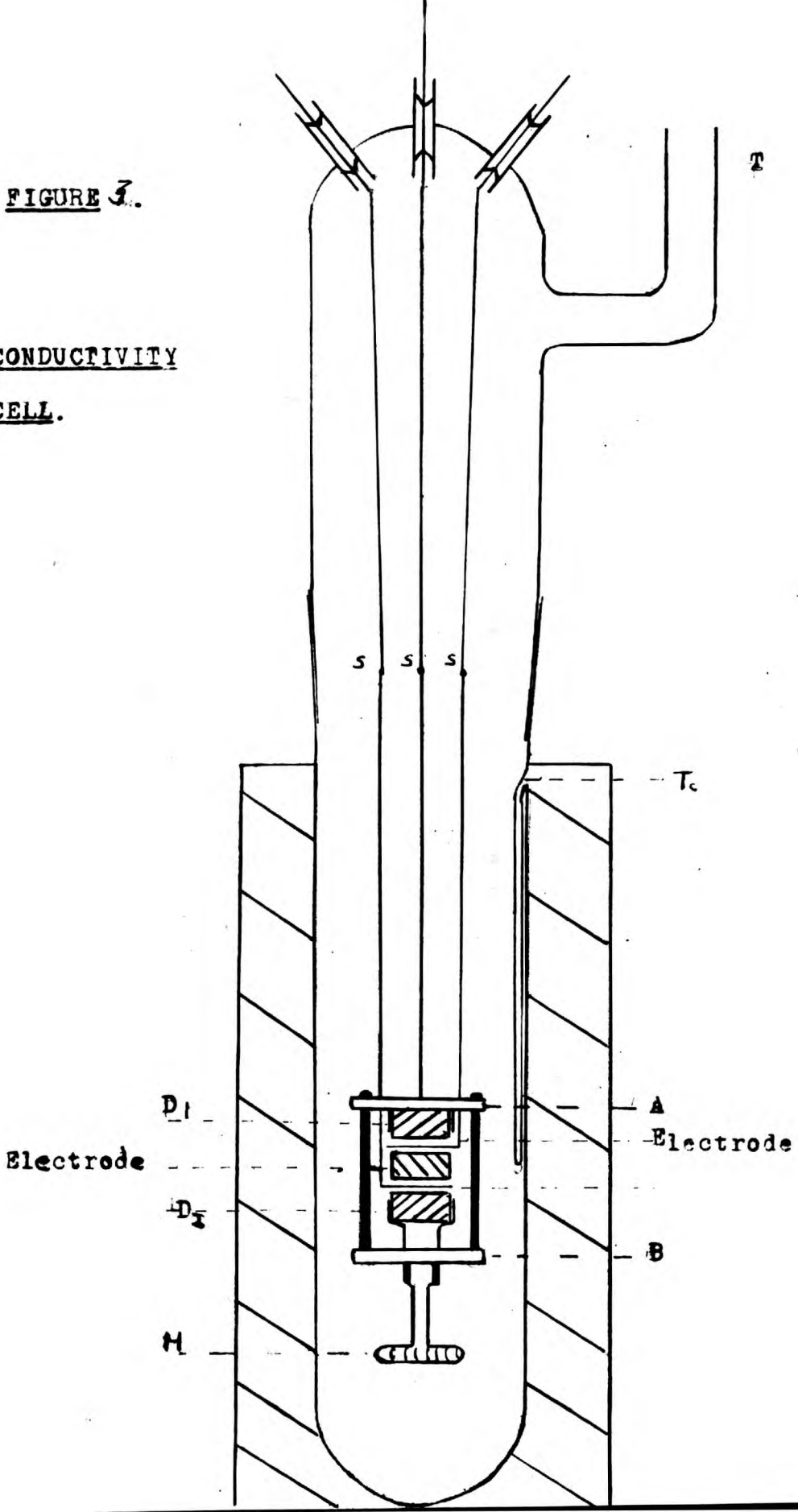
ho = " " " " " open capilliary

The lowest pressure obtainable was of the order of 10^{-6} mm., and was consistently obtained during runs.

The conductivity cell was attached to the line at D.

FIGURE 3.

CONDUCTIVITY CELL.



The Conductivity Cell

The conductivity cell is shown in diagram (3). The framework consisted of two ¼ 2.5cm brass plates, A, B, and two 0.25 cm. brass rods, secured by lock-nuts. A circular brass cup, external diameter I.¼ cm. and height 0.3 cm. was silver-soldered to the upper plate B. The cup is machined to fit the quartz insulating disks D 1, D2. A similar cup, silver-soldered to a threaded brass rod, terminated in a knurled head H. Both quartz disks, D1, D2, were of grade-B "plate-glass finish" fused quartz, of height 0.7 cm. and diameter 1.¼ cm. The electrodes consisted of smooth platinum foil, spot-welded to 0.05 mm. platinum wire, which was soft-soldered to the copper conducting leads. The cell was supported in the apparatus by a length of 18 S.W.G. copper wire silver-soldered to the centre of the base of plate B.

The containing cell consisted of a pyrex tube, fitted with a thermocouple inlet Tc, and terminating in a B-50 pyrex ground-glass socket. Connection to the main vacuum-line was via the T-piece T.

The cell was heated by an electric furnace of conventional design operating off 110v. D.C. mains, the temperature being hand-regulated by a rheostat in

series with the furnace. The furnace was encased in a fibre box packed with asbestos wool.

In any run, the pellet under investigation was firmly clamped in position by movement of the knob H. The copper support and the platinum leads were then soft-soldered to the copper-wire hooks, S_1, S_2, S_3. The B-50 joint was originally secured by Apiezon vacuum grease, but much trouble was experienced through the joint sticking on subsequent dismantling of the cell. After experimenting with various greases, picein vacuum wax was adopted; this worked very satisfactorily. The cell thus hung freely in vacuum, the only leak being through the quartz insulator disks. The thermocouple inlet was arranged to lie adjacent to the pellet, and the whole system was evacuated for ca. eighteen hours before any measurement.

The thermocouple used was of chromel-alumel and was calibrated at the following points: Melting-ice, boiling-water at known external pressure, melting point of tin, melting point of lead. The calibration was checked after ca. two months; no correction was necessary

Preparation of Oxalates

All compounds were prepared in a standard manner.

M/5 solutions of A.R. oxalic acid dihydrate and a soluble compound of the metal required were added at the same slow rate to 500.ml. of water in a three-litre beaker, with vigorous mechanical stirring. The crystals were washed by decantation, transferred to a Büchner funnel, washed with distilled water, and dried at the pump. The compounds were stored over phosphorous pentoxide. All operations were carried out under dark-room conditions. The quantities used are shown below, with relevant experimental details.

a) Silver Oxalate 1,000 ml. each of silver nitrate and oxalic acid solutions were run into water at 30°C.

b) Lead Oxalate 1,000 ml. each of lead acetate and oxalic acid solutions were mixed at the boiling-point. The precipitate was dried in an electric oven at 110°C.

c) Mercuric Oxalate Equal volumes of mercuric acetate solution and oxalic acid solution were mixed at 30°C.

d) Thallous Oxalate

1. Equivalent quantities of thallous sulphate and oxalic acid were mixed and the solution allowed to crystallise. The crystals were twice rapidly recrystallised from hot water, and dried

at 110°C in an electric oven and stored over phosphorous pentoxide.

An attempt to prepare samples of thallous sulphate containing foreign ions was made. Thallous oxalate was selected since

(a) It crystallises well.

(b) No interference due to thermal decomposition is likely and temperatures below at least 500°C.

(c) It possesses a conductivity whose magnitude is easily measureble at normal working temperatures.

2. Equivalent quantities of thallous sulphate solution containing barium oxalate and oxalic acid were allowed to crystallise. Barium was selected since the closeness in size of the barium and thallous ions (1.43, 1.49 respectively) made incorporation of the barium ion into the lattice seem possible. The crystals were not further purified.

3. Crystals of thallous oxalate were prepared as in d), 1. The crystals were recrystallised a) quickly and b) slowly, from M/500 $BaCOO_2$ solution.

e) <u>Barium Oxalate</u> 1,000 ml. solutions of barium

chloride and oxalic acid solution were mixed at the boiling-point. The precipitate was washed and dried at 50°C in an electric oven.

Since none of the compounds were available in single crystals sufficiently large to permit direct measurement, compressed pellets were used. The pellets were prepared in a Millen hydraulic Mounting Press, under a pressure of ca. 10 tons/sq.inch. The pellets produced were all perfectly white and hard. Pellets of thallous oxalate were translucent, as were pellets of sodium chloride and potassium bromide. At first difficulty was experienced in making pellets of barium oxalate, but it was found that satisfactory pellets were formed by a very slow increase of pressure in the press. All pellets were stored in the dark, over phosphorous pentoxide.

Experimental Procedure

A pellet was placed in the cell, and clamped in position by turning the knob H (Fig.3) until finger-tight. The cell was soldered in position to the leads and copper support. The apparatus was evacuated for ca. eighteen hours before any run, at a temperature determined by the decomposition temperature of the compound concerned. Thus silver oxalate was outgassed

at room-temperatures whereas lead oxalate was outgassed at 120°C. Measurements were made at both ascending and descending points in the temperature range used, about one hour being allowed at each temperature to ensure establishment of thermal equilibrium. At the end of each run the pellet was removed and its thickness measured.

Results were tabulated and platted with $\log \sigma$ as a function of $\frac{1}{T^{\circ}K.}$ ...K. The variation of conduction with temperature is given by the Arrhenius-type eqn.:

$$\sigma = Ae^{-\frac{E}{RT}} = A \exp. \frac{-E}{RT},$$

whence the pre-exponential term A, and the activation energy E, were found from the graph of $\log \sigma \sim \frac{1}{T}$

The specific conductance was calculated from the formula

$$\sigma = \frac{1}{R} \frac{l}{a}$$

$\frac{1}{R}$ = Measured conductance

l = thickness of pellet in cm.

a = cross-sectional area = 1.786 cm^2.

The apparatus was tested by measuring the conductance of a pellet of A.R. potassium bromide in the

temperature range 110° to 220°C. Potassium bromide was selected, since a direct comparison could be made with the results of Jacobs (40) using the same technique, and the results of Phipps and Partridge (7), who used a simple D.C. bridge with a sensitive galvonometer. The results obtained are shown below. Since the measurements were in the region of structure-sensitivity, the agreement with the results obtained by other workers was considered satisfactory.

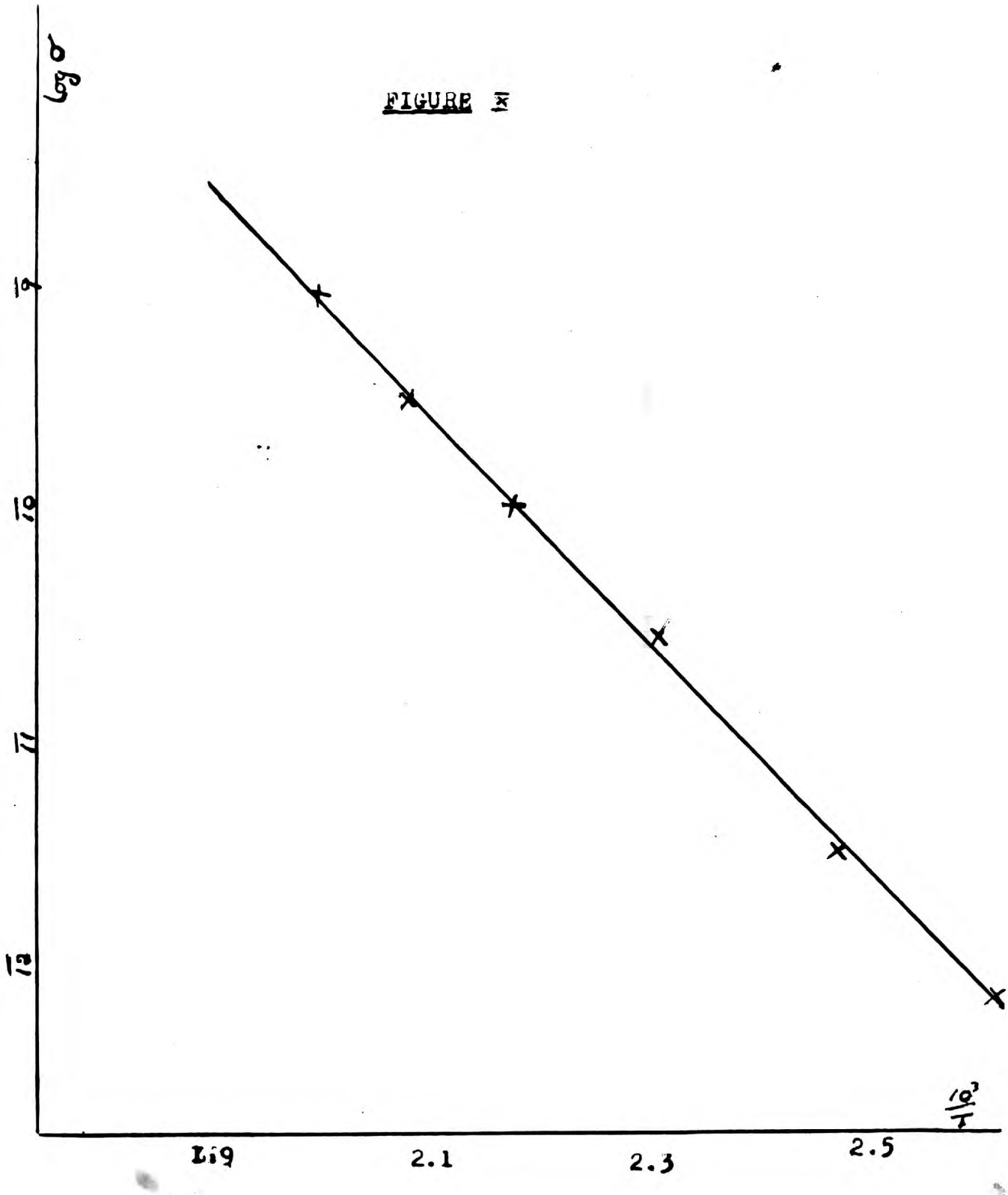
Values of the energy of activation do not in general vary because of structure-sensitive effects. The value of the pre-exponential factor, however, may vary considerably. Thus for Na Cl Smekal (57) reported values for A of 0.055, 0.42 and 0.62 for specimens corresponding to different single crystals.

The actual measurements are shown in Table $\bar{X}$

TABLE $\bar{X}$ $l = \cdot 42$ cm.

$T^{\circ}K$	$\frac{10^3}{T}$	s	u	p	log
384.6	2.60	1.201	0.03	5	15.86
406.5	2.46	1.220	.985	9	12.51
460.0	2.175	1.200	.640	2	10.05
500.0	2.00	1.200	1.09	2	10.99
480.0	2.08	1.310	0.92	2	10.50
434.8	2.30	1.210	0.278	2	11.46

FIGURE IX



From the graph, the characteristic equation for the conductivity of potassium bromide was derived, viz.;

$$\log_{10}\sigma = 0.850 - \frac{24,000}{4.576}\,\frac{1}{T}$$

The results obtained are compared below with those obtained by other workers.

TABLE XI

K Br	A	log A	Ek.cals	Author
"	9.63	0.984	22.40	Phipps & Partridge
"	6.85	0.838	25.76	P. Jacobs
"	7.08	0.850	24.00	

The reproducibility of the conductance measurements is affected by three factors:-

a) Variation in conductance due to measurements at different applied voltages. This is an instrument error, which in no case was found to be greater than 1%, and was, as Jacobs reports, frequently much smaller. Ohm's Law was verified for each compound used; this showed that the precautions taken to avoid polarisation were effective.

b) Variations due to differences in physical form of pellet or electrode. The process for making pellets appeared satisfactory. Density determinations were carried out on potassium bromide pellets; the

variation between two pellets amounted to ca. 2%. The actual density is compared below with the reported value (2.75) for the crystal modification. This indicates ca. 10% "Space" in the pellet.

	Pellet 1	Pellet 2	Mean	Crystal	
Density	2.455	2.505	2.480	2.756	(25°)C.

The electrodes were of smooth platinum foil, and were washed with alcohol between runs. Care was taken to mount the pellets in a standard manner.

c) Variation due to the nature of the structure-sensitive temperature-range in which all measurements were made. This variation is indeterminate, and reference to each particular compound is necessary.

The ionic conductances of silver, mercuric, thallous, lead and barium oxalates were measured in the temperature range of stability of each compound, and the characteristic equation relating conductance to temperature derived. Two further series of experiments were attempted.

First, an attempt to find a relation between conductance and method of preparation of thallous oxalate was made. Preparations (d) 1, —3a, 3b, were employed. It was expected, by analogy with previous investigators, (58,59) that a marked difference in the structure-sensitive conductance would result. The results obtained, however, varied from the "stoicheiometric results" by no more than the normal experimental limits of reproducibility. In general, the results are similar to those obtained by Jacobs (40) in work on the conductance of potassium azide. The results obtained are summarised below.

Preparation	E k.cals	log A	E (Mean)	log A (Mean)
d i Run 8	6.35	$\bar{7}.65$	6.15	$\bar{7}.57$
d i Run 9	5.96	$\bar{7}.49$		
d i	6.10	$\bar{7}.79$	5.77	$\bar{7}.46$
d iii (a)	5.50	$\bar{7}.11$		
d iii (b)	5.70	$\bar{7}.33$		

Hence the average value of the pre-exponential factor is not significantly increased by any of the different methods of preparation. By comparison, the addition of 1% of $Ca\ cl_2$ to Ag Cl was found to increase the conductivity more than 1,000 times (60).

Secondly, the effect of pre-irradiation on the conductance of silver oxalate was studied. This experiment is of especial interest, since the lack of positive evidence for photo-conductance in barium azide (40), has led to a new theory of photolysis (35), which does not postulate the existence of electrons in the conduction band.

The experiments were carried out in two ways. In the first, light from a 150-watt tungsten-filament lamp was focussed on a slit, and passed through a quartz cell containing distilled water. This served as a filter for infra-red radiation. The slit of light was adjusted to fall on the side of the pellets mounted on the press, such that a band of ca. 1-2 mm. was illuminated. Care was taken to prevent illumination of the electrodes.

In the second modofication a small hole was blown in the wall of the pyrex tube, enclosing the pellet, and a quartz window sealed thereon with picein vacuum wax. Light from a low-pressure mercury-vapour lamp was focussed through a slit onto the pellet in the apparatus. It was found possible to cause slight discolouration of the pellet in a strip corresponding to the incident light, showing that some decomposition had

occured.

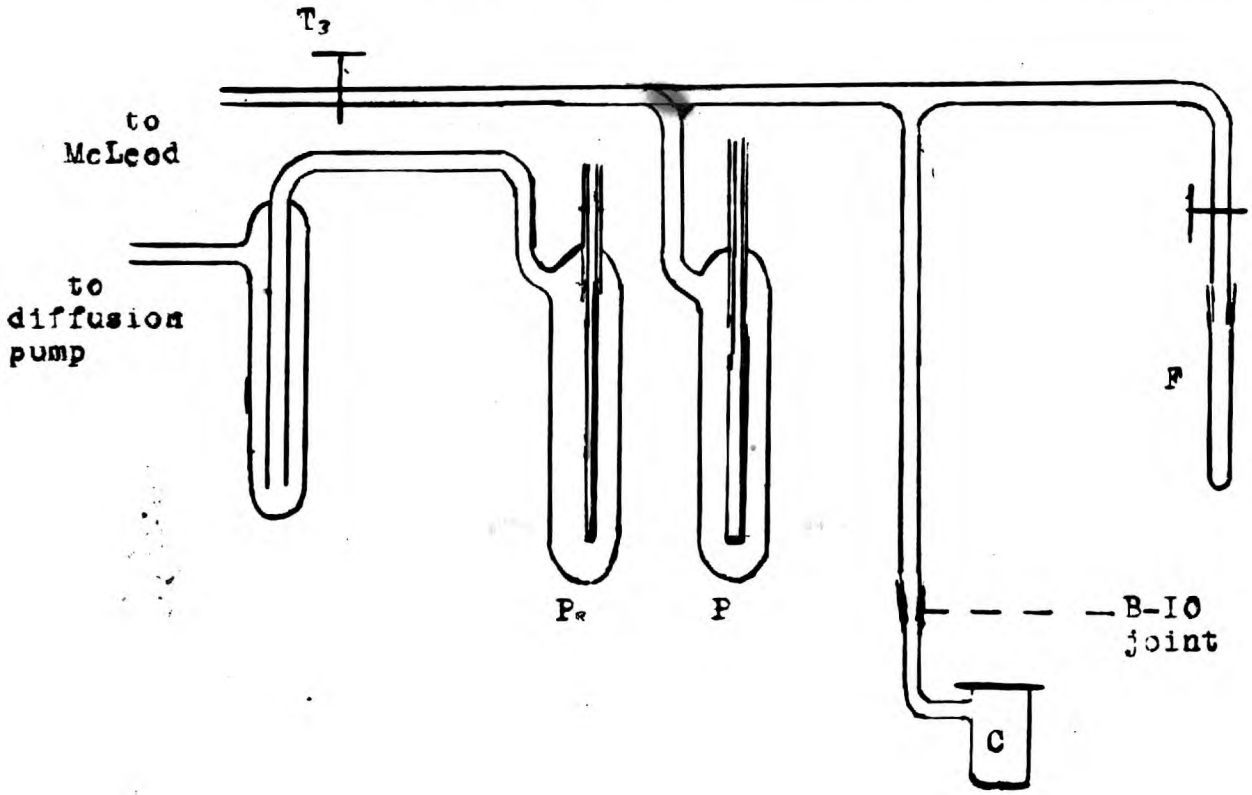
In neither modification of the apparatus was it found possible to demonstrate any difference in conductance on switching on the light. It is concluded, therefore, that silver oxalate does not show photoconductance, of currents greater than 10^{-12} amp. under the above conditions.

Photolysis

The pumping system used in the conductance measurements was retained and extended as shown in Figure (7). The reaction cell C consisted of a 6.5 x 2.5 cm. pyrex tube, connected to the vacuum line in a B-10 ground glass joint. The upper edges of the cell were extended to a rim, with two small indentations, for thermocouple wires. A 1.0 mm. Grade "B" 'plate-glass-finish' quartz plate was sealed to the rim by picein vacuum wax.

The Pirani gauges were constructed as shown in Figure (8). The tungsten filament consisted of a spiral unflashed electric-light bulb filament, resistance 240 ohms, welded between two strips of nickel foil, which in turn were welded to 1 mm. diameter tungsten wire. The Pirani heads consisted of 20 x 2.5 cm. pyrex tubing, and were immersed in a Dewar containing ethanol and solid carbon dioxide, the level of the liquid being kept above the internal seal. No attempt was made to flash the wires, as this resulted in a loss of elasticity; a small amount of mercury was condensed in each gauge and hence all measurements were made with the Piranis in an atmosphere saturated with mercury vapour. The gauges were operated at a

FIGURE 7 APPARATUS USED FOR PHOTOLYSIS.



constant current of ten ma. Measurements were made using a conventional Wheatstone net circuit, component parts for which are given in Figure (15a). The Piranis were calibrated against decomposition gas and carbon dioxide from commercial solid 'cardice', introduced into the apparatus via the finger f. The reference Pirani was maintained permanently at high vacuum by direct connection to the diffusion pump, and the reading taken to balance the bridge with both gauges in hard vacuum was taken as the resistance zero Ro. After initial fluctuations, the difference $\Delta R = (Ro - R)$ where ΔR = the resistance needed to balance the bridge at a pressure P, remained constant. A graph of $\Delta R \sim P$ was constructed, and used in the subsequent measurements. The gauge had a sensitivity of ca. 100 ohms/micron and the bridge could be balanced accurately to within 0.5 ohm. Pressures of 10^{-5} mm. could, therefore, be measured to $\pm$ 5%.

The temperature of the photolysis cell was measured by a copper/constantin thermocouple standardised at the following fixed points: Boiling-water, melting-ice, boiling oxygen and the temperature of a water-bath measured by an N.P.L.-calibrated thermometer. Several cm. of the thermocouple wire were coiled

inside the cell, to minimise conduction along the leads, and the spot-welded metal junction arranged to lie in the centre of the surface of the oxalate layer. The cold junction was maintained at 0°C in a Dewar of melting-ice. Variation in temperature of the cell was effected by immersion in various temperature-baths. Above 0°C, a water-bath, the temperature of which was controled to $\pm$0.05°C by a conventional toluene regulator was employed. At lower temperatures Dewars containing suitable refrigerant mixtures, e.g. melting ice, ethanol and solid carbon dioxide, melting carbon tetrachloride were used.

Experimental Procedure: This was standardised as far as possible. A thin layer of oxalate was spread over the base of the cell, and the position of the thermocouple adjusted. The quartz window was sealed, and the apparatus allowed to out-gas for ca. 18 hours before any run. Dark-room conditions were observed. Before beginning a run, the cell was isolated from the pumps, and the outgassing rate measured. The lamp was switched on for ca. 10 minutes before irradiation, and the current in the primary winding of the lamp transformer measured. The cell was opened to the pumps, and the resistance-zero checked. The shutter was removed,

$P_1 P_2$ - measuring & compensating heads
R_1 - decade resistance box, 0-10000 ohms
R_2 - 5000 ohm resistance
H - two, 2-volt, 120 A.H. accumulators
G - Tinsley galvonometer, sensitivity of $1.6\ 10^{-9}$ amp/mm.

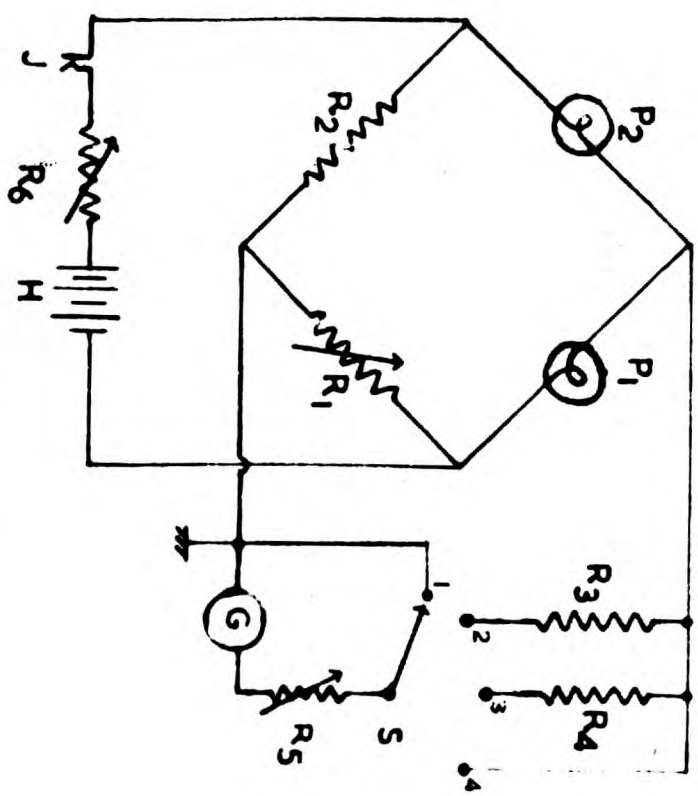


FIGURE 15a

the reaction system isolated from the pumps, and a stop-clock started. Readings were taken at suitable time-intervals, usually of one minute. At the end of a run, the shutter was replaced, and readings continued in order to test for the existence of a 'dark-rate'. In the reactions considered, evolutions of gas ceased with cessation of irradiation, and the small original out-gassing rate was reëstablished within a few minutes. Photolysis rates were measured both at different temperatures and at different intensities of incident light. In order to preserve unaltered the relative positions of lamp and reaction-cell, the intensity was varied by adjustment of the primary lamp-current. It was found by aligning the lamp with a Kipp thermopile, that a square-law relationship between primary current i_p and intensity I existed, although a point source was not employed.

i.e. $i_p^{\frac{1}{2}} \propto$ e.m.f. $\propto$ Intensity I.

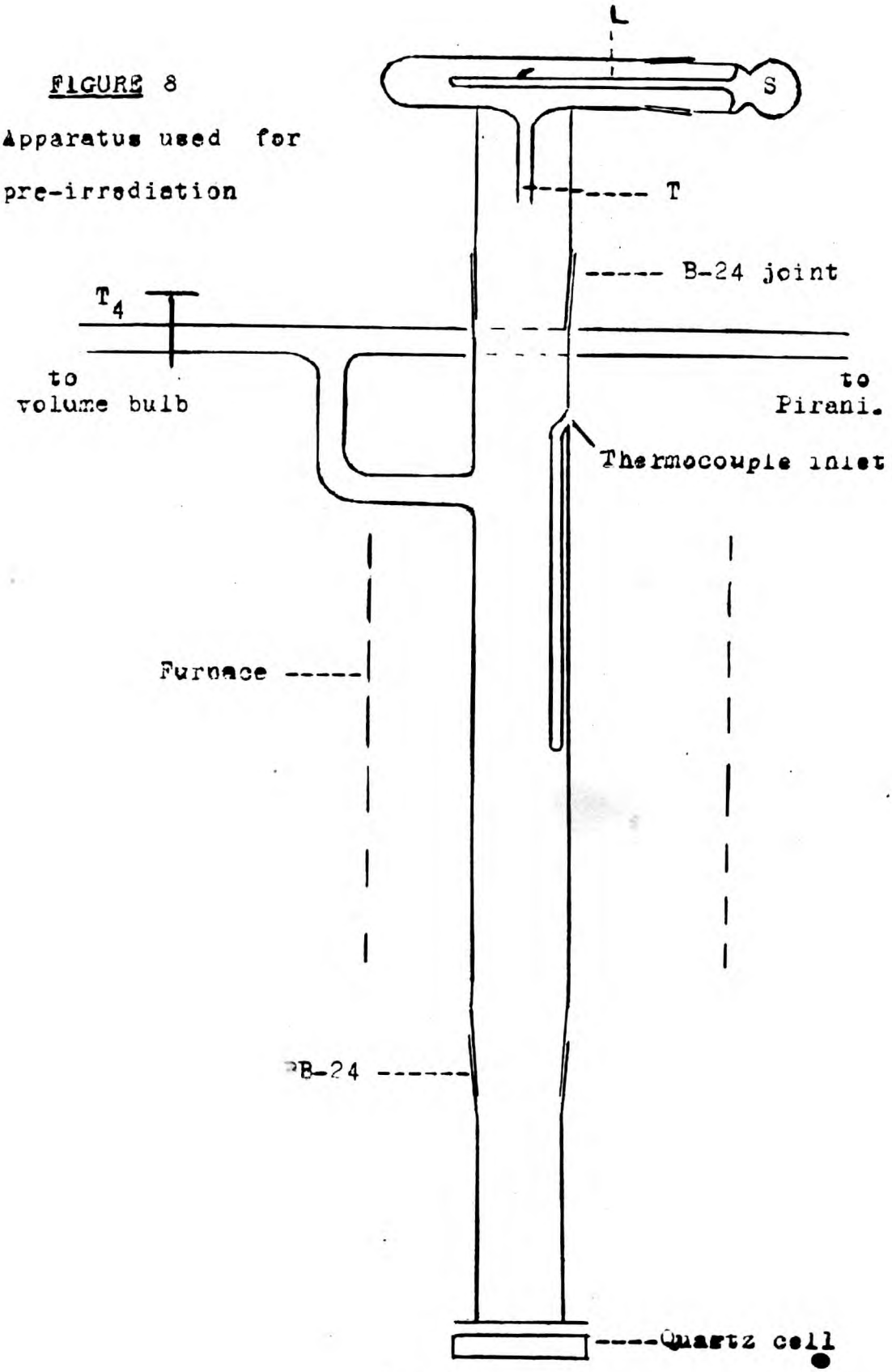
Apparatus used in Pre-Irradiation

The apparatus used in the photolysis experiments was modified as shown in Fig. (8), a reaction-tube and calibrated volume being added.

The sample was contained in a quartz bucket, the bottom of which was plane, and of "plate-glass-finish".

FIGURE 8

Apparatus used for pre-irradiation



The bucket was suspended from the winch by 0.01 cm. platinum wire. Apiezon-N grease was used as lubricant for the movable joints in the winch, due to its plasticity at working temperatures. The bucket could be raised to the centre of the furnace, so as to touch the thin-walled tip of the thermocouple inlet. The thermocouple was of copper-constantin, and was calibrated at the melting-points of lead, tin and ice. The temperature of the reaction vessel was maintained by an electric furnace which fitted closely over the reaction tube. The core of the furnace consisted of an iron tube, 26 x 2.2 cm. and of thickness 0.3 cm. The furnace was constructed for use with an electronic control unit, and was made of three separate windings. In practice it was perfectly satisfactory to operate on one winding, control being obtained manually by a 500 ohm. lamp series rheostat. The winding used was the external winding, of 140 ohms of 18 ohm/metre nickrame, and the 110 D.C. mains were employed as power supply. Used thus, the temperature of the reaction vessel remained constant for several hours at temperatures between 90° and 130°C. to within $\pm$ 0.2°C. The irradiation cell was provided with a $\frac{1}{4}$" rim at the lower end to facilitate sealing of the quartz window

by picein vacuum wax. To prevent infra-red irradiation a quartz cell filled with distilled water was fastened to the window by elastic bands. A fibre box shielded the lower portion of the reaction vessel from draughts during irradiation, which was always carried out at room temperature.

Experimental Procedure: A fixed quantity of silver oxalate was weighed into the quartz bucket, and mounted in the irradiation cell. The apparatus was pumped for ca. 18 hours before any rum. Before a run, the outgassing rate was measured, and the Pirani zero checked. Irradiation was carried out with the cell open to the pumps. The cell was then raised to the centre of the furnace by a known number of revolutions of the winch, the apparatus closed to the pumps, and a stop-clock started. Readings of pressure were noted at convenient time intervals.

Preparation of Silver Oxalate: All samples were prepared in dark-room conditions, washed by decantation and then at the pump, and stored over phosphorus pentoxide in a desicator.

1. "Stoicheiometric" Silver Oxalate: 200 ml. of N/5 A.R. oxalic acid dihydrate, and 200 ml. N/5 silver nitrate were run into 400 ml. of water at 30 C. at the

same slow rate, with vigorous mechanical stirring.

2. "Oxalate-Excess" Silver Oxalate: 2,000 ml. of N/20 oxalic acid solution were run into 400 ml. of N/20 silver nitrate solution, with vigorous mechanical stirring.

3. "Nitrate Excess" Silver Oxalate: 500 ml. of N/5 silver nitrate solution were run into 50 ml. of N/5 oxalic acid solution, with vigorous mechanical stirring.

4. "Nitrate-Excess" silver Oxalate: 500 ml. of N/5 silver nitrate solution were run into 50 ml. of N/5 A.R. sodium oxalate solution, with vigorous mechanical stirring.

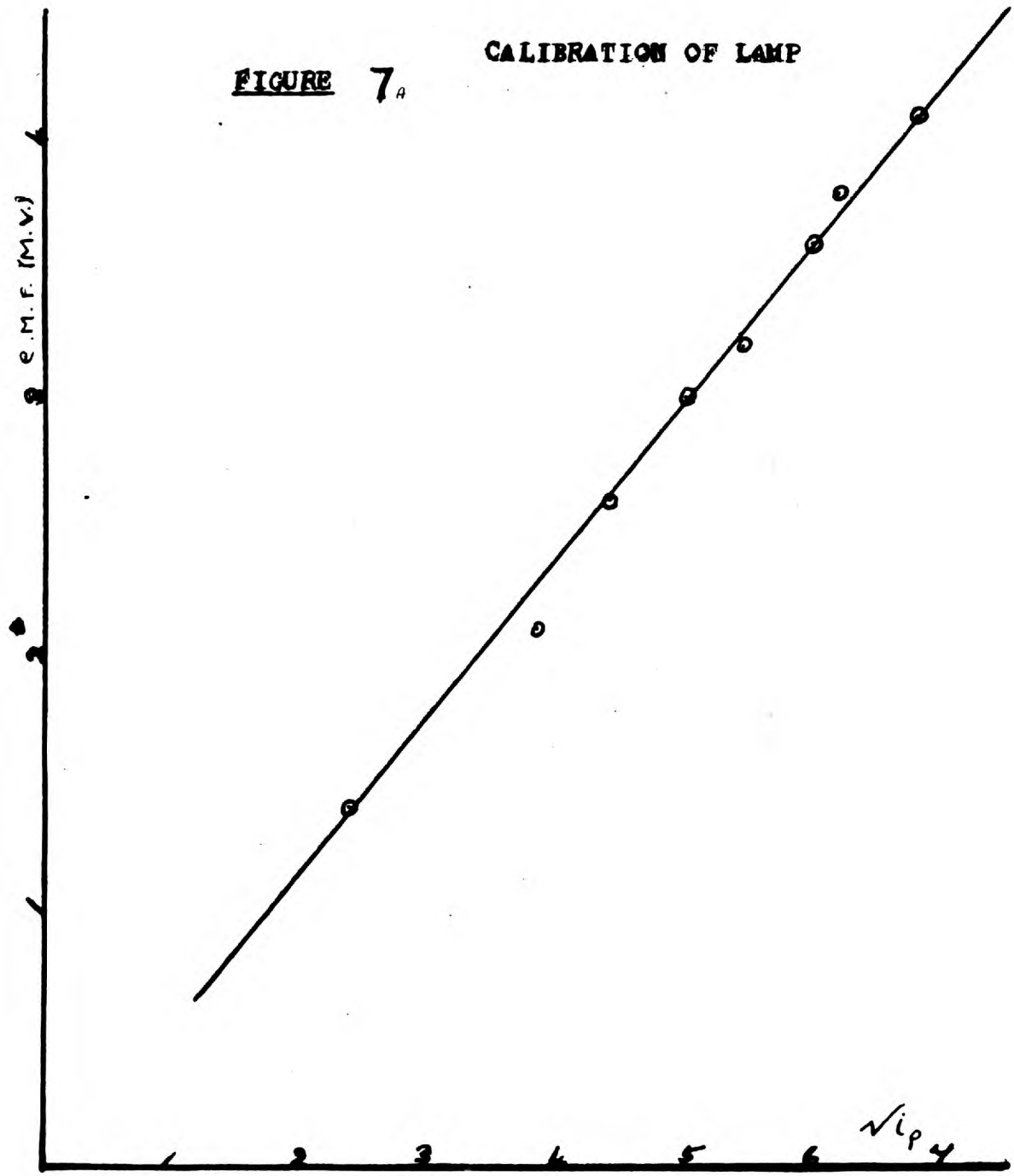
The ultra-violet lamp was placed before a Kipp thermopile, in the same position as it had been with respect to the cell. The e.m.f. registered was measured on a Doran potentiometer. The results are tabulated below.

i_p amp.	E.M.F. mv.	$i_p^{\frac{1}{2}}$
0.0	0.00	0
0.41	0.41	0.640
0.36	0.36	0.600
0.30	0.32	0.546
0.25	0.30	0.500
0.20	0.26	0.447
0.15	0.21	0.387
0.06	0.14	0.240
0.36	0.38	0.616

Results are shown on Figure 7A

FIGURE 7A

CALIBRATION OF LAMP

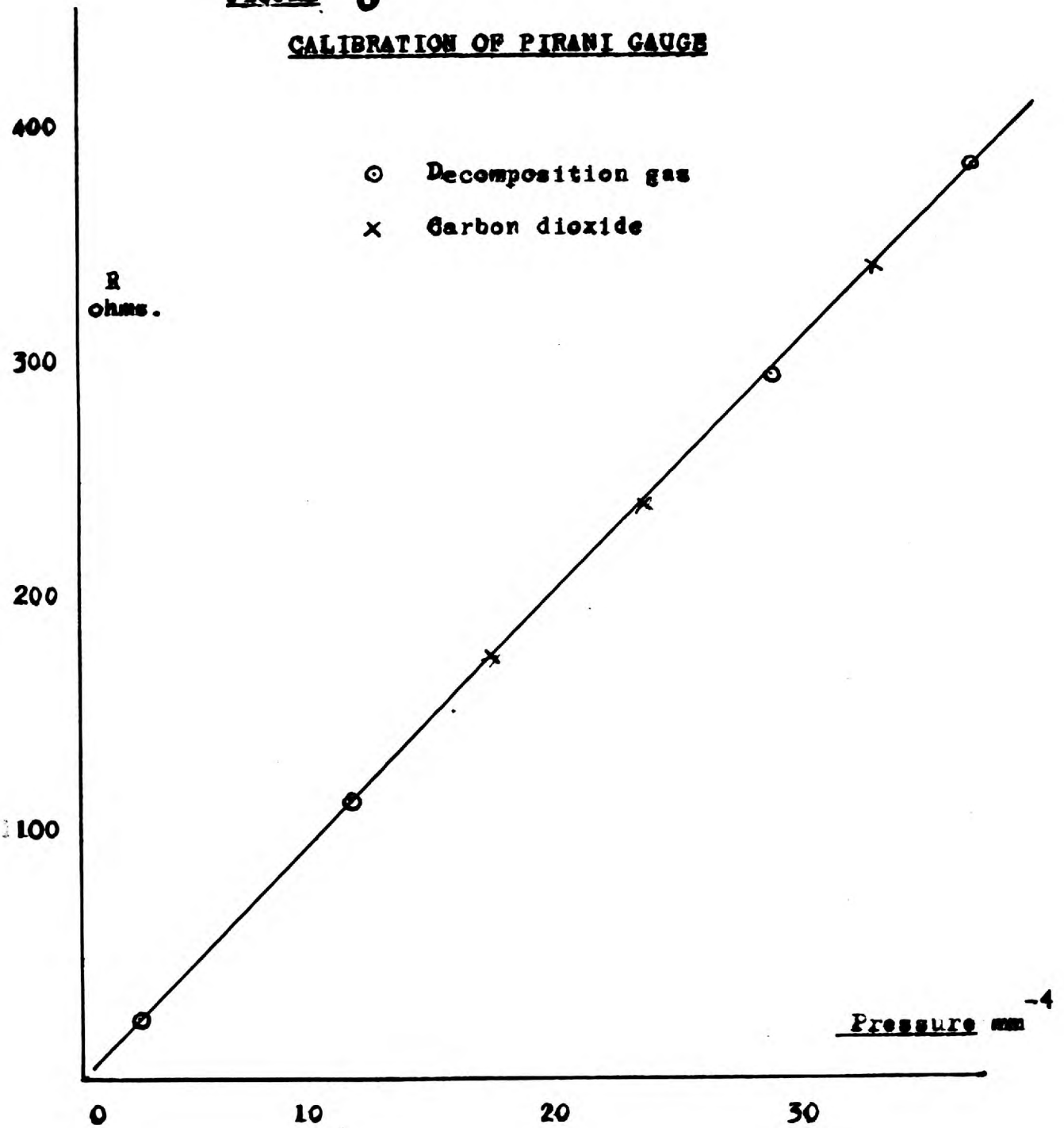


A typical Pirani calibration curve is shown in Figure 6. It is seen that the curve is strictly linear in the range required. The curve was independent of whether the gas was prepared by heating silver oxalate, or from commercial solid carbon dioxide

$p\ mm^{-4}$	R ohms.
37.51	375.0
33.50	340.0
29.49	293.0
19.20	190.0
17.50	175.0
12.42	124.0
2.50	25.0

FIGURE 6

CALIBRATION OF PIRANI GAUGE



EXPERIMENTAL RESULTS

IONIC CONDUCTANCE

1. Lead Oxalate

Runs 8 ℓ = 0.315 cm.

TABLE 3

T°K	s	U	P	logσ	$\frac{10^3}{T}$
377.4	1.238	.024	11	$\bar{1}4.293$	2.650
395.3	1.242	.088	11	$\bar{1}4.84$	2.530
425.5	1.220	.315	11	$\bar{1}3.4$	2.350
435.0	1.215	.535	11	$\bar{1}3.64$	2.300
452.5	1.216	.932	11	$\bar{1}3.88$	2.210
433	1.225	.474	11	$\bar{1}3.58$	2.310
423.7	1.227	.327	11	$\bar{1}3.42$	2.360
405.0	1.219	.142	11	$\bar{1}3.06$	2.469
396.8	1.215	.100	11	$\bar{1}4.90$	2.520
390.5	1.232	.093	11	$\bar{1}4.92$	2.560

A second run was carried out, using another pellet of lead oxalate, the run lasting over two days. Results are given in Tables, 4,5,.

Runs 9a, 9b. l = 0.221 cm.

TABLE 4

T°K	s	U	P	log σ	$\frac{10^3}{T}$
393.0	1.247	.068	11	$\bar{1}4.73$	2.544
403.2	1.232	.086	11	$\bar{1}4.84$	2.480
435.0	1.219	.375	11	$\bar{1}3.46$	2.300
448.3	1.220	.681	11	$\bar{1}3.73$	2.231
442.5	1.223	.552	11	$\bar{1}3.65$	2.260
433.0	1.217	.329	11	$\bar{1}3.42$	2.310
418.1	1.221	.058	10	$\bar{1}3.27$	2.391
405	1.216	.095	11	$\bar{1}4.884$	2.469

TABLE 5

399.0	1.236	.075	11	$\bar{1}4.77$	2.508
434.8	1.233	.331	11	$\bar{1}3.42$	2.300
445.0	1.231	.497	11	$\bar{1}3.60$	2.250
438.6	1.231	.374	11	$\bar{1}3.47$	2.280
423.4	1.231	.242	11	$\bar{1}3.28$	2.362
420.6	1.221	.184	11	$\bar{1}3.17$	2.379
413.3	1.233	.136	11	$\bar{1}3.03$	2.420

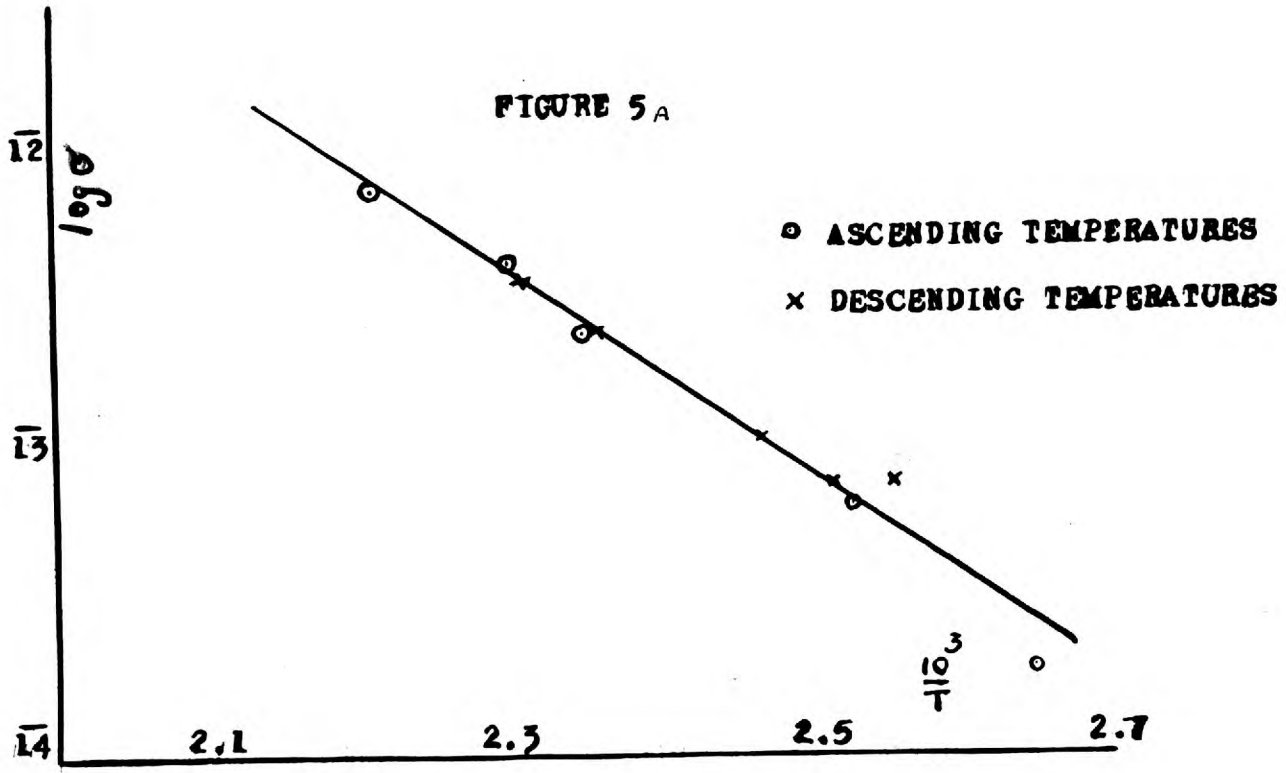
From the slopes of the lines in Figure (5A), the constants in the conductance equation were evaluated

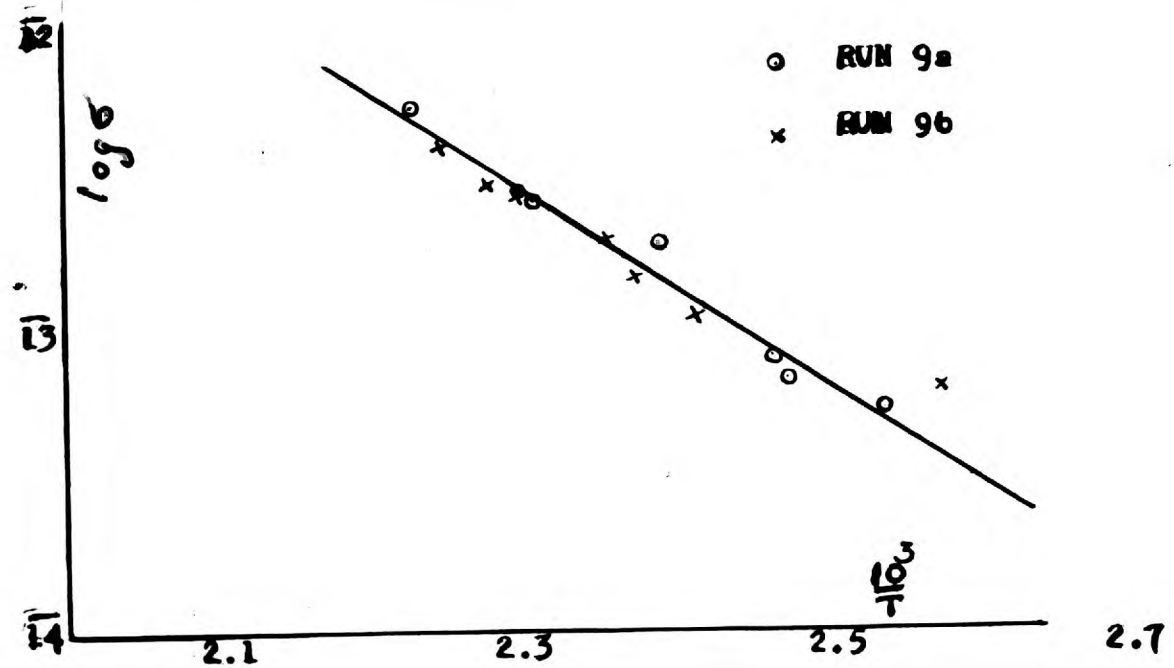
Run	E kcal.	log A
8	15.4	$\bar{6}.26$
9a, 9b.	14.75	$\bar{7}.93$

The conductance of lead oxalate is given by:

$$\log \sigma = -5.95 - \frac{15000}{4.576\,T}$$

FIGURE 5A


log σ
$\bar{1}2$
$\bar{1}3$
$\bar{1}4$
2.1
2.3
2.5
2.7
$\frac{10^3}{T}$
o ASCENDING TEMPERATURES
× DESCENDING TEMPERATURES


log σ
$\bar{1}2$
$\bar{1}3$
$\bar{1}4$
2.1
2.3
2.5
2.7
$\frac{10^3}{T}$
o RUN 9a
× RUN 9b

2. Silver Oxalate

Run 10 — TABLE 6 — l = .334 cm.

T°K	s	U	P	log σ	$\frac{10^3}{T}$
305.7	1.21	.130	11	$\bar{1}3.02$	3.271.
308.6	1.193	.039	10	$\bar{1}3.136$	3.240
310.6	1.232	.171	11	$\bar{1}3.133$	3.219
309.6	1.708	.024	11	$\bar{1}3.045$	3.230
306.7	1.205	.119	11	$\bar{1}4.99$	3.261
310.7	1.194	.045	10	$\bar{1}3.176$	3.218
316.5	1.204	.254	11	$\bar{1}3.32$	3.160
318.5	1.176	.065	10	$\bar{1}3.53$	3.140
303.8	1.196	.043	11	$\bar{1}3.156$	3.292

Runs 11, 12. TABLE 7 — l = .255 cm.

304.0	1.217	.180	11	$\bar{1}3.26$	3.292
305.7	1.210	.300	11	$\bar{1}3.38$	3.270
313.0	1.196	.101	10	$\bar{1}3.52$	3.195
318.2	1.204	.136	11	$\bar{1}3.615$	3.143
315.5	1.207	.111	11	$\bar{1}3.57$	3.170
310.6	1.204	.070	10	$\bar{1}3.35$	3.220
301.3	1.191	.061	10	$\bar{1}3.22$	3.320
333.2	1.193	.242	10	$\bar{1}3.96$	3.000
307.8	1.183	.360	11	$\bar{1}3.44$	3.248
292.4	1.206	.108	11	$\bar{1}4.95$	3.420

The three points in Run 12 were carried out after the crystal had been maintained at 70°C for some time. That some decomposition has occured was demonstrated by the darkening of the pellet. Nevertheless, the points obtained lay on the original curve of Run 11, indicating that slight decomposition has no pronounced effect on conductivity.

From the graphs the following constants were calculated:

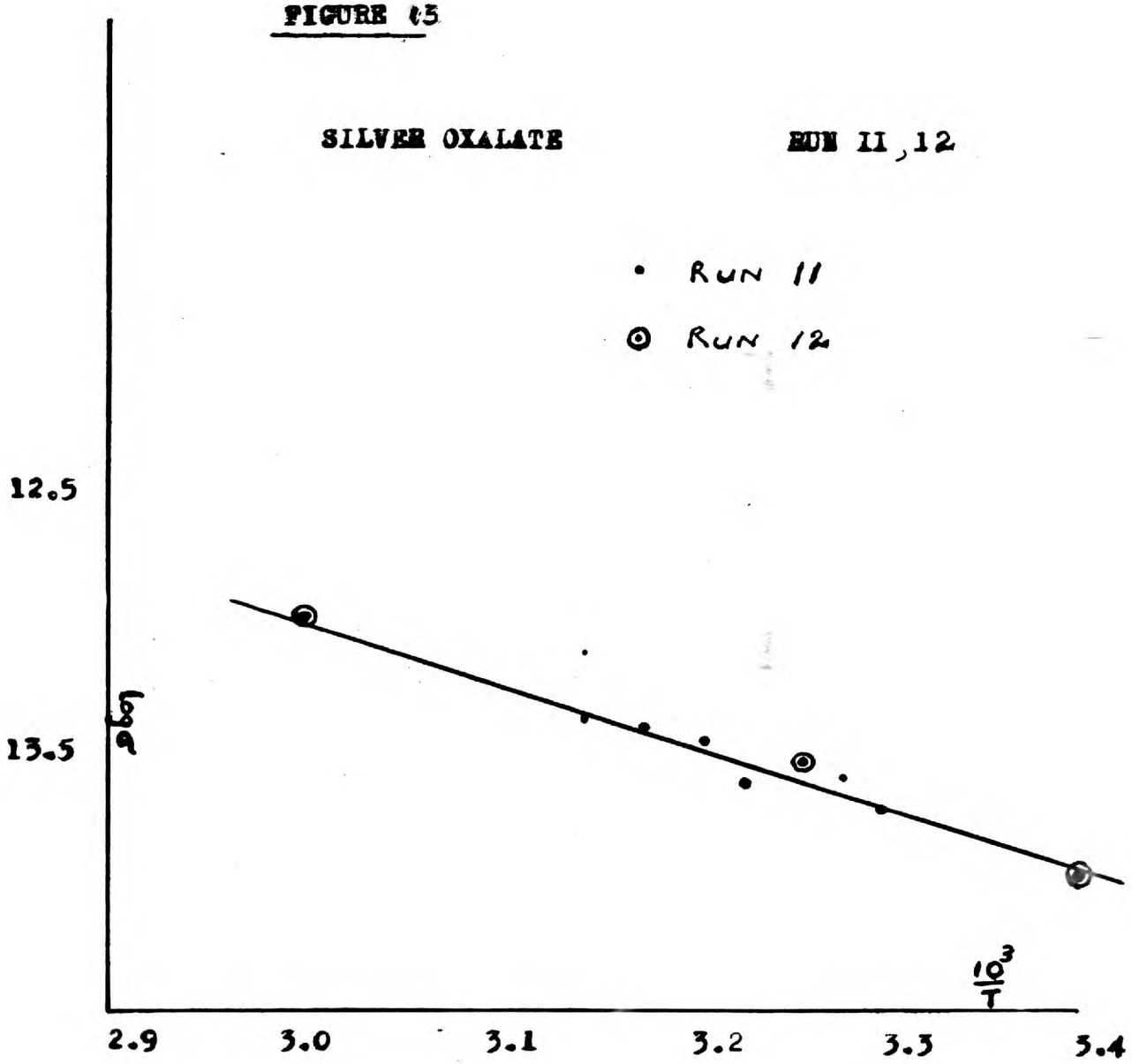
Run	log A	E kcal.
10	$\bar{7}.97$	10.7
11, 12	$\bar{6}.01$	10.6

The equation for the specific conductance of silver oxalate is hence:

$$\log \sigma = -6.01 - \frac{10{,}700\ 1}{4.576\ T}$$

FIGURE 13

SILVER OXALATE RUN 11, 12



3. Mercuric Oxalate

TABLE 8

Run 13 l = .162 cm.

T°K	s	u	p	log $\frac{1}{\rho}$	$\frac{10^3}{T}$
390.5	1.206	.047	11	$\bar{1}4.58$	2.560
398.6	1.198	.057	11	$\bar{1}4.68$	2.509
408.2	1.198	.106	11	$\bar{1}4.94$	2.452
415.0	1.170	.163	11	$\bar{1}3.13$	2.410
423.7	1.175	.203	11	$\bar{1}3.23$	2.360
425.5	1.172	.208	11	$\bar{1}3.24$	2.350
413.0	1.178	.131	11	$\bar{1}3.04$	2.421
398.5	1.178	.021	11	$\bar{1}4.22$	2.510

TABLE 9

Run 14 l = 0.173 cm.

406.5	1.204	.049	11	$\bar{1}3.20$	2.460
403.6	1.206	.103	11	$\bar{1}4.92$	2.479
413.2	1.189	.146	11	$\bar{1}3.08$	2.420
423.7	1.188	.238	11	$\bar{1}3.29$	2.360
435.1	1.186	.317	11	$\bar{1}3.42$	2.298
423.7	1.193	.168	11	$\bar{1}3.14$	2.360
418.4	1.189	.123	11	$\bar{1}3.10$	2.390
392.2	1.190	.050	11	$\bar{1}4.65$	2.550

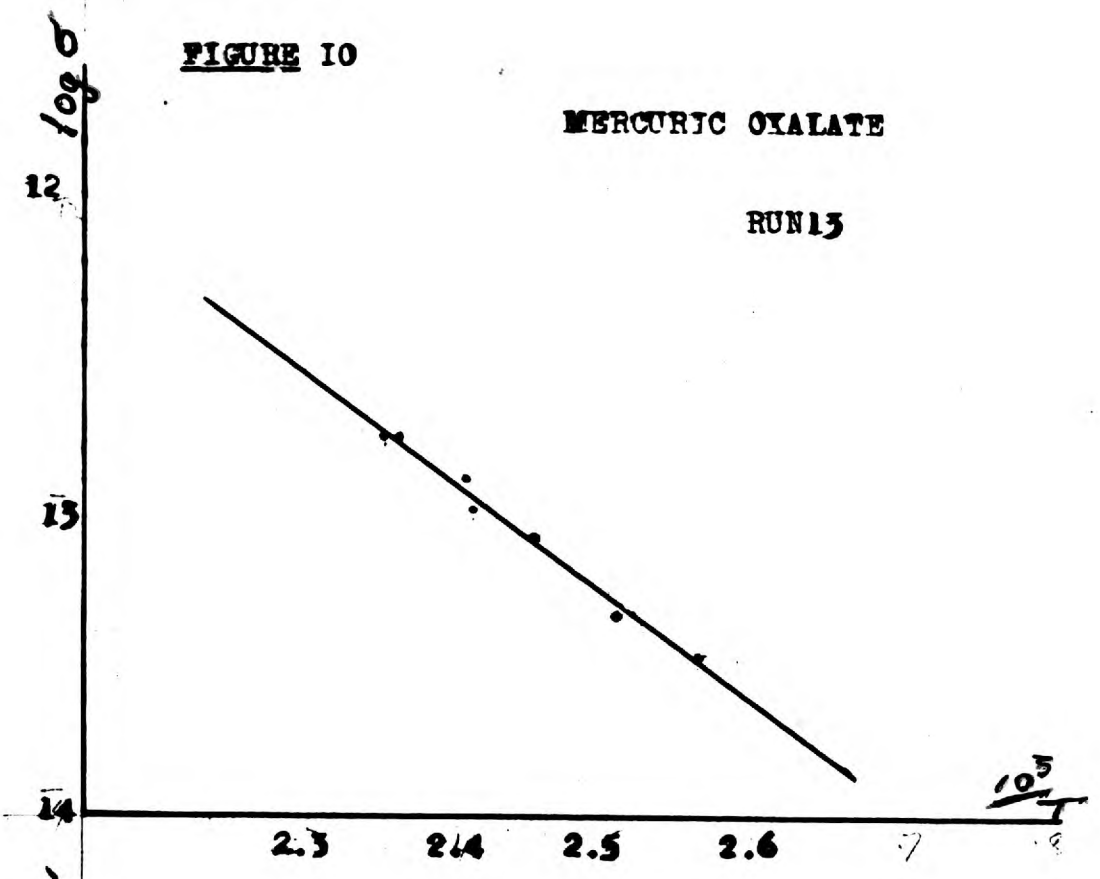
From the results the following constants were evaluated

Run	E. kcal.	log A
13	14.3	$\bar{7}.59$
14	14.2	$\bar{7}.57$

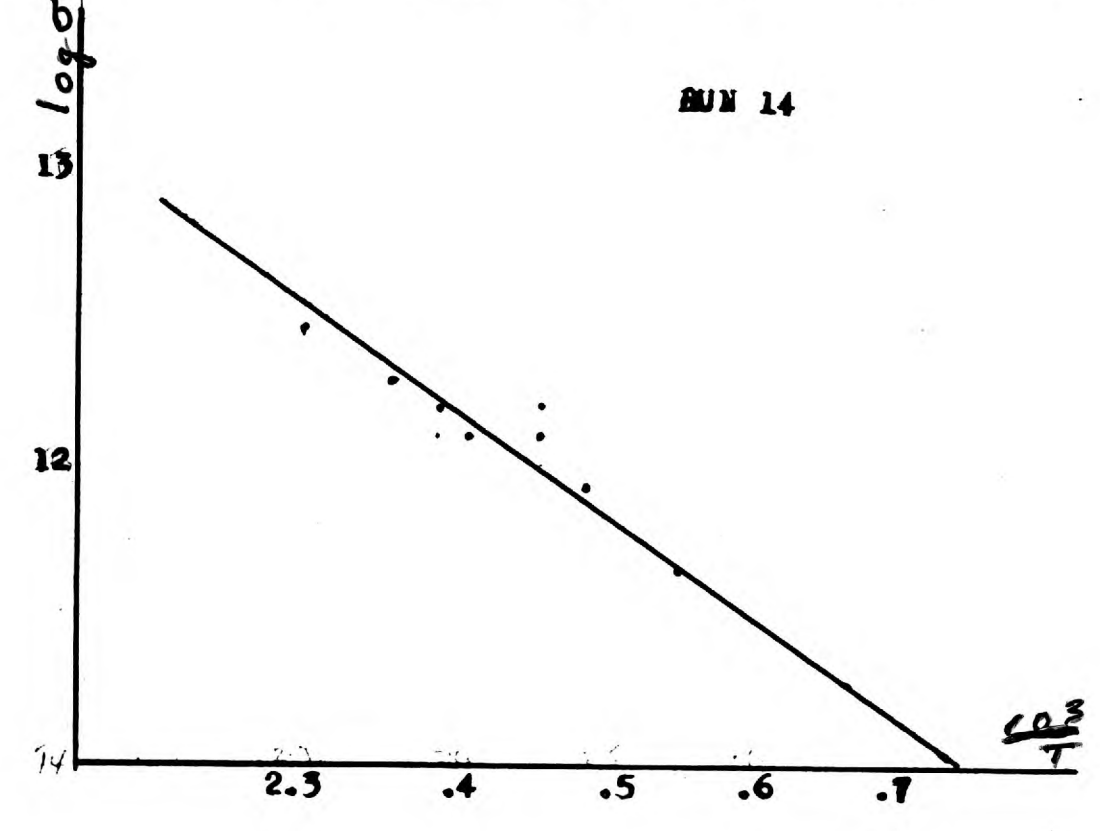
FIGURE 10

MERCURIC OXALATE

RUN 13



RUN 14



The conductance of mercuric oxalate is thus given by the following equation:

$$\log \sigma = -6.42 - \frac{14.150}{4.576} \frac{1}{T}$$

4. Thallous Oxalate

TABLE 10

Run 15 $l = .27$ cm.

$T^{\circ}K$	s	U	P	$\log \sigma$	$\frac{10^3}{T}$
324.8	1.204	.857	8	$\bar{1}0.38$	3.080
336.7	1.208	.901	8	$\bar{1}0.46$	2.970
362.0	1.212	1.036	8	$\bar{1}0.76$	2.762
380.1	1.209	1.058	8	$\bar{1}0.84$	2.631
377.4	1.209	1.079	8	$\bar{1}0.91$	2.650
369.0	1.210	1.018	8	$\bar{1}0.71$	2.710
356.1	1.208	1.037	8	$\bar{1}0.76$	2.808
356.0	1.207	.980	8	$\bar{1}0.63$	2.810

Run 16

TABLE 11

$l = .262$ cm

293.4	1.212	.247	8	$\bar{1}1.4$	3.408
310.6	1.202	.587	8	$\bar{1}1.97$	3.220
315.5	1.210	.662	8	$\bar{1}0.08$	3.170
327.0	1.210	.735	8	$\bar{1}0.18$	3.058
333.4	1.213	.814	8	$\bar{1}0.4$	3.00
342.5	1.211	.878	8	$\bar{1}0.4$	2.920
352.1	1.214	.940	8	$\bar{1}0.53$	2.840
357.3	1.212	.962	8	$\bar{1}0.58$	2.798
295.9	1.209	.130	8	$\bar{1}1.07$	3.380

FIGURE I2 Run I5

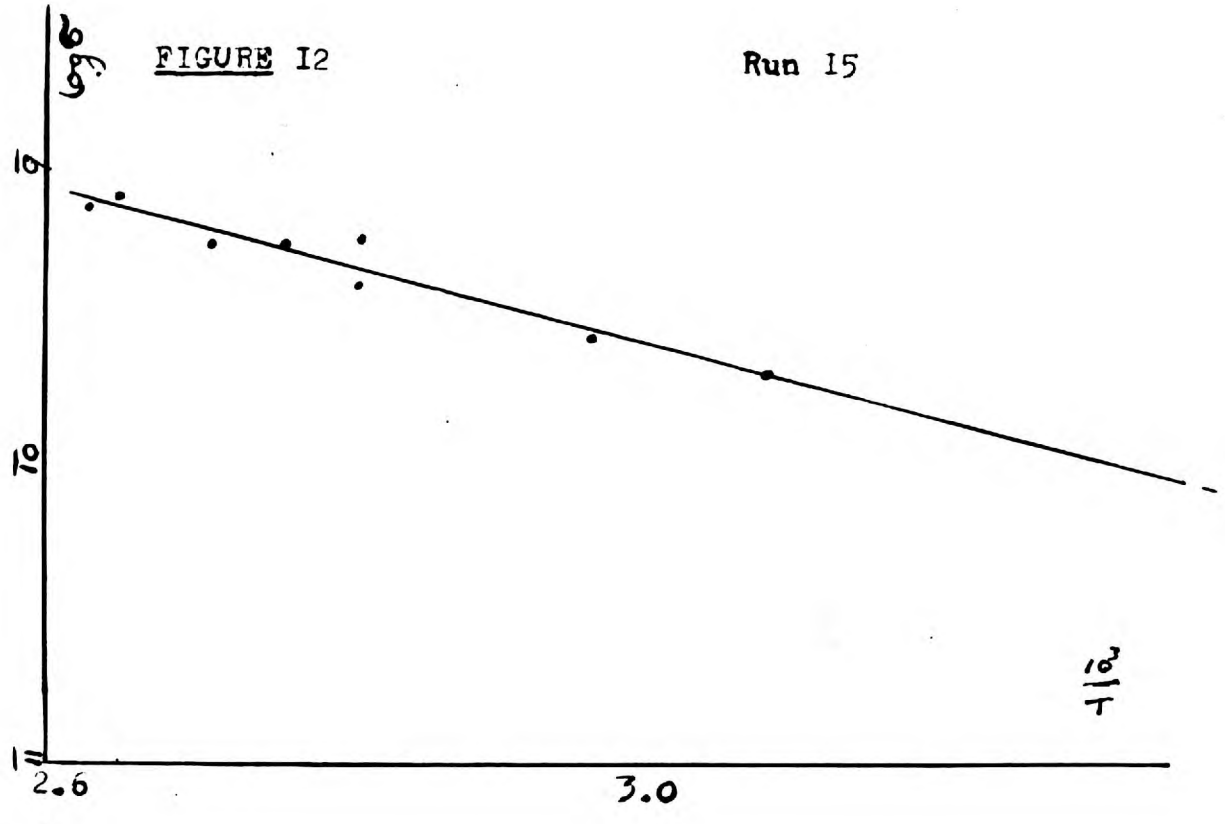
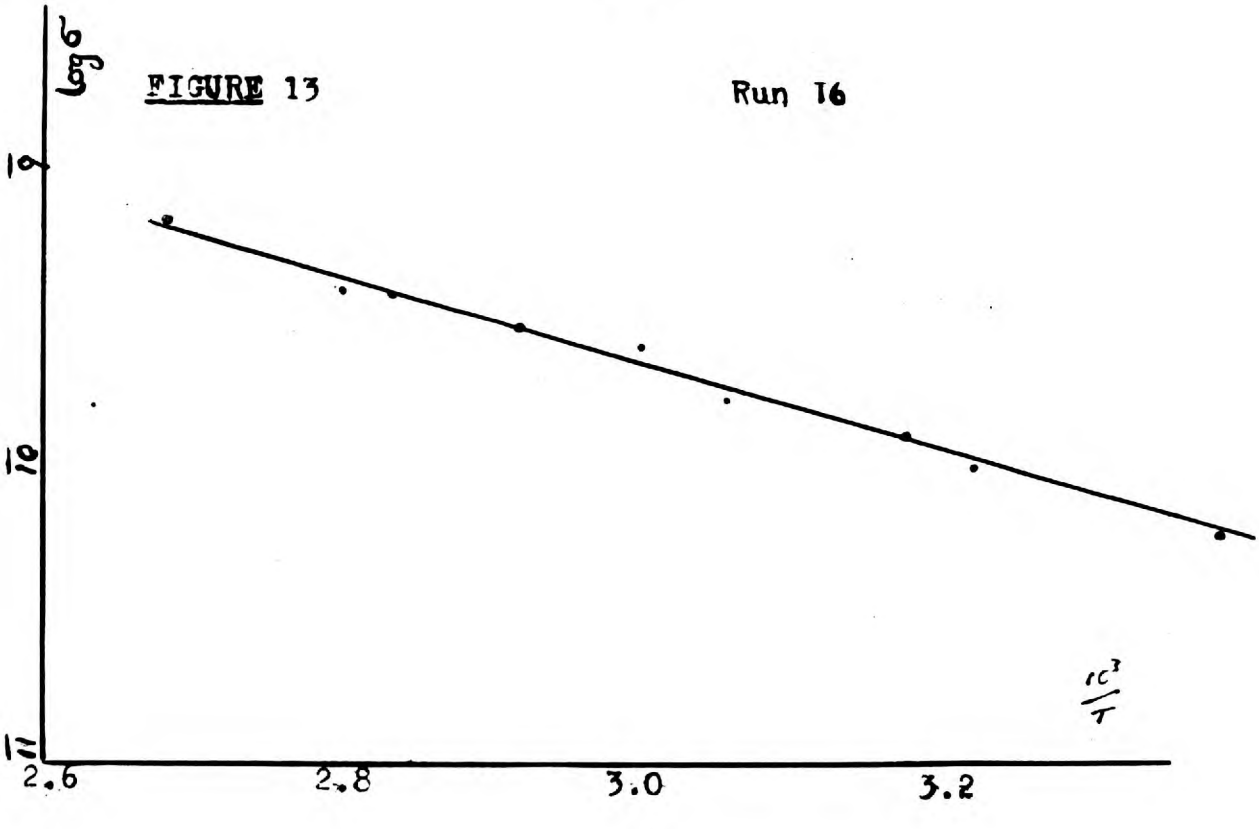


FIGURE 13 Run I6



At the end of run 15 the pellet of thallous oxalate, which had previously been quite translucent, appeared grey.

From these results the following constants were calculated

Run	E	log A
15	6.35	$\bar{7}.65$
16	5.96	$\bar{7}.49$

Hence the characteristic equation for thallous oxalate is:

$$\log \sigma = -6.43 - \frac{6.15.10^3}{4.576} \frac{1}{T}$$

The following results are for pellets of thallous oxalate made from samples prepared under different experimental conditions.

Run 17	Table 12	l = 0.22cm.	Run 18	Table 13	l = 0.25
T^oK	$\frac{10^3}{T}$	$\log \sigma$	T^oK	$\frac{10^3}{T}$	$\log \sigma$
305.8	3.270	$\bar{1}0.350$	298.5	3.350	$\bar{1}0.00$
320.5	3.120	$\bar{1}0.500$	305.3	3.275	$\bar{1}0.10$
339.6	2.950	$\bar{1}0.750$	329.5	3.035	$\bar{1}0.43$
362.9	2.755	$\bar{9}.025$	350.9	2.850	$\bar{1}0.58$
384.3	2.602	$\bar{9}.200$	369.7	2.705	$\bar{1}0.82$

FIGURE I2

Run I5

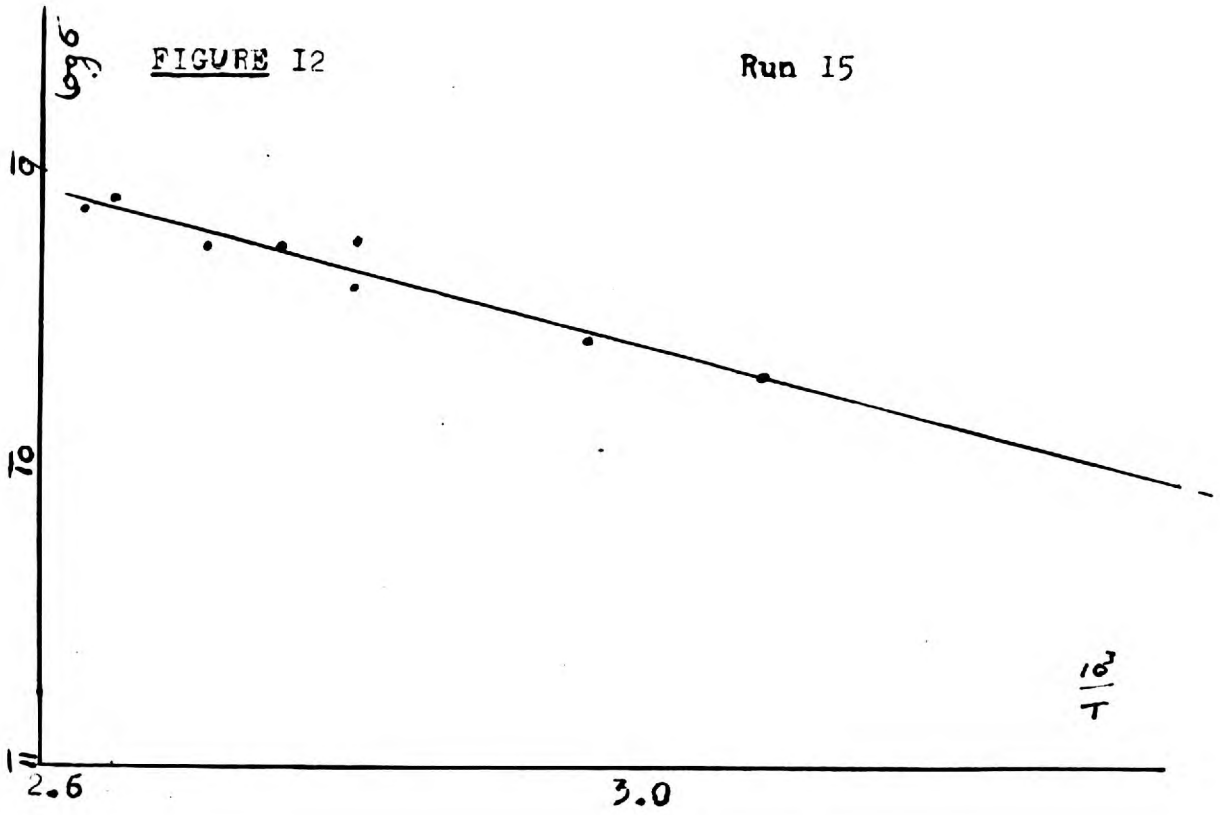
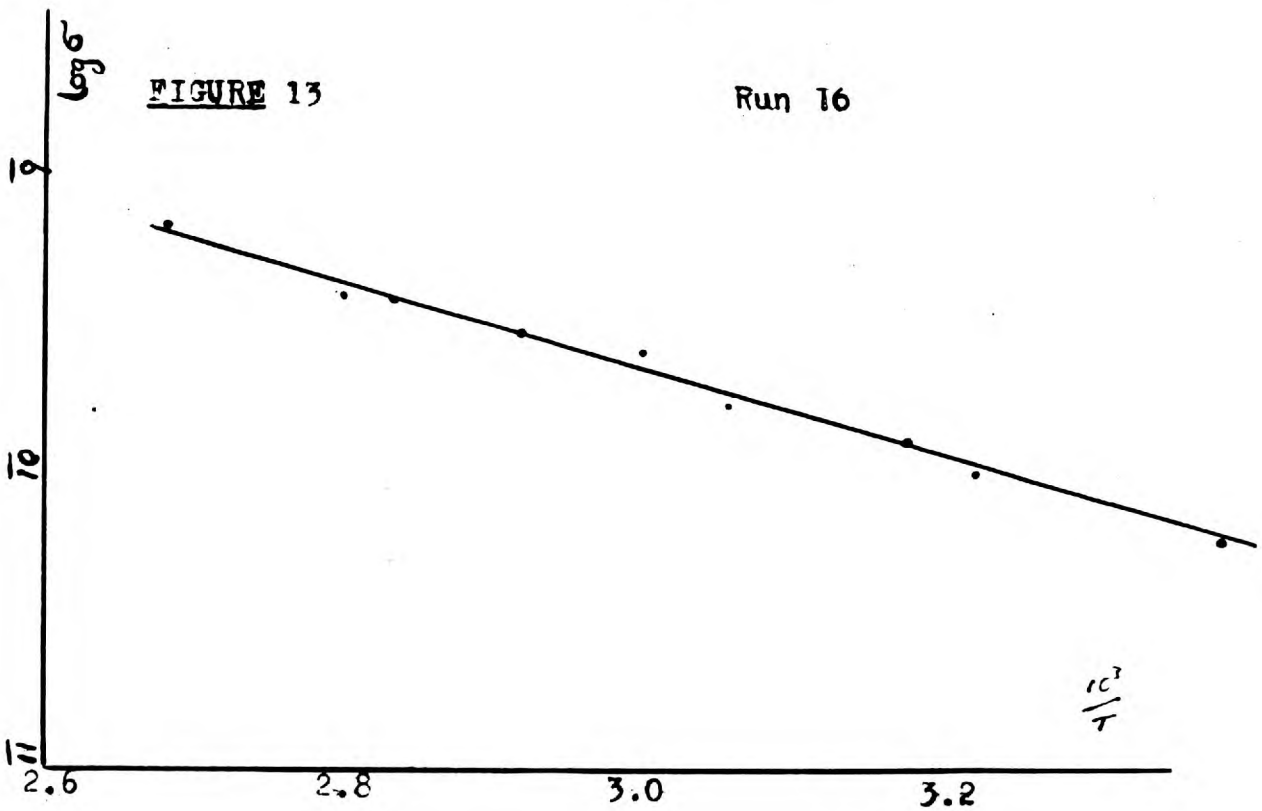


FIGURE 13

Run I6



Run 19 TABLE 14 l = 0.47 cm.

T°K	$\frac{10^3}{T}$	log σ
299.4	3.340	$\bar{1}1.70$
308.6	2.240	$\bar{1}1.82$
317.5	3.150	$\bar{1}1.98$
329.5	3.035	$\bar{1}0.075$
341.3	2.930	$\bar{1}0.20$
352.5	2.837	$\bar{1}0.32$
365.6	0.735	$\bar{1}0.425$

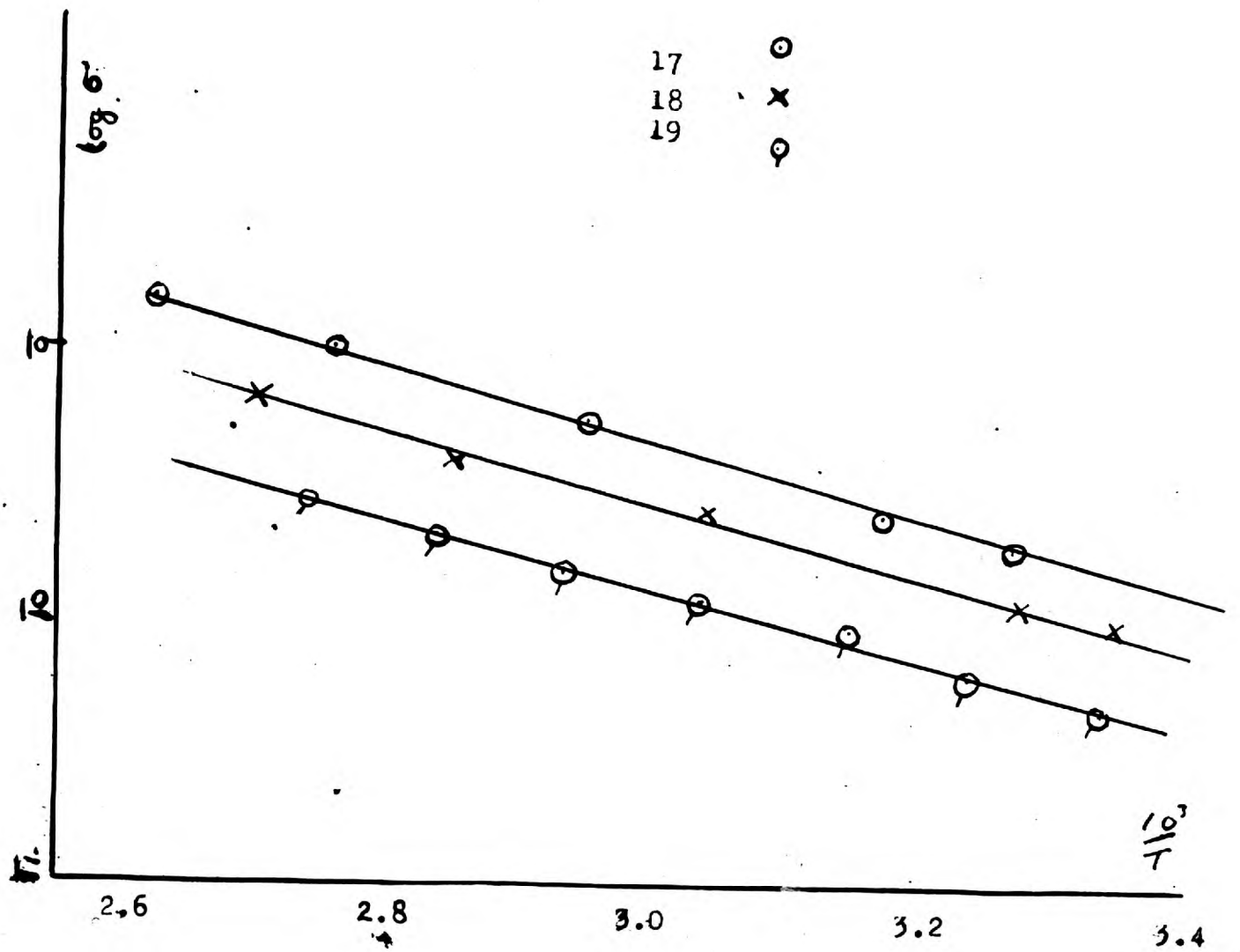
The values for E and A are collected in Table 15, and compared with the values obtained from the "stoicheiometric" pellet.

TABLE 15

Run	Preparation	E kcal	log A	Mean E	log A (Mean)
15	d i	6.35	$\bar{7}.65$	6.15	$\bar{7}.57$
16	d i	5.96	$\bar{7}.49$		
17	d ii	6.10	$\bar{7}.79$	5.77	
18	d iii (a)	5.50	$\bar{7}.11$		$\bar{7}.76$
19	d iii (b)	5.7	$\bar{7}.33$		

Thus the mean values of log A do not differ by as much as individual values for log A carried out under identical conditions.

Figure I4 Runs 17 to 19



5. Barium Oxalate

Run 20 TABLE 46 l = .210

$T^{o}K$	s	u	p	$\log \frac{1}{R}$	$\frac{10^3}{T}$
350.9	1.205	.540	10	$\bar{1}2.25$	285.0
370.3	1.200	1.63	10	$\bar{1}2.75$	270.0
400.0	1.208	.65	5	$\bar{1}1.25$	250.0
425.9	1.210	.518	3	$\bar{1}1.63$	235.2
408.2	1.205	.814	5	$\bar{1}1.37$	245.0
380.2	1.212	.393	5	$\bar{1}1.0$	263.0
357.1	1.205	.755	10	$\bar{1}2.4$	280.0

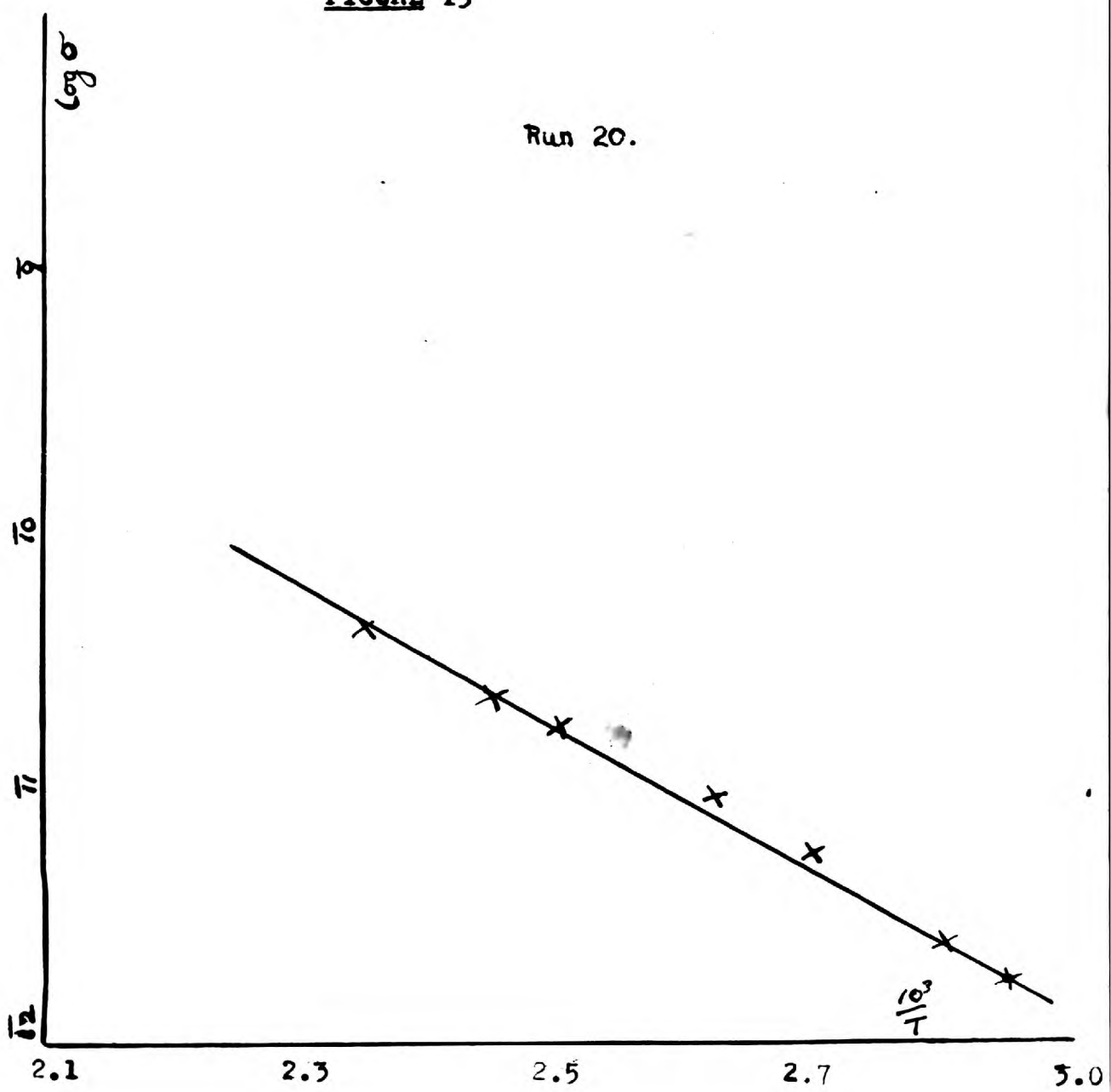
From these results the following constants were evaluated:

E kcal.	log A
18.7	$\bar{5}.71$

The specific conductance of barium azide is thus given by:

$$\log \sigma = -4.29 - \frac{18700}{4.576} \frac{1}{T}$$

FIGURE 15



PHOTOLYSIS RESULTS

1. Photolysis of Silver Oxalate

The photolysis of silver oxalate was carried out at temperatures ranging from -70°C to + 32°C, and at varying intensities.

The p - t curves were accurately linear, with slight acceleration. Gas evolution commenced immediately on switching on the light, and ceased on cessation of irradiation. The ratio obtained from any one sample were strictly reproducible within ± 1%, and it was not, therefore, found necessary to determine relative rates of photolysis.

A. Variation of Rate of Photolysis with Intensity

Runs 26 - 32 give the results obtained for photolysis at varying intensities, the cell being immersed throughout in a Dewar of melting ice. All runs were performed on the same sample without letting down the vacuum. The evolution of gas is given in units of 10^{-4} mm. of mercury. Rates of evolution, k_c are expressed in units of 10^{-6} mm. of carbon dioxide evolved in an apparatus volume of 705 cm^3 per minute, and are collected in Table (17). A curve relating ip, the primary lamp current, to k_c, together with a typical run, is given in Figure 18.

Run 26

$T = 1^{\circ}C$; $i_p = .40$ a.

t	p
2	.5
4	1.65
6	1.55
8	2.00
10	2.47
12	2.95
14	3.50
16	4.00
18	4.50
20	5.00
22	5.50
24	6.00
26	6.50
28	7.05
30	7.60
32	8.10
34	8.60
36	9.10
38	
40	

Run 27

$T = 1^{\circ}$; $i_p = .27$a.

t	p
0	0
2	.4
4	.75
6	1.05
8	1.37
10	1.70
12	2.40
14	2.37
16	2.75
18	3.10
20	3.40
22	3.80
24	4.15
26	4.50
28	4.85
30	5.18
32	5.5
34	5.85
36	6.25
38	6.57
40	6.96

Run 28

$T = 1^{\circ}$; $i_p = .18$a.

t	p
2	.22
4	.4
6	.65
8	.9
10	1.1
12	1.4
14	1.55
16	1.80
18	2.02
20	2.25
22	2.50
24	2.75
26	2.98
28	3.04
32	3.65
36	4.10
40	4.60
44	5.07
50	5.75

Run 29

$T = 1^{\circ}$; $i_p = .32$ a.

p	t
.4	2
.8	4
1.25	6
1.62	8
2.00	10
2.45	12
2.85	14
3.25	16
3.65	18
4.01	20
4.50	22
4.90	24
5.30	26
5.75	28
6.15	30
6.55	32
6.45	34
7.35	36
8.18	40
9.00	44

Run 30

$T = 1^{\circ}$; $i_p = .23$ a.

p	t
.3	2
.57	4
.85	6
1.10	8
1.40	10
1.70	12
1.95	14
2.25	16
2.55	18
2.82	20
3.40	24
3.95	28
4.50	32
5.10	36
5.70	40
6.22	44
6.80	48
7.37	52
7.95	56
8.55	60

Run 31

$T = 1^{\circ}$; $i_p = .15$

p	t
.20	2
.35	4
.55	6
.73	8
.92	10
1.10	12
1.30	14
1.50	16
1.70	18
1.85	20
2.25	24
2.65	28
3.00	32
3.40	36
3.80	40
4.20	44
4.55	48
4.95	52
5.35	56
5.70	60

Run 32

$T = 1^{o}$; $i_p = .1$ a.

p	t	p	t
.15	2	1.50	24
.25	4	1.75	28
.35	6	2.00	32
.45	8	2.25	36
.60	10	2.50	40
.72	12	3.75	44
.85	14	3.02	48
1.00	16	3.27	52
1.10	18	3.58	56
1.25	20	3.80	60

TABLE 18

Run	i_p a.	k_c mm^{-6}/ minute
26	.40	25.4
27	.27	17.3
28	.18	11.5
29	.32	20.4
30	.23	14.2
31	.15	9.6
32	.10	6.3

PHOTOLYSIS OF SILVER OXALATE

• — RUN 27

× — VARIATION OF i_p WITH RATE

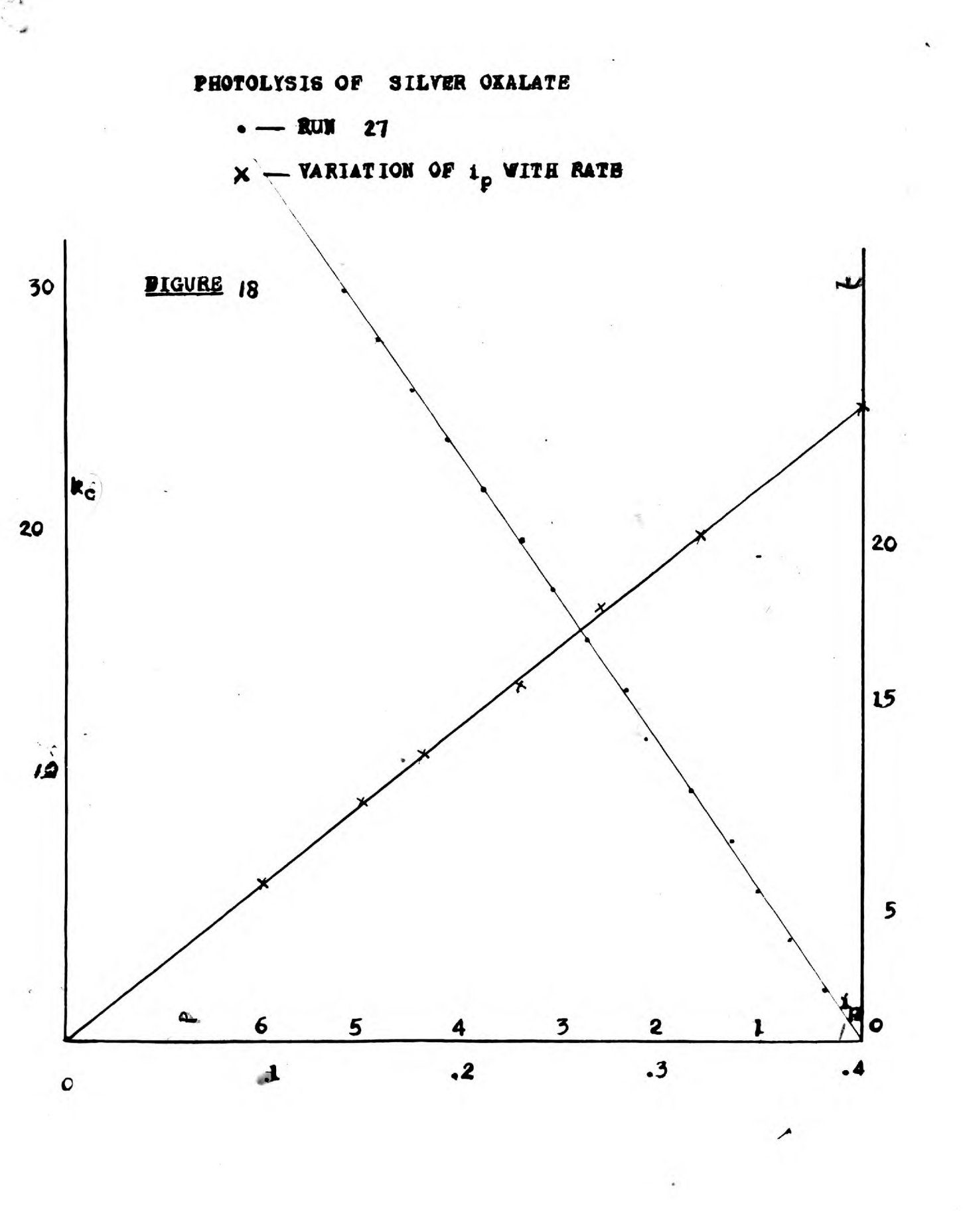


FIGURE 18

B. Variation of Rate of Photolysis with Temperature

The result of runs 33 to 43 show the influence of temperature on the rate of photolysis. The primary current was fixed at .40 amp. for runs 33 to 38, and at .27 amp. for runs 39 to 43. Values of k_c for different temperatures are collected in Table (19) and are plotted in Figure 9. From the graphs, the energy of activation of photolysis was found to be 920 and 882 cal.

Run 33 T = - 70°C

t	p
2	.25
4	.52
6	.8
8	1.1
10	1.35
14	1.95
18	2.51
22	3.07
26	3.65
30	4.2
34	4.75
38	5.34
42	5.9
46	6.47
50	7.05

Run 34 T = -40°

t	p
0	0
2	.3
4	.7
6	1.10
8	1.45
10	1.78
12	2.20
16	2.95
20	3.77
24	4.47
28	5.26
32	6.00
36	6.75
40	7.5
44	8.75

Run 35 T = -10

t	p
0	0
4	.9
8	1.85
10	2.30
12	2.80
16	3.75
20	4.75
24	5.72
28	6.68
32	7.66
36	8.60
40	9.60
44	10.55
48	
52	

Run 36

T = 1°C

p	t
0	0
2	.49
4	.95
6	1.45
8	1.95
10	2.45
12	2.96
14	3.47
16	3.97
18	4.47
20	5.00
22	5.50
24	6.00
26	6.50
28	7.00
30	7.50
32	8.05
34	8.60
36	9.10

Run 37

T = 25°

p	t
0	0
4	1.00
6	1.75
8	2.30
10	2.95
12	3.55
14	4.15
16	4.75
18	5.46
20	5.95
22	6.55
24	7.15
26	7.80
28	8.37
30	8.95
32	9.55
34	10.17

Run 38

T = 35°

p	t
2	.51
4	1.15
6	1.75
8	2.40
10	3.02
12	3.60
14	4.21
16	5.80
18	5.35
20	6.07
22	6.66
24	7.25
26	7.85
28	8.50
30	9.06
32	9.67
34	10.25
36	10.85
40	12.05

Run 39

T = -47°C

p	t
.25	2
.50	4
.75	6
1.02	8
1.25	10
1.50	12
2.05	16
2.60	20
3.10	24
3.60	28
4.10	32
4.62	36
5.15	40
5.65	44
6.15	48
6.68	52

Run 40

T = -11°

p	t
.3	2
.65	4
.95	6
1.25	8
1.60	10
1.90	2
2.52	16
3.20	20
3.80	24
4.45	28
5.07	32
5.70	36
6.35	40
7.00	44
7.60	48

Run 41

T = 1

p	t
.70	4
.95	8
2.15	12
2.85	16
3.55	20
4.25	24
5.00	28
5.70	32
6.40	36
7.10	40
7.80	44
8.55	48
9.25	52
9.97	56
10.70	60

Run 42

T = 22

t	p
2	.35
4	.80
6	1.20
8	1.60
10	2.00
12	2.08
16	3.20
20	4.00
24	4.80
28	5.60
32	6.42
36	7.20
40	8.00
44	8.80
48	9.60

Run 43

T = 38

t	p
2	.4
4	.85
6	1.30
8	1.75
10	2.15
12	2.55
16	3.45
20	4.30
24	5.15
28	6.00
32	6.90
36	7.75
40	8.60
44	9.47
48	10.35
50	10.75

TABLE 19

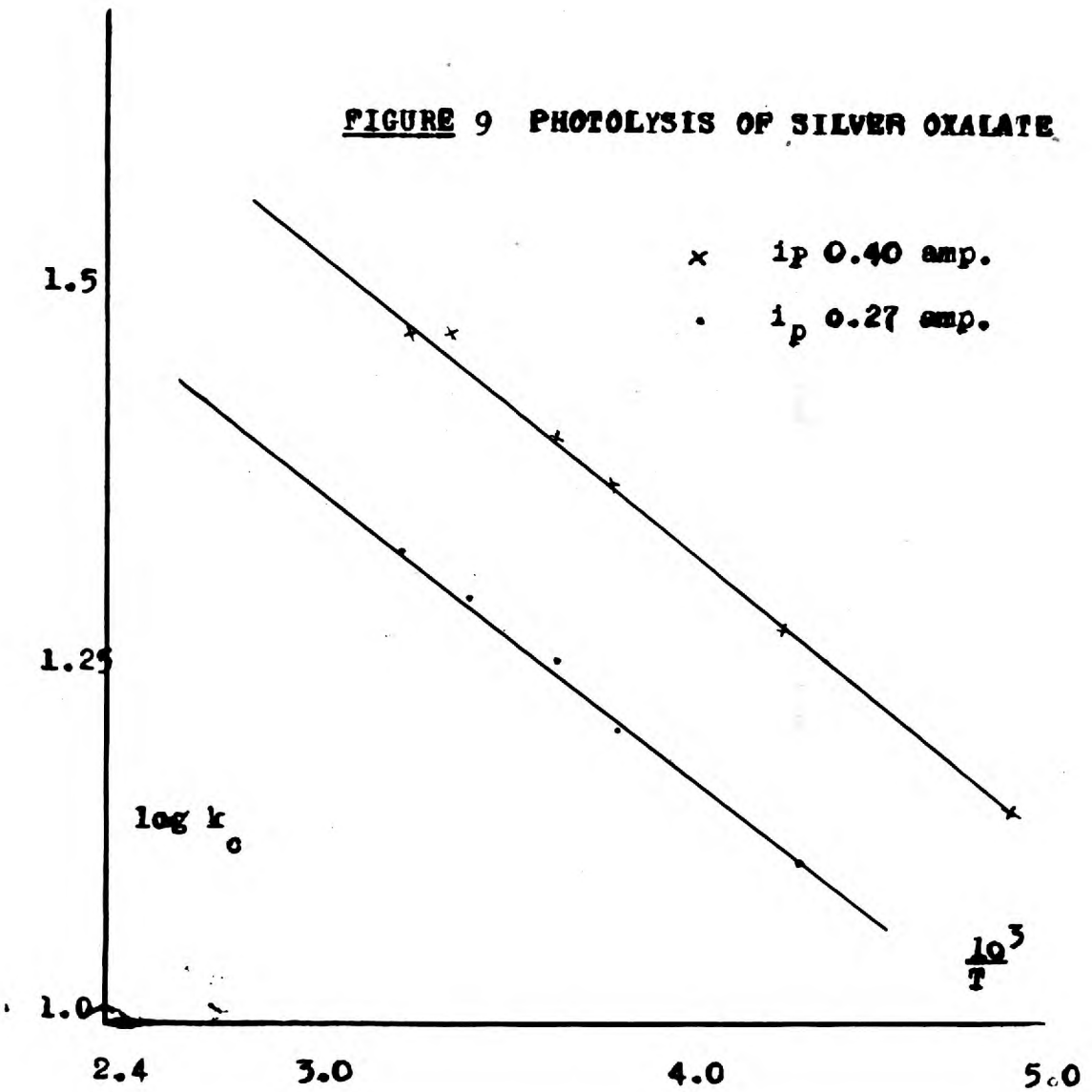
ip = .40 amp.

Run	T° C	T°K	$\frac{10^3}{T}$	kc	log kc.
33	-70.0	203	4.93	14.1	1.149
34	-40.0	233	4.29	18.8	1.274
35	-10.0	263	3.80	24.0	1.380
36	1.0	274	3.65	25.2	1.401
37	25.0	298	3.35	29.9	1.476
38	35.0	308	3.25	30.8	1.488

TABLE 20

ip = .27 amp.

39	-42.0	231	4.33	12.9	1.110
40	-11.0	262	3.82	15.9	1.201
41	1.0	274	3.65	17.8	1.250
42	22.0	295	3.39	20.0	1.301
43	38.0	311	3.21	21.6	1.334


FIGURE 9 PHOTOLYSIS OF SILVER OXALATE
× ip 0.40 amp.
• ip 0.27 amp.
1.5
1.25
1.0
log k
o
10³/T
2.4
3.0
4.0
5.0

2. Photolysis of Mercuric Oxalate

This was carried out in exactly the same manner as for silver oxalate. The rates of photolysis were lower than for the silver salt, but the activation energy of photolysis in the same temperature range, -70° to 33°, though still small, was much larger. As before, rates of photolysis were found to be reproducible to ± 1%, and were proportional to the square of the intensity of irradiation. During photolysis, the salt changed from a perfectly while to a light-brown colour.

Runs 44 to 48 show the variation of rate with intensity. Results are collected in Table (21) and plotted on Figure 11A

Runs 49 to 53 show the variation of rate with temperature. Results are plotted on Figure 11 and tabulated in Table (22). From the curve, the activation energy of photolysis is 1.55 kcal.

Run 44

ip = .4 amp.

t	p
0	0
2	.3
4	.7
6	1.15
8	1.57
10	2.00
12	2.35
16	3.20
20	4.00
24	4.80
28	5.57
32	6.50
36	7.20
40	8.00
44	8.80
48	9.60
52	
56	
60	

Run 45

ip = .32 amp.

t	p
2	.25
4	.55
6	.90
8	1.25
10	1.60
16	2.55
20	3.20
24	3.80
28	4.50
32	5.15
36	5.75
40	6.40
44	7.05
48	7.70
52	
56	
60	

Run 46

ip = ;22 amp.

t	p
2	.18
4	.40
8	.85
12	1.25
16	1.75
20	2.20
24	2.60
28	3.05
32	3.50
36	3.95
40	4.40
44	4.80
48	5.25
52	5.70
56	6.15
60	6.60

Run 47

ip = .15

t	p
2	.10
4	.25
8	1.56
12	0.90
16	1.20
20	1.50
24	1.80
28	2.10
32	2.40
36	2.70
40	3.00
44	3.35
48	3.60
52	3.95
56	4.25
60	4.55

Run 48

ip = .11

t	p
4	.18
8	.40
12	.65
16	.85
20	1.05
24	1.25
28	1.50
32	1.70
36	1.95
40	2.13
44	2.37
48	2.60
52	2.80
56	3.05
60	3.25

Run 49

T = -40°C

t	p
2	.2
4	.4
8	.9
12	1.4
16	1.85
20	2.35
24	2.80
28	3.25
32	3.75
36	4.20
40	4.67
44	5.15
48	5.6
52	6.1
56	6.55
60	7.05

Run 50

T = -18°

t	p
2	.2
4	.52
8	1.20
12	1.80
16	2.45
20	3.05
24	3.64
28	4.30
32	4.90
36	5.50
40	6.10
44	6.75
48	7.35
52	7.97
60	9.15

Run 51

T = 1°

t	p
2	.23
4	.65
6	1.10
8	1.50
10	1.90
12	2.30
16	3.05
20	3.85
24	4.65
28	5.44
32	6.20
36	7.00
40	7.80
44	8.57
48	9.35

Run 52

$T = 22^{\circ}$

t	p
2	.45
4	.76
8	1.85
10	2.35
12	2.80
16	3.80
20	4.75
24	5.70
28	6.70
32	7.65
36	8.60
40	9.60

Run 53

$T = 33^{\circ}$

t	p
2	.51
4	.90
6	1.45
8	2.00
10	2.50
12	3.00
14	3.53
16	4.05
18	4.55
20	5.10
24	6.10
28	7.15
30	7.64
34	8.70

TABLE 2.1 T = 1°C

Run	ip	kc mm^{-6}/minute
44	.40	20.0
45	.32	16.1
46	.22	11.0
47	.15	7.6
48	.11	5.4

TABLE 2.2

ip amp.	Run	T°C	T°K	$\frac{10^3}{T}$	k	log k
.40	49	-40	233	4.29	11.7	1.07
.40	50	-18	255	3.92	15.31	1.103
.40	51	1	274	3.65	19.5	1.29
.40	52	22	295	3.39	24.0	1.38
.40	53	33	306	3.27	25.7	1.41

FIGURE II MERCURIC OXALATE

VARIATION OF RATE WITH TEMPERATURE

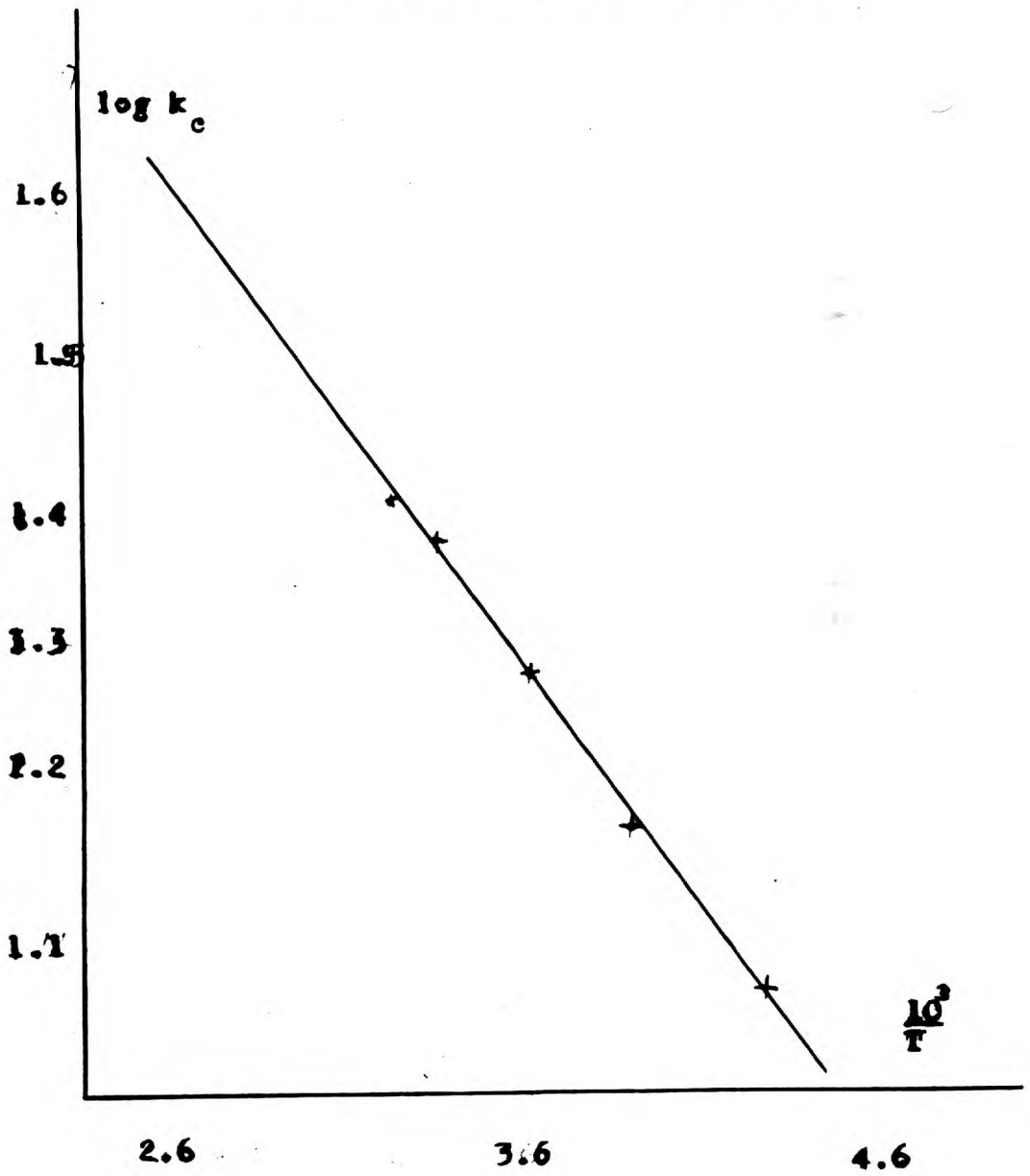
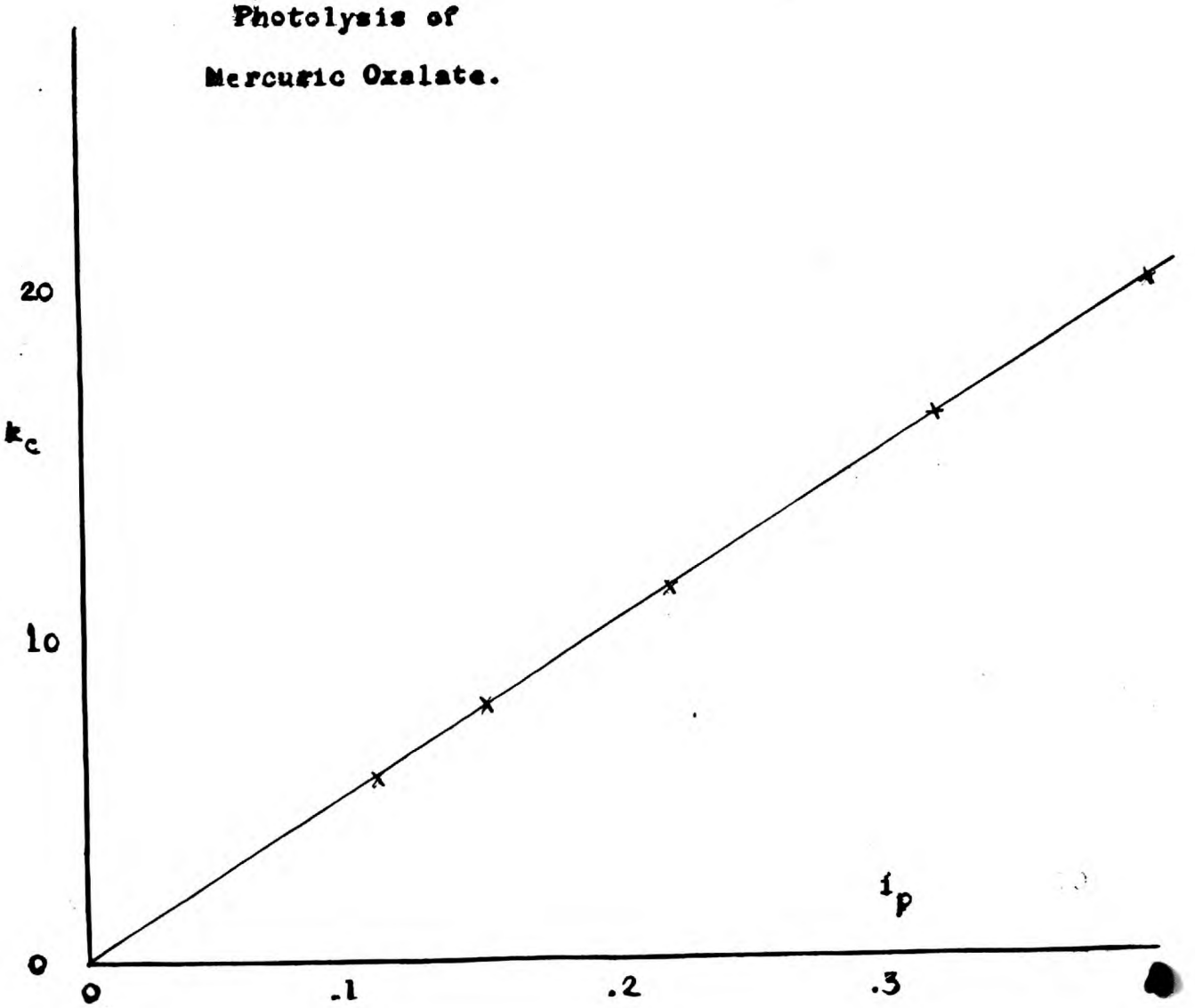


FIGURE 1

Photolysis of

Mercuric Oxalate.



3. Photolysis of Lead Oxalate

It was found that the photolysis rates obtained from lead oxalate were not strictly reproducible over a long period of time. Two effects contributing to this were distinguished: A) The rates of gas evolution, though at first linear, decreased progressively after ca. thirty minutes irradiation. It was found that if the sample were pumped for some hours and again irradiated, the constant rate was reproduced.

B) After prolonged photolysis, the oxalate layer became quite brown, and the rate of photolysis decreased steadily, finally reaching a very small constant value. Further irradiation and pumping had no effect on the rate. It was not found possible to reproduce the time taken to reach this saturation stage, but the onset of the reduced rate occured after ca. 3½ to 4½ hours irradiation at a lamp current of .4 amp. The irradiation of rate with intensity was, therefore, investigated with runs of short duration, (~20 minutes). At the end of the series of runs the original rate at the first intensity used was measured to check whether or not the effect had become operative. Due to the low rates of photolysis, measurements below 0°C were of insufficient accuracy to permit the temperature variation

to be studied. Results of runs 54 to 59 are summarised in Table (23) and plotted in Figure 15. As for the silver and mercuric salts, the rate of reaction was proportional to the square of the intensity of irradiation.

Run 54

ip = .42 amp.

t	p
1	-
2	.20
3	.31
4	.50
5	.70
6	.81
7	.95
8	1.10
10	1.37
12	1.65
14	1.92
16	2.20
18	2.50
20	2.76

Run 55

ip = .31

t	p
2	.20
3	.34
4	.40
6	.65
8	.85
10	1.05
12	1.28
14	1.50
16	1.70
18	1.90
20	2.15
2	

Run 56

ip = .23

t	p
2	.15
4	.30
6	.45
8	.60
10	.75
12	.87
14	1.00
16	1.15
18	1.32
20	1.47

Run 57

ip = .20 amp.

t	p
1	(.05)
2	.1
3	.2
4	.25
6	.40
8	.51
10	.65
12	.80
14	.941
16	1.05
18	1.15
20	1.30

Run 58

ip = .15

t	p
2	0.10
4	.17
6	.25
8	.37
10	.45
12	.55
14	.65
16	.74
18	.82
20	.96

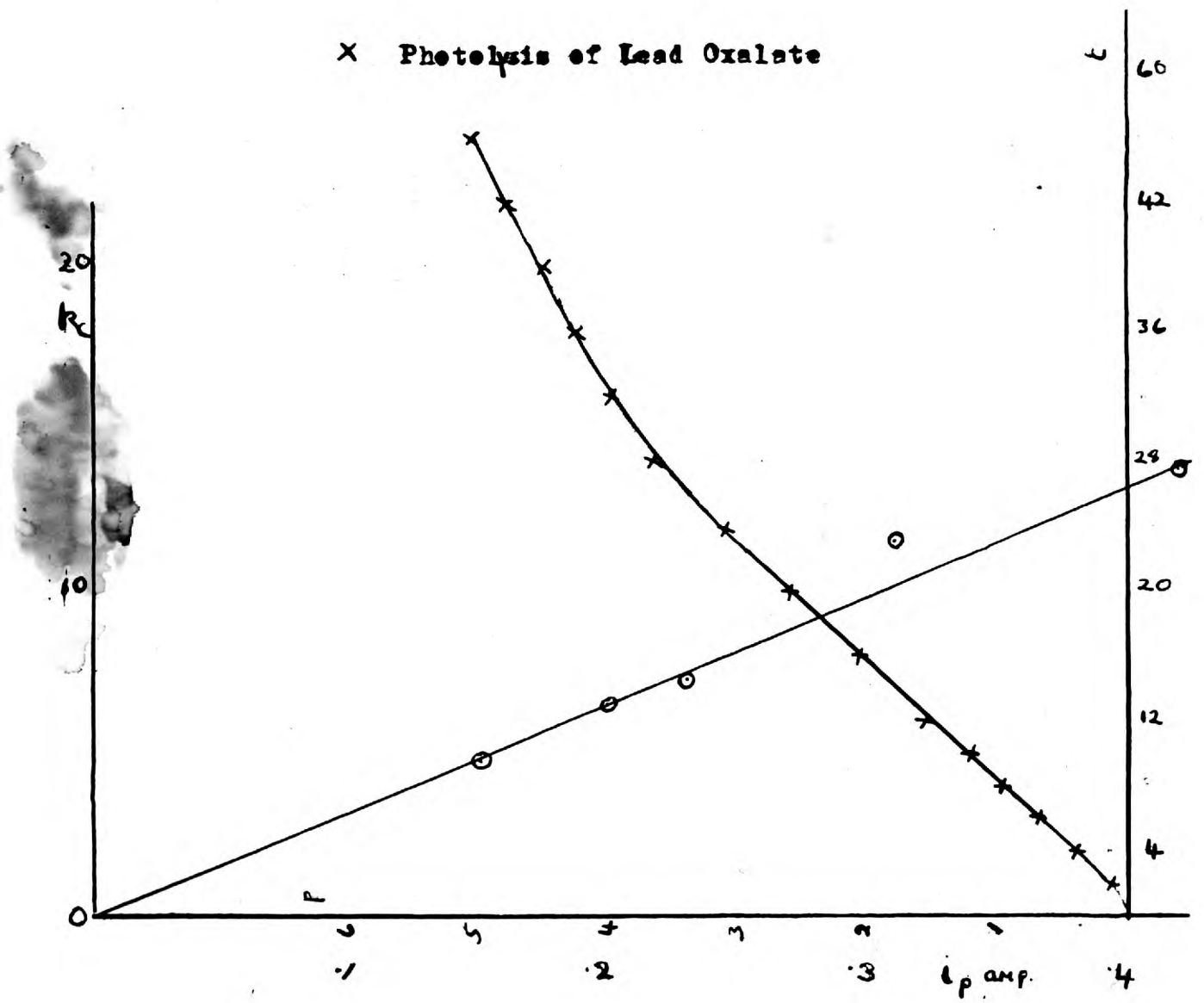
23

Run	ip	Rate mm^{-6}
54	.42	13.8
55	.31	10.4
56	.23	7.3
57	.20	6.5
58	.45	4.8
59	.42	13.8

FIGURE 15.

⊙ Variation of rate with intensity

× Photolysis of Lead Oxalate



Thermal Decomposition of Silver Oxalate

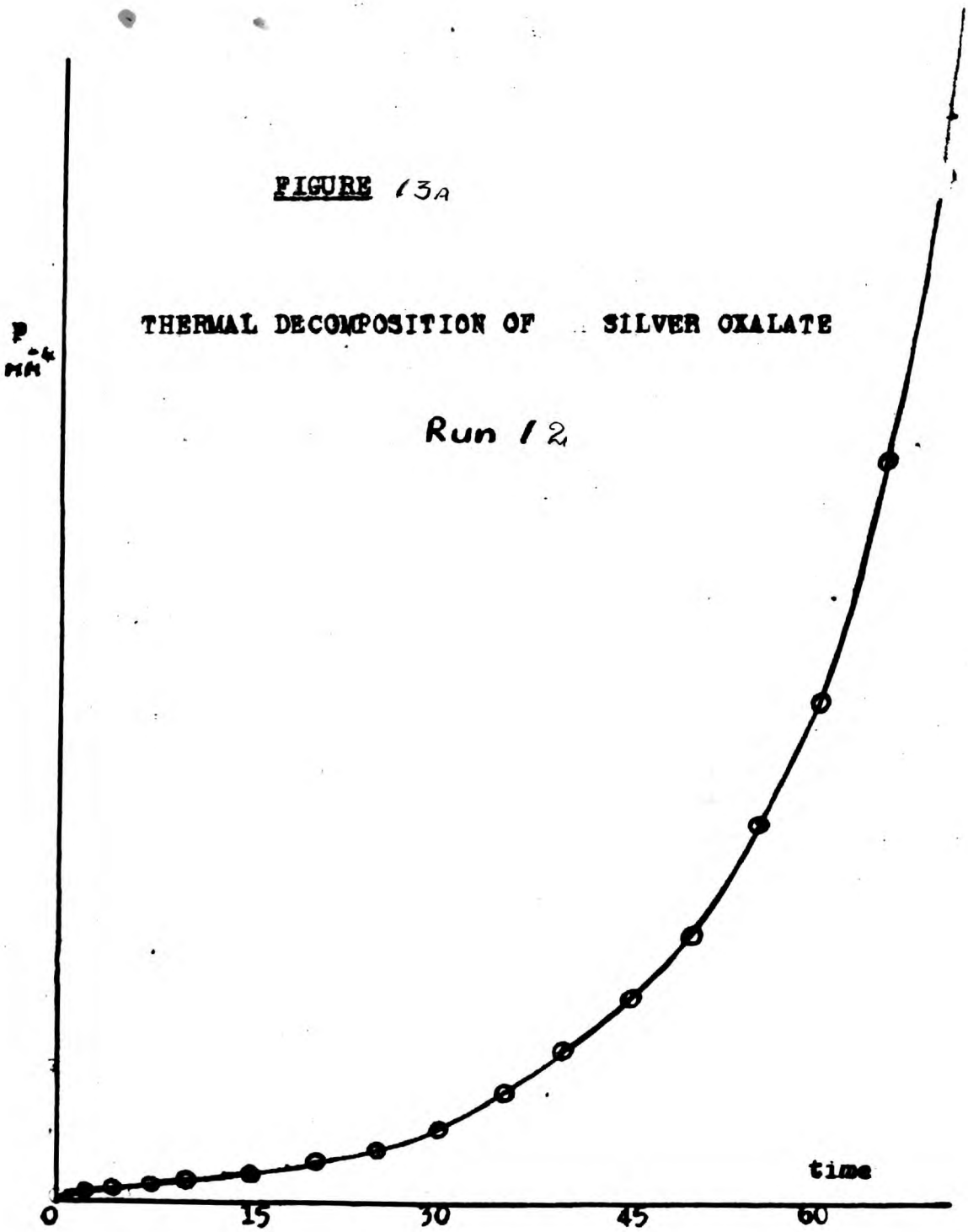
The thermal decomposition of silver oxalate was investigated over the temperature range 105° to 125° C. In runs 7 to 12 are shown the results obtained for decompositions on a "stoicheiometric" sample. A typical curve is shown in Figure 13. It was found that the p-t curves were well fitted after the first five minutes by an expression of the form $p = Ce^{kt}$ where t = time, and C, k, are constants. Graphs of log p-t for two runs are shown in Figure 13, and are linear throughout the range of decomposition studied, viz. up to ca. 30% decomposition.

The constant k was reproducible to within $\pm$ 2% at constant temperature for samples of oxalate selected from the same preparation. The constant C was found to be sensitive to pre-irradiation; this effect was studied later. For an unirradiated sample, C varied slightly from run to run. However, since the value of C was very small, this variation has little effect on the subsequent decomposition. Constants from runs 7 to 12 are collected in Table (24) and plotted in Figure 14A. From the graph an activation energy of 27.5 kcal. was derived. Pressure readings are given throughout in units of 10^{-4} mm. of mercury. Time readings are given in minutes.

FIGURE 13A

THERMAL DECOMPOSITION OF SILVER OXALATE

Run 12



Run 7. T = 108°C

t	p	log P
0	0	0
2	.16	$\bar{5}$.20
4	.19	$\bar{5}$.28
6	.21	$\bar{5}$.32
8	.22	$\bar{5}$.34
10	.23	$\bar{5}$.36
15	.25	$\bar{5}$.40
20	.27	$\bar{5}$.43
25	.30	$\bar{5}$.48
30	.32	$\bar{5}$.50
40	.42	$\bar{5}$.62
50	.44	$\bar{5}$.64
60	.57	$\bar{5}$.76
70	.76	$\bar{5}$.88
80	.83	$\bar{5}$.92
100	1.3	$\bar{4}$.11
120	1.9	$\bar{4}$.28
140	2.75	$\bar{4}$.44
160	4.0	$\bar{4}$.60
180	5.75	$\bar{4}$.76
200	9.12	$\bar{4}$.96
20	13.2	$\bar{3}$.12

Run 8. T = 112°

t	p	log P
0	0	0
2	0.18	$\bar{5}$.26
4	0.20	$\bar{5}$.30
6	0.22	$\bar{5}$.34
8	0.25	$\bar{5}$.40
10	0.26	$\bar{5}$.42
15	0.29	$\bar{5}$.46
20	0.35	$\bar{5}$.54
30	0.50	$\bar{5}$.70
40	0.66	$\bar{5}$.82
50	0.87	$\bar{5}$.94
60	1.23	$\bar{4}$.09
70	1.62	$\bar{4}$.21
80	2.24	$\bar{4}$.35
90	3.02	$\bar{4}$.48
100	4.01	$\bar{4}$.60
120	7.94	$\bar{4}$.90
140	14.4	$\bar{3}$.16
160	25.7	$\bar{3}$.41
180	44.7	$\bar{3}$.65
200	87.1	$\bar{3}$.94

Run 9 T = 113.7°

t	p	log t
2	.19	$\bar{5}.28$
6	.22	$\bar{5}.34$
10	.26	$\bar{5}.42$
15	.32	$\bar{5}.50$
20	.40	$\bar{5}.60$
25	.50	$\bar{5}.70$
30	.62	$\bar{5}.79$
40	.85	$\bar{5}.93$
50	1.15	$\bar{4}.04$
60	1.82	$\bar{4}.36$
70	2.51	$\bar{4}.40$
80	3.31	$\bar{4}.52$
90	5.01	$\bar{4}.70$
100	7.76	$\bar{4}.89$
110	10.2	$\bar{3}.01$
120	15.5	$\bar{3}.19$
130	21.3	$\bar{3}.33$
140	31.6	$\bar{3}.50$

Run 11 T = 118°

t	p	log P
2	.16	$\bar{5}.2$
5	.220	$\bar{5}.34$.
10	.29	$\bar{5}.46$.
15	.38	$\bar{5}.58$.
20	.47	$\bar{5}.67$.
30	.81	$\bar{5}.91$.
40	1.32	$\bar{4}.12$.
50	2.01	$\bar{4}.30$.
60	2.85	$\bar{4}.46$.
70	5.50	$\bar{4}.74$.
80	8.51	$\bar{4}.93$.
90	113.2.	$\bar{3}.12$.
100	22.4.	$\bar{3}.35$.
110	34.7.	$\bar{3}.54$.
120	52.4.	$\bar{3}.72$.
130	87.0.	$\bar{3}.94$.

Run 10 T = 116°

t	p	log p
10	.29	$\bar{5}.46$
15	.32	$\bar{5}.50$
20	.39	$\bar{5}.60$
25	.46	$\bar{5}.66$
30	.60	$\bar{5}.78$
35	.69	$\bar{5}.84$
40	.91	$\bar{5}.96$
50	1.32	$\bar{4}.13$
60	2.00	$\bar{4}.30$
70	2.69	$\bar{4}.43$
80	4.57	$\bar{4}.66$
90	7.24	$\bar{4}.86$
100	10.00	$\bar{3}.00$
110	15.5	$\bar{3}.19$
120	24.5	$\bar{3}.39$
130	33.9	$\bar{3}.53$
140	53.7	$\bar{3}.73$
150	75.8	$\bar{3}.88$

Run 12 T = 119.9°

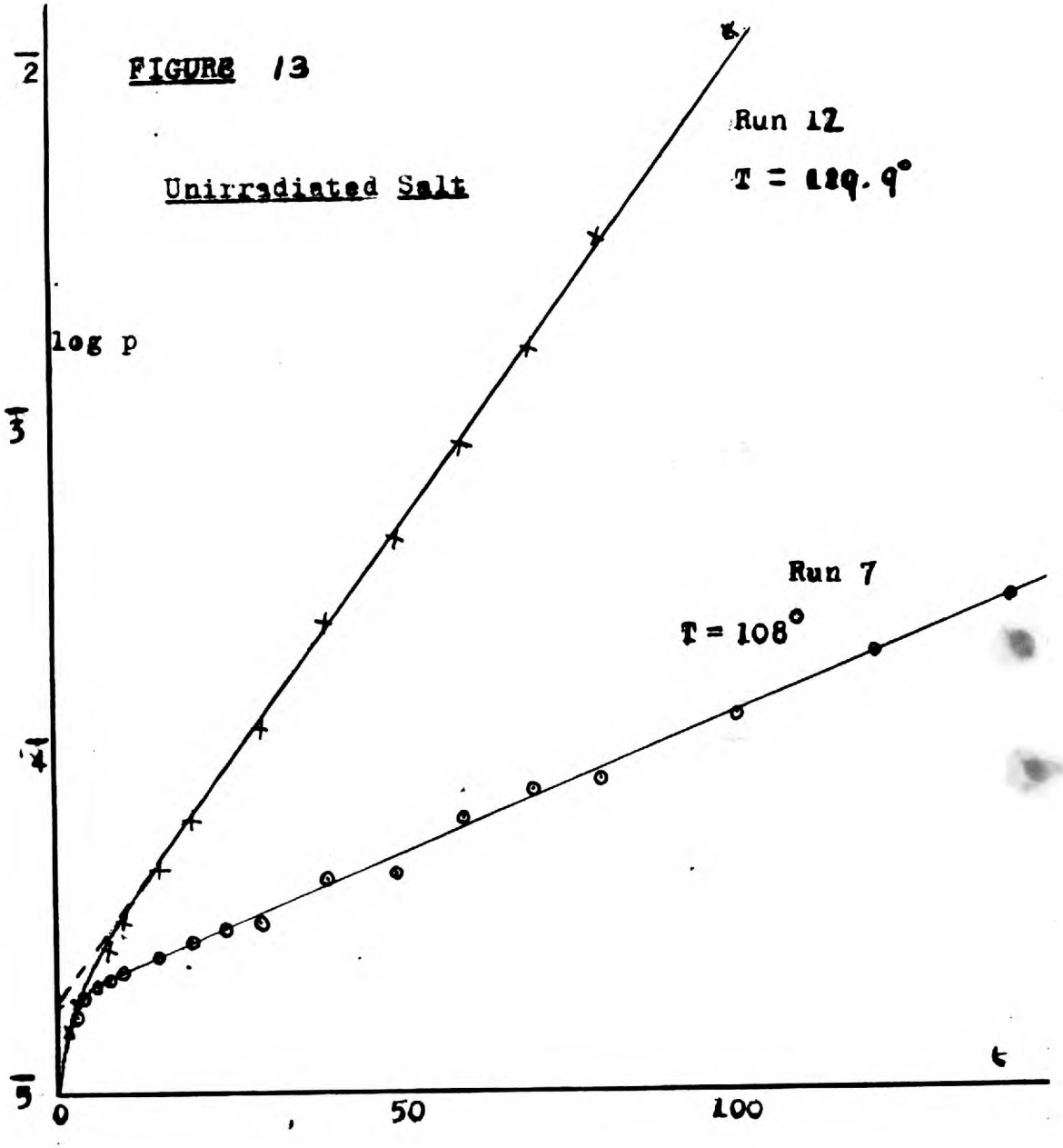
t	p	log p
0	0	0
2	.18	$\bar{5}.26$
4	.22	$\bar{5}.34$
8	.26	$\bar{5}.47$
10	.31	$\bar{5}.50$
15	.46	$\bar{5}.66$
20	.63	$\bar{5}.80$
25	0.80	$\bar{5}.90$
30	1.17	$\bar{4}.07$
35	1.80	$\bar{4}.26$
40	2.40	$\bar{4}.38$
45	3.21	$\bar{4}.50$
50	4.26	$\bar{4}.63$
55	6.00	$\bar{4}.78$
60	7.94	$\bar{4}.90$
65	11.70	$\bar{3}.07$
70	16.22	$\bar{3}.21$
80	31.60	$\bar{3}.50$
90	55.00	$\bar{3}.74$
100	126.0	$\bar{2}.10$

Run 7a T = 108°

t	p	log P	t	p	log P
10	.20	$\bar{5}$.30	70	.71	$\bar{5}$.81
15	.24	$\bar{5}$.38	75	.80	$\bar{5}$.90
20	.26	$\bar{5}$.41	80	.90	$\bar{5}$.96
25	.30	$\bar{5}$.48	85	1.00	$\bar{4}$.00
30	.31	$\bar{5}$.50	90	1.1	$\bar{4}$.04
35	.37	$\bar{5}$.57	100	1.13	$\bar{4}$.13
40	.40	$\bar{5}$.60	110	1.16	$\bar{4}$.21
45	.45	$\bar{5}$.65	120	2.00	$\bar{4}$.30
50	.48	$\bar{5}$.68	130	2.40	$\bar{4}$.38
55	.55	$\bar{5}$.74	140	2.95	$\bar{4}$.47
65	.66	$\bar{5}$.82	160	4.36	$\bar{4}$.64
			200	9.55	$\bar{4}$.98

TABLE 24

Run	T°C	T°K	$\frac{10^3}{T}$	k.10^3	log k.
7a	108	381.8	262.5	8.69	$\bar{3}$.94
7	108	381.8	262.5	8.51	$\bar{3}$.93
8	112	385.0	259.7	13.2	$\bar{2}$.12
10	116	389.0	257.1	17.8	$\bar{2}$.25
11	118	391.0	255.8	20.9	$\bar{2}$.32
12	119.9	392.9	254.5	25.8	$\bar{2}$.46
9	113.7	386.7	258.6	15.5	$\bar{2}$.19


FIGURE 13
Unirradiated Salt
Run 12
T = 129.9°
log p
Run 7
T = 108°
t
0
50
100

THERMAL DECOMPOSITION OF SILVER OXALATE

VARIATION OF RATE WITH TEMPERATURE

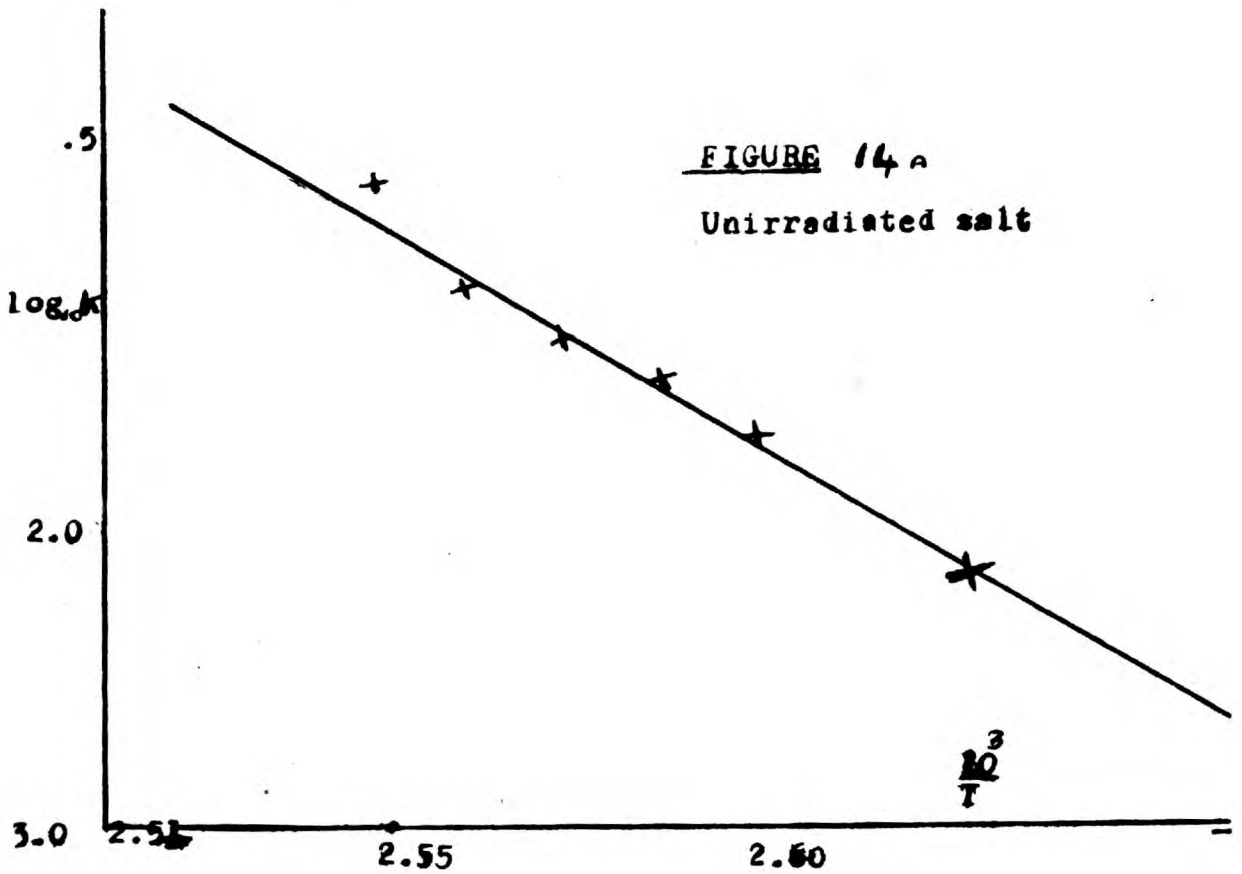


FIGURE 14 a

Unirradiated salt

A series of runs at various temperatures on specimens which had been irradiated for a constant time was performed (Runs 1-6). The curves followed the same course as for unirradiated salt, the plots of log p-t being linear. Values of log C were almost constant throughout the series of runs, the value being larger than for unirradiated salt. Results are given in Table (26) and are plotted in Figure 16. An activation energy of 28.2 kcal. is reported. Plots of typical runs are shown in Figure 15A

In runs 1 to 5, all samples of silver oxalate were irradiated for 5 minutes at a primary lamp current of 0.2 amp.

T = 106 Run 5

t	p	log p
0	0	0
2	.44	$\bar{5}.64$
4	.52	$\bar{5}.72$
6	.60	$\bar{5}.78$
8	.66	$\bar{5}.82$
10	.72	$\bar{5}.86$
15	.85	$\bar{5}.93$
20	.93	$\bar{5}.97$
30	1.14	$\bar{4}.06$
40	1.32	$\bar{4}.12$
50	1.66	$\bar{4}.22$
60	1.91	$\bar{4}.28$
70	2.09	$\bar{4}.32$
80	2.51	$\bar{4}.41$
90	3.02	$\bar{4}.48$
100	3.63	$\bar{4}.56$
110	4.17	$\bar{4}.62$
120	5.13	$\bar{4}.71$
130	6.02	$\bar{4}.78$
140	7.24	$\bar{4}.86$
160	10.2	$\bar{3}.01$
180	14.1	$\bar{3}.15$
200	19.1	$\bar{3}.28$

T = 105.5 Run 1

t	p	log p
10	.72	$\bar{5}.86$
20	.91	$\bar{5}.96$
40	1.26	$\bar{4}.10$
60	1.66	$\bar{4}.22$
80	2.29	$\bar{4}.36$
100	3.02	$\bar{4}.48$
120	3.98	$\bar{4}.60$
130	5.25	$\bar{4}.72$
140	5.49	$\bar{4}.74$
150	6.02	$\bar{4}.78$
160	7.24	$\bar{4}.86$
170	8.51	$\bar{4}.93$
180	10.0	$\bar{3}.00$
200	13.5	$\bar{3}.13$

Run 3 T = 114.0			Run 4 T = 110°		
t	p	log p	t	p	log p
0	0	$\bar{\infty}$.0	0	0	$\bar{\infty}$
2	.630	5.80	2	.52	$\bar{5}$.72
4	.690	5.84	4	.57	5.76
6	.79	5.90			
8	.871	5.94	8	.72	$\bar{5}$.86
10	.98	5.99	10	.79	5.90
15	1.15	$\bar{4}$.06	15	.91	$\bar{5}$.96
20	1.31	$\bar{4}$.12	20	1.00	$\bar{4}$.00
25	1.62	$\bar{4}$.21	28	1.31	$\bar{4}$.12
30	1.91	$\bar{4}$.28	36	1.55	$\bar{4}$.19
35	2.40	$\bar{4}$.38	44	1.91	$\bar{4}$.28
40	2.82	$\bar{4}$.45	52	2.34	$\bar{4}$.37
45	3.39	$\bar{4}$.53	60	2.88	$\bar{4}$.46
50	4.17	$\bar{4}$.62	66	3.16	$\bar{4}$.50
55	5.01	$\bar{4}$.70	74	4.17	$\bar{4}$.62
60	5.90	$\bar{4}$.77	80	4.79	$\bar{4}$.68
65	6.90	$\bar{4}$.84	90	6.17	$\bar{4}$.79
70	8.70	$\bar{4}$.94	100	7.76	$\bar{4}$.89
80	12.3	$\bar{5}$.09	120	13.2	$\bar{5}$.12
90	18.2	$\bar{5}$.26	130	17.4	$\bar{5}$.24
100	25.1	$\bar{5}$.40	150	28.2	$\bar{5}$.45
110	38.0	$\bar{5}$.58	160	36.3	$\bar{5}$.56
120	53.7	$\bar{5}$.73	170	45.7	$\bar{5}$.66
130	67.6	$\bar{5}$.83	185	66.1	$\bar{5}$.82
140	10.9	2.04	190	75.8	$\bar{5}$.88

$T = 120^{\circ}$ Run 6

t	p	log P
0	0	0
4	0.96	$\bar{5}.98$
6	1.12	$\bar{4}.05$
8	1.31	$\bar{4}.12$
10	1.44	$\bar{4}.16$
2	1.58	$\bar{4}.20$
4	1.90	$\bar{4}.28$
6	2.13	$\bar{4}.33$
8	2.50	$\bar{4}.38$
20	2.81	$\bar{4}.45$
24	3.80	$\bar{4}.58$
28	5.01	$\bar{4}.70$
32	6.31	$\bar{4}.80$
36	9.12	$\bar{4}.97$
40	12.0	$\bar{3}.08$
44	15.8	$\bar{3}.20$
50	25.1	$\bar{3}.40$
54	31.6	$\bar{3}.50$
60	50.1	$\bar{3}.70$
65	72.4	$\bar{3}.86$
70	100.0	$\bar{2}.00$
75	151.01	$\bar{2}.18$

Run 2 $T = 115.9^{\circ}$

t	p	log P
0	0	0
2	.575	$\bar{5}.76$
4	.724	$\bar{5}.86$
6	.832	$\bar{5}.92$
8	.980	$\bar{5}.99$
10	1.07	$\bar{4}.03$
12	1.20	$\bar{4}.08$
15	1.41	$\bar{4}.15$
20	1.82	$\bar{4}.26$
25	2.30	$\bar{4}.36$
30	2.88	$\bar{4}.46$
35	3.63	$\bar{5}.56$
40	4.47	$\bar{4}.65$
45	5.49	$\bar{4}.74$
50	6.92	$\bar{4}.84$
55	8.31	$\bar{4}.92$
60	10.71	$\bar{3}.03$
65	13.20	$\bar{3}.12$
70	16.60	$\bar{3}.22$
75	20.89	$\bar{3}.32$
80	25.11	$\bar{3}.40$
85	31.6	$\bar{3}.50$
90	41.69	$\bar{3}.62$
100	60.25	$\bar{3}.78$
110	95.5	$\bar{3}.98$

TABLE 26

Run	T°C	T°K	$\frac{10^3}{T}$ °K	K.10^{-3}	log K
1	105.5	378.5	2.643	6.45	$\bar{3}$.81
2	115.9	388.9	2.571	19.0	$\bar{2}$.28
3	114.0	387.0	2.584	16.0	$\bar{2}$.20
4	110	383.0	2.611	11.0	$\bar{2}$.05
5	106.1	379.0	2.638	7.24	$\bar{3}$.86
6	120	393.0	2.544	30.2	$\bar{2}$.40

Figure 15A

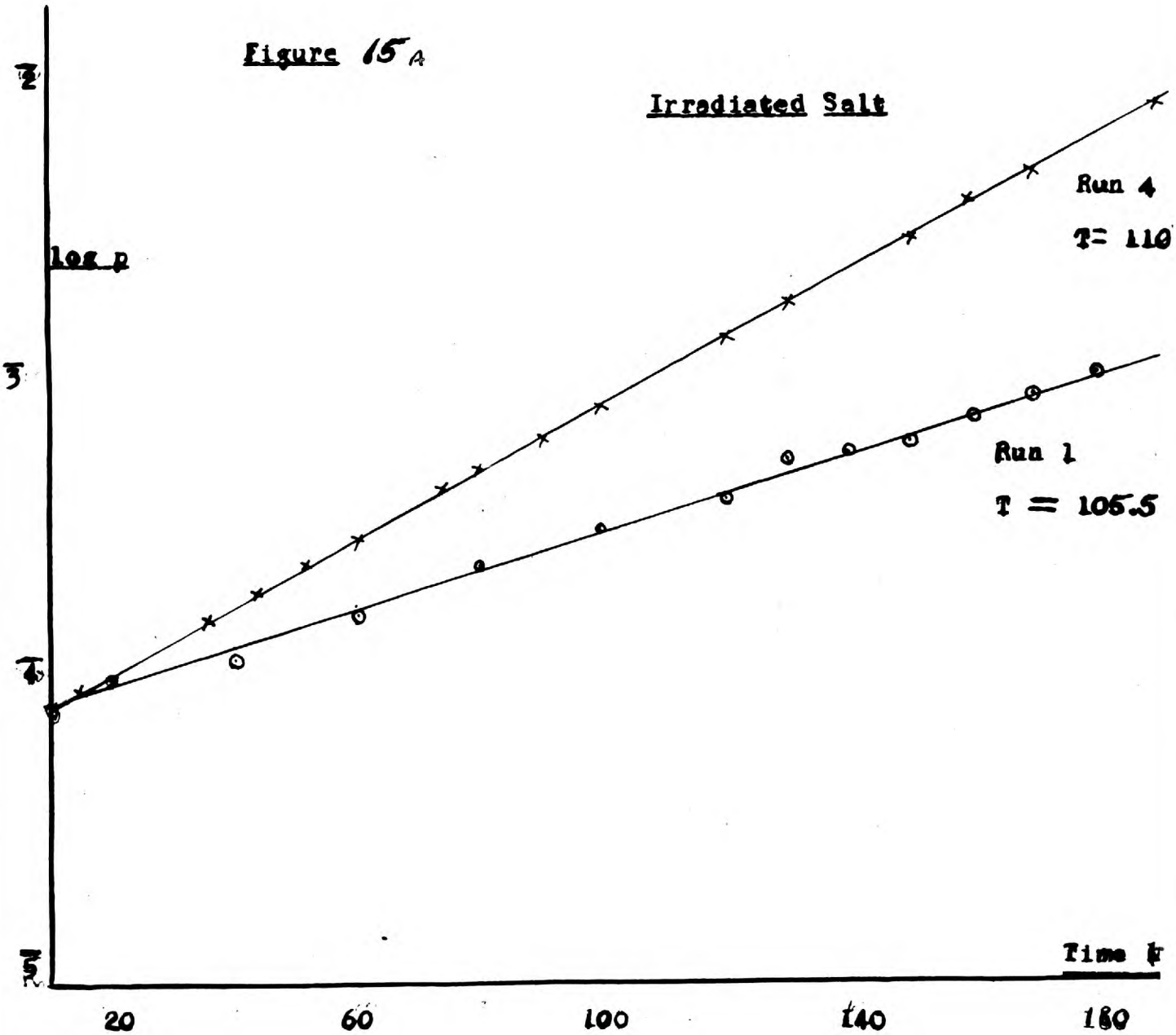
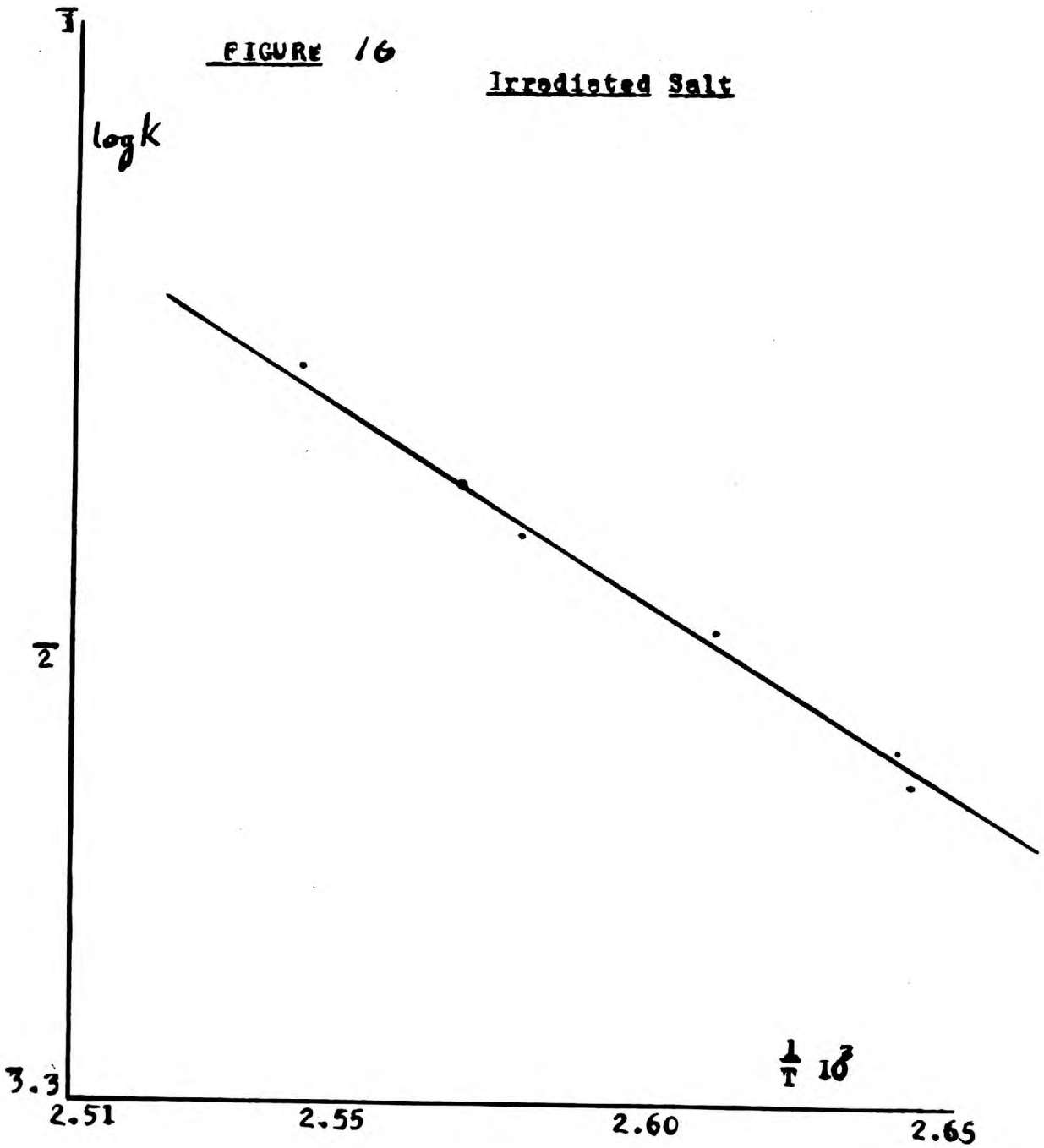

Irradiated Salt
Run 4
T= 110
Run 1
T = 105.5
log p
Time t
20
60
100
140
180

FIGURE 16

Irradiated Salt



Thermal decompositions were carried out with samples of oxalate prepared a) in presence of excess oxalate ion and b) in presence of excess silver ion. It was found that although the form of p-t curve was unaltered, the rate of reaction was markedly altered, the rate being increased and reduced respectively. Values of log C remained small, as for non-irradiated "stoicheiometric" salt. Activation energy curves are plotted in Figures 19 and 19a. The values of activation energies reported are a) 27.0 and b) 27.3 kcal.

Runs 20 to 25 were carried out on samples prepared in presence of excess oxalate ion.

Run 20		Run 21		Run 22	
T = 111.6°C.		T = 108.6°C		T = 106.8°	
t	p	p	t	p	t
		.162	2	.20	5
4	0.30	.22	6	.32	10
8	.43	.27	10	.38	15
10	.50	.44	20	.44	20
5	.66	.91	30	.69	30
20	1.05	1.30	40	1.15	40
30	2.00	2.20	50	1.82	50
40	3.60	5.01	60	2.90	60
50	7.25	7.40	70	4.25	70
60	15.90	13.80	80	6.61	80
70	31.60	21.90	90	10.00	90
80	57.50	40.10	100	16.70	100
85	95.50	72.44	110	22.90	110
90	120.0			38.90	120
				55.00	130

Run 23		Run 24		Run 25	
T = 105.0°		T = 101.5°		T = 96.7°	
t	p	p	t	p	t
2	.15	.25	10	.15	5
6	.18	.32	20	.20	10
10	.21	.42	30	.24	15
20	.31	.59	40	.26	20
30	.46	.79	50	.44	40
40	.65	1.26	60	.63	60
50	.93	1.44	70	.87	80
60	1.00	1.91	80	1.17	100
70	1.71	2.51	90	1.62	120
80	2.51	3.55	100	2.19	140
90	3.54	6.17	120	2.95	160
100	5.01	7.94	130	4.17	180
110	5.62	10.72	140	7.08	200
120	7.94	13.18	150		
130	14.8	19.50	160		

Runs 26 to 31 were performed on samples prepared in presence of excess silver ion.

Run 26		Run 27		Run 28	
T = 140.2°C		T = 136°		T = 127°	
p	t	p	t	p	t
.12	2	0.20	10	.13	4
.15	4	.32	20	.18	8
.18	8	.42	30	.19	10
.20	10	.60	40	.24	20
.36	20	.79	50	.27	30
.59	30	1.07	60	.33	40
1.00	40	1.55	70	.39	50
1.74	50	2.09	80	.45	60
3.30	60	3.38	90	.56	70
5.74	70	4.27	100	.63	80
6.31	80	6.02	110	.68	90
17.40	90	8.31	120	.83	100
27.50	100	12.30	130	1.00	10
46.80	110	17.40	140	1.18	20
83.18	120	25.10	150	1.41	30
131.0	130	37.10	160	1.60	40
				2.29	60
				2.75	70

Run 29

T = 124.6

p	t
.16	5
.19	10
.22	20
.25	30
.33	50
.44	70
.57	90
.66	100
.91	120
1.00	130
1.20	140
1.59	160
1.80	180

Run 30

T = 130.2

p	t
.18	10
.27	20
.45	30
.47	40
.60	50
.79	60
1.00	70
1.26	80
1.67	90
2.09	100
2.75	110
3.55	120
4.57	130
5.90	140
7.57	150
10.00	160
12.59	170

Run 31

T = 137

p	t
.12	2
.14	4
.19	8
.20	10
.31	20
.48	30
.72	40
1.05	50
1.95	60
2.29	70
3.31	80
4.79	90
7.24	100
15.50	20
33.11	40
70.80	60

TABLE 27

Run	$T^{\circ}C$	$T^{\circ}K$	k	log k	$\frac{10^3}{T^{\circ}K}$
23	105.0	378.0	15.1	$\bar{2}.18$	264.6
24	101.5	374.5	12.3	$\bar{2}.09$	267.0
25	96.7	369.7	6.76	$\bar{3}.83$	270.5
20	111.6	384.6	30.20	$\bar{2}.48$	260.0
21	108.6	381.6	24.0	$\bar{2}.38$	262.1
22	106.8	379.8	19.1	$\bar{2}.28$	263.3
26	140.2	413.2	23.4	$\bar{2}.37$	241.9
31	137.0	410.0	16.6	$\bar{2}.22$	243.9
27	136.0	409.0	14.4	$\bar{2}.16$	244.5
30	130.2	403.0	11.0	$\bar{2}.04$	248.0
28	127.0	400.0	7.2	$\bar{3}.86$	250.0
29	124.6	397.6	6.1	$\bar{3}.79$	251.5

FIGURE 19

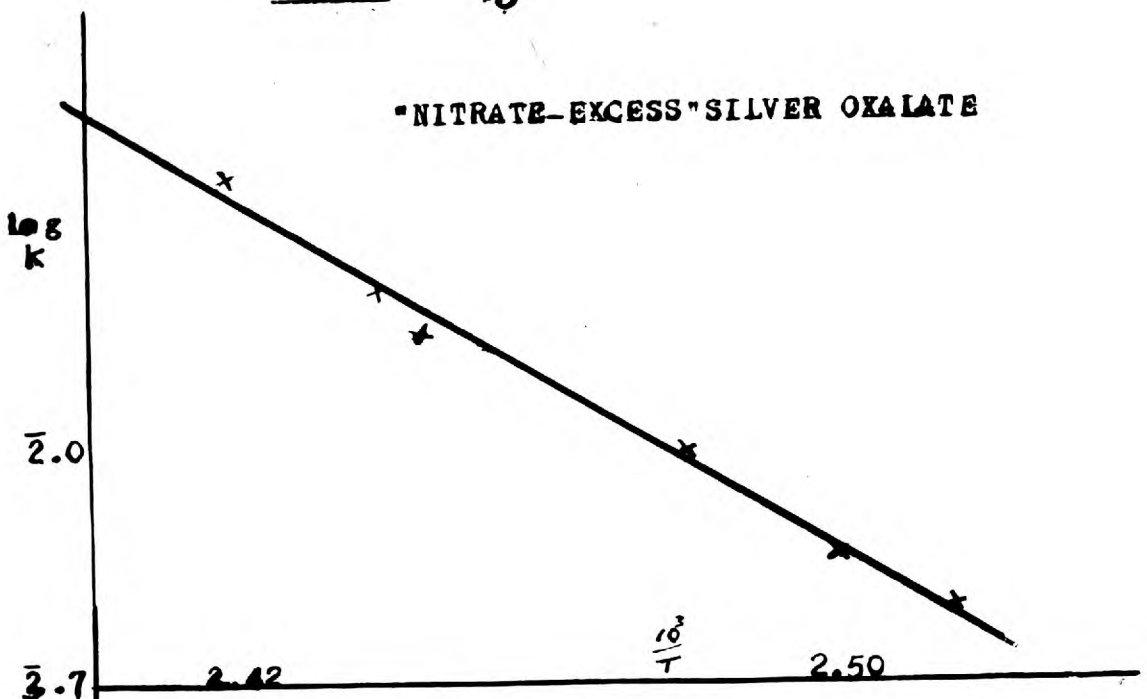
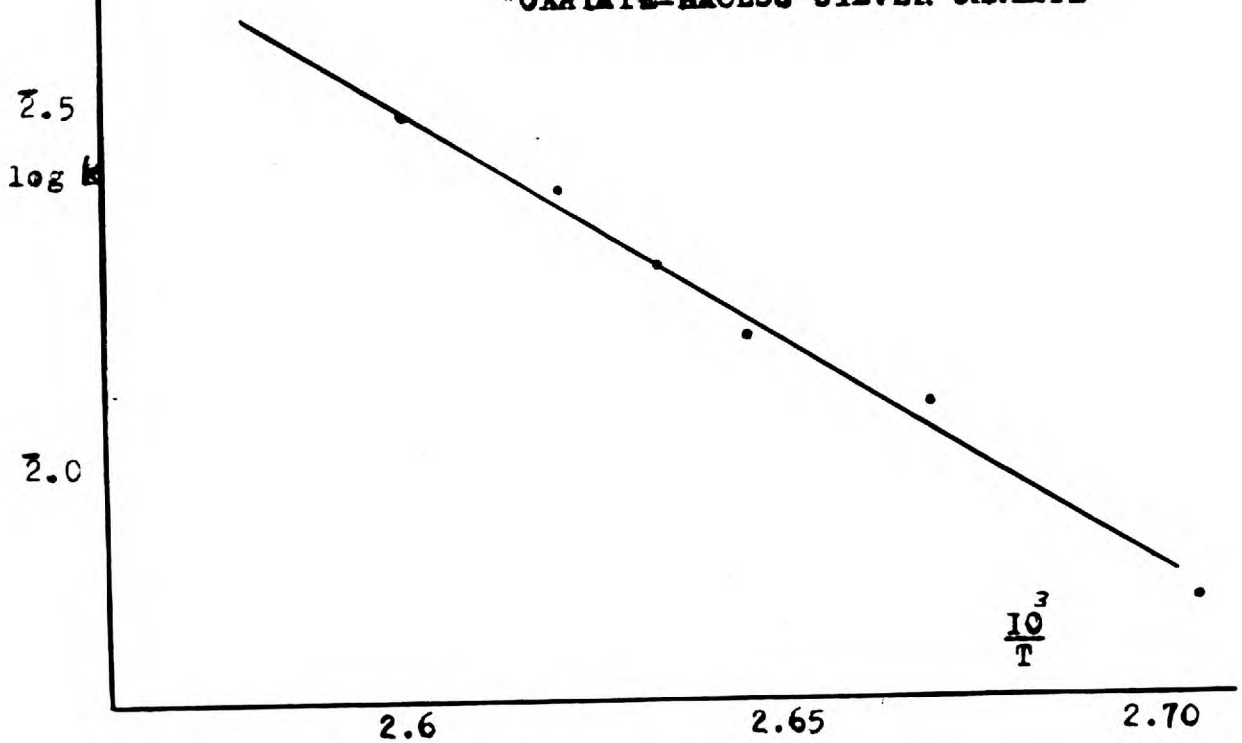


FIGURE 19_A



A quantitative study of the effect of pre-irradiation on thermal decomposition was made on a "stoicheiometric" sample of silver oxalate (Runs 13 to 21). In runs 13, 14, 15, 19, 21 and 22 the sample was irradiated for varying times, t_i, at a constant lamp current, i_p, of 0.2 amp. In runs 16, 17, and 18 the lamp current was varied, values of 0.4, 0.1 and 0.3 amp. being used. All decompositions were carried out at a temperature of 110°C. The results are summarised in Table (28) and Figure 19, where it is shown that the plot of log $(t_i\ i_p)$ log $(C - C_u)$ is linear, with a slope of 1.1. C_u is the value of C for unirradiated salt. This value was determined as the mean of three runs, in which the utmost care was taken to mount the sample in the bucket in a standard manner. The values obtained for log C were as follows 5.23, 5.21, 5.25 giving a mean value of 5.23. Values of log C for previous runs (7 to 12) had varied from 5.20 to 5.30.

i_p = 0.2 amp.
t_i = 2 min.

Run 19

t	p
10	.54
15	.63
20	.69
30	.85
40	1.07
50	1.38
60	1.74
70	2.23
80	2.75
90	3.39
100	4.36
110	5.25
120	7.08
130	9.12

i_p = 0.2 amp.
t_i = 3.5 min.

Run 20

t	p
10	.87
20	1.0
30	1.3
40	1.7
50	2.0
60	2.5
70	3.2
80	4.3
90	5.0
100	7.2
110	8.7
120	10.2
130	13.5
140	17.8
150	22.9
160	27.5

i_p = 0.2 amp.
t_i = 10 min.

Run 21

t	p
10	1.8
20	2.5
30	2.9
40	4.0
50	4.8
60	6.3
70	7.7
80	10.2
90	12.9
100	14.4
110	19.5
120	24.5
130	31.6
140	40.7
150	50.1

i_p = 0.2 amp.
t_i = 15 min.
Run 13

t	p
10	1.9
15	3.4
20	3.6
30	4.7
40	5.9
50	7.6
60	9.8
70	12.0
80	15.5
90	19.5
100	25.1
110	31.6
120	39.8
130	47.9
140	61.7
150	81.3
160	100.0

i_p = 0.2 amp.
t_i = 20 min.
Run 14

t	p
10	3.6
20	4.7
30	6.0
40	7.9
50	10.0
60	12.9
70	15.9
80	21.9
90	25.7
100	33.9
110	43.7
120	53.8
130	75.9
140	93.3
150	117.5
160	

i_p = 0.2 amp.
t_i = 5 min.
Run 15

t	p
10	0.9
20	1.1
30	1.5
40	2.0
50	2.4
70	3.8
80	4.9
90	6.3
110	8.9
120	12.6
130	16.2
140	19.5
150	22.9
160	30.9

i_p = 0.4 amp.
t_i = 5.2 min.

Run 16

t	log p
10	1.3
20	1.7
30	2.0
40	2.7
50	3.4
60	4.3
70	5.4
80	6.9
90	8.9
100	10.5
110	13.8
120	17.8
130	23.4
140	29.5
150	35.5
160	45.7

i_p = .1 amp.
t_i = 25.1 min.

Run 17

t	log p
10	2.3
20	2.8
30	3.5
40	4.3
50	6.2
60	7.2
70	8.9
80	11.5
90	14.4
100	18.6
110	22.9
120	30.2
130	34.7
140	46.8

i_p = 0.3 amp.
t_i = 13.0 min.

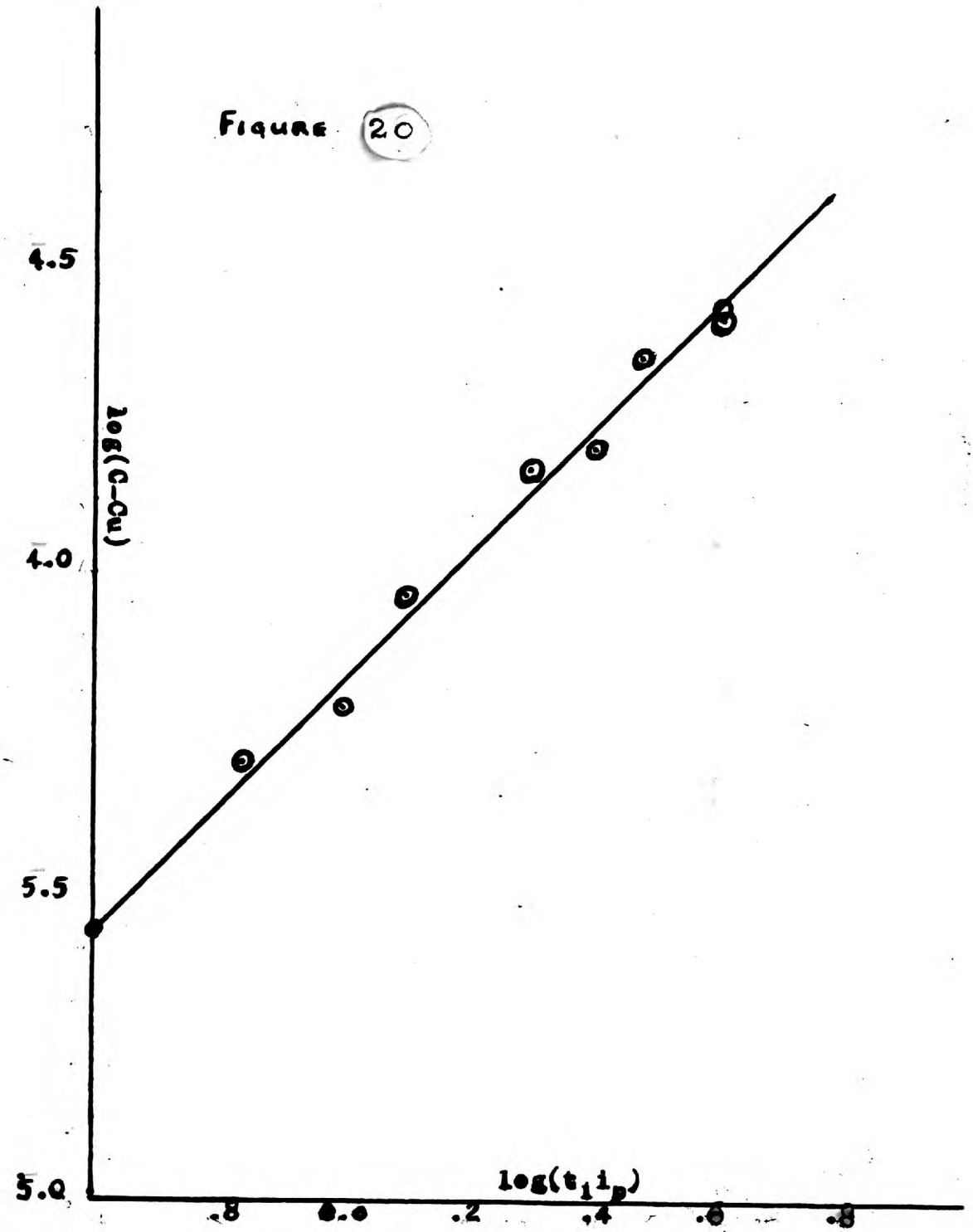
Run 18

t	log p
10	3.4
20	4.2
30	5.5
40	6.9
50	8.9
60	11.7
70	15.1
80	18.2
90	24.0
100	30.2
110	40.0
120	58.9
130	85.1

TABLE

Run	t_i	log t_i	log $(t_i i_p)$	log C.C.10^5	$C-C_u$	log $(C-C_u)i_p$	
19	2	.30	$\bar{1}.6$	$\bar{5}.64$	4.4	2.7	$\bar{5}.43$	0.2
20	3.5	.54	$\bar{1}.84$	$\bar{5}.82$	6.7	5.0	$\bar{5}.70$	0.2
15	5	.70	$\bar{0}.0$	$\bar{5}.86$	7.2	5.5	$\bar{5}.79$	0.2
21	10	1.00	$\bar{0}.3$	$\bar{4}.18$	15.1	13.4	$\bar{4}.13$	0.2
13	15	1.18	$\bar{0}.48$	$\bar{4}.38$	24.0	22.3	$\bar{4}.35$	0.2
14	20	1.30	$\bar{0}.60$	$\bar{4}.46$	28.8	27.1	$\bar{4}.43$	0.2
16	3.2	5.05	0.10	$\bar{4}.04$	11.0	9.31	$\bar{5}.97$	0.4
17	25.1	1.40	$\bar{0}.40$	$\bar{4}.24$	17.4	15.7	$\bar{4}.20$	0.1
18	13.0	1.13	$\bar{0}.60$	$\bar{4}.44$	27.5	25.8	$\bar{4}.41$	0.3

FIGURE 20



DISCUSSION

The Conductance of Metallic Oxalates

The conductance of a number of metallic oxalates was measured as part of a general programme of research concerning the solid-phase decomposition of a related series of compounds. Since modern theories of both ionic conductance and solid decomposition involve the number and mobility of lattice defects, it was hoped that some correlation between the two phenomena might be obtained. Thus, as a result of the measured conductance of barium azide, (40) Thomas and Tompkins were able to show that the Mott theory of the rate of growth of nuclei could not be applied to the thermal decomposition of this salt (61). Moreover, the lack of evidence for the existence of photoconductance in barium and potassium azide, cannot be explained on the basis of Mott's theory, and this has led to a new theory of photolysis for these compounds (35). Before undertaking further research on the decomposition of metallic oxalates, therefore, it was of value to see whether similar conclusions would follow as a result of the study of the ionic conductance of these compounds.

The ionic conductances of lead, silver, mercuric, thallous and barium oxalates were all measured in the

structure-sensitive region of temperature. For each compound the characteristic constants in the equation expressing the variation of conductance with temperature were derived. The constants for the three divalent metal compounds are listed below:

	Barium	Mercuric	Lead
E kcal.	12.7	14.1	15.0
log A	-4.3	-6.4	-6.0

As can be seen, the specific conductance is very low at normal temperatures. Compare Li Cl, KBr, BaN_6, values for which are shown:

	Li Cl	KBr	BaN_6
log A	2	.98	-6.0
E kcal	13.6	22.4	11.6

The values for E here refer to the activation energy for mobility of the conducting species, since the measurements were made in the structure-sensitive region. The nature of the conducting species can only be determined by transport number measurements which are impracticable due to the low conductance of these compounds at temperatures below the decomposition point. However, by analogy with lead and barium halides, for which $t_{cation} = 0$, it is presumed that anionic conductance predominates. It may be noted from the list

that the value of E decreases, as expected, with increasing size of cation i.e. in the order $E_{Ba} < E_{Hg} < E_{Pb}$

The constants obtained for silver and thallous oxalates are:

	Thallium	Silver
E kcal.	6.15	10.7
log A	-6.45	-6.0

The small value of E obtained for thallous oxalate is surprising, and may mean that surface conduction is operative. The value of the specific conductance of silver oxalate is of the same order as that of the analogous property for barium azide (E = 11.6 kcal.; log A = 6.0). No observations of nuclei in silver oxalate have been recorded, and hence quantitative calculations of ion conductance from experimental rates of nucleus growth are not possible. Nevertheless, since both conductance and rates of decomposition of the two compounds are comparable in order of magnitude, it is reasonable to expect the conclusions derived for barium azide to be applicable to silver oxalate. Thus it is almost certain that the measured conductance is too small to account for the rate of reaction actually found, and hence Mott's theory of internal electrolysis can not apply to silver oxalate.

An attempt was made to see whether different methods of preparation would result in the inclusion of different numbers of defects in the lattice. Although the decomposition of silver oxalate was of most interest in this investigation, the solubility of this compound is so small that it was thought advisable to attempt first to introduce foreign ions into the lattice of the more soluble thallous oxalate. Thallous oxalate was selected since it is freely soluble and is quite stable at temperatures below at least 500°C. Barium was chosen as interstitial ion since 1) barium oxalate is fairly soluble, and 2), the closeness in size of the barium and thallous ions made inclusion of the former into the lattice of thallous oxalate seem possible. Thallous oxalate was, therefore, allowed to crystallise from solutions of barium oxalate. The results obtained, however, were negative, i.e. the values of conductance were within experimental error equal to that of "pure" thallous oxalate. Although at this stage it seemed evident that similar results would be obtained from experiments on similar oxalate, a sample of silver oxalate was prepared by precipitation from a solution containing calcium ion. As before, however, no increase in conductance was detected, and it is concluded that

incorporation of a significant number of ions into the lattice is not effected by this means.

It was shown that no photo-current as large as 10^{-12} amp. could be detected when a pellet of silver oxalate was irradiated with ultra-violet light. The significance of this result is discussed more fully in the photolysis discussion, but the conclusion is that irradiation results in the formation of excitons, and not of electrons in the conduction band.

In general, then, the results of the conductance measurements are analogous to those found for the azides. Similar conclusions can be drawn, and, as will be shown, a theory for their decomposition can be developed. The theory, whilst in terms of lattice defects, differs from the Mott theory, and is consistent both with conductance and decomposition results.

The Photolysis of Silver Oxalate

The main features of the photo-chemical decomposition of silver oxalate may be summarised as follows:-

1. At constant intensity of irradiation the pressure of carbon dioxide evolved varies linearly with time, slight acceleration being present. Evolution of gas commences simultaneously with irradiation, ceases immediately on cessation of irradiation, and is strictly reproducible. The temperature coefficient is small, the activation energy of photolysis in the temperature range -70° to + 40°C being ~ 900 cal. These results confirm the results of Tompkins (32), who reported an activation energy of 850 cal.

2. At constant temperature the rate varies as the second power of the intensity of illumination, as found for barium and potassium azides, (35,40), and for barium styphnate. The corresponding power found in the previous investigation was 1.67. It will be shown later that this value is not inconsistent with the theory developed to explain the present results.

3. The quantum efficiency η may be calculated from the equation: Rate, in molecules of CO_2 evolved per second. / = Area of irradiation in cm^2 x energy of irradiation absorbed. = η

The area exposed to irradiation in the photolysis cell = 3.8 cm^2, and the intensity corresponded to 1.44×10^4 erg./cm. sec. The energy of 1 quantum of light at $\lambda = 2357A = 7.83 \times 10^{-12}$ erg., so the intensity used is equivalent to 1.9×10^{15} quanta/cm^2 second, since the radiation is almost entirely concentrated in this line.

The rate at this intensity is equal to 4.75×10^{14} molecules of CO_2 per second, hence assuming 20% of the light is scattered by the quartz window,

$$\eta = 7.6 \times 10^{-2}$$

The value previously recorded is of the order of 0.1, in satisfactory agreement with the present result, since it has been shown that η decreases with time (40).

4. No photo-current as large as 10^{-12} amp. could be observed when a pellet of silver oxalate was irradiated with the full intensity of a low pressure mercury-vapour lamp, of intensity $\sim 10^{15}$ quanta/sec. cm^2. If irradiation results in the production of electrons, and all electrons are in the conduction band, then a photo-current of

$$\sim \frac{10^{15} \times 7.6 \times 10^{-2} \times 4.8 \times 10^{-10}}{3 \times 10^9}$$

i.e. $\sim 1 \times 10^{-5}$ amp.

would be expected. Hence either irradiation does not

produce electrons, or the electrons are immobilised in traps.

The maximum fraction ψ of free electrons which actually reached the electrode is given by

$$\psi = \frac{1 \times 10^{-12}}{1 \times 10^{-5}} = 10^{-7}$$

The mean range w of the photo-electrons is given by the formula

$$\psi = \frac{W}{l}$$ where l = width of the pellet illuminated.

Here $l \sim .2$ cm.

hence $W = 2 \times 10^{-8}$

Suppose that there are N traps of cross-sectional area a., then the mean life, t, of an electron in the conduction band will be given by

$$t = \frac{1}{Nav}$$ where v = velocity

$$W = t \times v$$

$$\therefore \quad N = \frac{1}{Wa}$$

If a value of 10^{-15} cm^2 is assigned to a, this value corresponds to that for a vacant anion site - then

$$N \sim \frac{1}{2 \times 10^{-8} \times 10^{-15}} \sim 5 \times 10^{22}/\text{cm}^3$$

which means that approximately every ion in the crystal acts as a trap, which is highly improbable. It is, therefore, concluded that absorption of light does not

result in the production of electrons in the conduction band.

Since the general features of the reaction show strong similarity to those exhibited by barium and potassium azides, a similar mechanism might be applicable. For barium azide it was assumed that decomposition occurred as a result of interaction of two excited azide radicals. It was shown that the radicals consisted of excitons, and not positive holes. Decomposition occurred when two excitons were trapped at neighbouring positions in the lattice and the I^2 term was explained by the bimolecular reaction of two species. The analogous reaction here would consist in the interaction of two oxalate excitors. This process will now be considered.

For barium azide it was shown that the rate, R, was given by

$$R = \frac{p^2 N s \nu e^{-\frac{E}{RT}}}{\frac{1}{t_1}\left(\frac{1}{t_2} + s\nu e^{-\frac{E}{RT}}\right)}$$

where p = probability of trapping an exciton/sec.

N = Number of traps

t_1, t_2 = life-times of excitons at centres where 1, 2, of them were trapped.

ν = lattice frequency

E = Activation energy in cal./mole. for decomposition of two trapped excitons

s = entropy term

In order to convert this equation into a form which compared with the experimental expression, it is necessary to assume that the steric factor is, $\sim 10^{-2}$, in order that $\frac{E}{RT} < \frac{1}{t_2}$, to give

$$I \quad - - - R = s\nu Np^2 t_1 t_2 e^{-\frac{E}{RT}}$$

For silver oxalate the rate is well fitted by the equation

$$\left(R_{Expt.}\right) = 151 \times e^{-\frac{900}{RT}}$$

Since the rate in equation I refers to the number of exciton complexes decomposing per second,

$$R = R_{Expt.} \times \text{Factor}$$

$$\text{Factor} = \frac{.705 \times 6.02 \times 274 \times 10^{16}}{22.4 \times 76 \times 60 \times 2 \times 296}$$

$$= 1.9 \times 10^{11}$$

whence $R = 2.9 \times 10^{13} e^{-\frac{965}{RT}}$

On comparison with equation I

$$sp^2 t_1 t_2 = 2.9 \times 10^{13}$$

A necessary restriction in the derivation of I was that $p < \frac{1}{t_1}, \frac{1}{t_2}$. It is reasonable to suppose that $t_1 \approx t_2$,

and hence $p^2 t_1 t_2 \sim 10^{-4}$. $\nu = 5 \times 10^{-12}$, and hence on substitution

$$N \sim \frac{2.9}{5} \times 10^{13} \times 10^{-12} \times 10^{4} \times 10^{12}$$

$$\underline{N \sim 6 \times 10^{6}}$$

By analogy with Ag Br and Ag Cl, the ionic conductance of silver oxalate is supposed to be due to the motion of vacant cation sites. The number of these vacancies, N_s, may be calculated from the conductance results by substitution in the equation

$$\kappa = \frac{N_s e^2 a^2 \nu C}{kT} e^{-\frac{E}{RT}}$$

where

κ = Value of the conductance at $T^{\circ}K = 3.0 \times 10^{-15}$ ohm $^{-1}$ cm^{-3} at 274°K.

a = Lattice constant = 6×10^{-8} cm.

ν = Lattice frequency = 5×10^{12} 5^{1}.

C = A constant involving the variation of the activation energy for conductance, E, = 10.65 kcal., with the thermal expansion of the crystal. For bulk conductance in the alkali halides, this is of the order of 10^2 (Jacobs and Tompkins (A)), and this value is considered appropriate here, hence $N_s \sim 1.94 \times 10^{8}$ cm^{-3}

This value refers to the number of cation vacancies in the bulk of the crystal. To a first approximation, the number in the surface is given by $(n_2)^{2/3} = \underline{1.5 \times 105}$ cm^{-2}

This number also represents the number of anion vacancies in the surface, since in order to preserve electro-neutrality, an equal number of positive and negative sites is required. The discussion is thus independent of which species acts as a trapping centre. On comparison of this figure with N, the number of traps calculated from the photolysis results, it is seen that good agreement between the two values is obtained.

Thus the theory developed for barium azide can describe the kinetics of the silver oxalate photo-decomposition. There are, however, two factors which have not yet been considered. There is some evidence from Mac. Donald that the $(COO)_2^-$ ion is stable in the solid state, and reaction between two $(COO)_2^-$ excitons would require greater activation energy than the small value actually found. Further, if, as suggested later, an electron from the oxalate exciton is partially trapped by a vacant anion site, then the resulting 'positive-hole' would bear a net negative charge. Considerable electrostatic repulsion between two such charged radicals is expected, and once again a bimolecular reaction of low activation energy (900 cal.) is unlikely. In the azide theory, this difficulty does not arise, since the azide ion has only one valency electron. An alternative

mechanism is, therefore, proposed. It is suggested that reaction occurs by the unimolecular decomposition of a single (divalent) oxalate radical. The dependence of rate on I^2 is explained by the double excitation of the oxalate radical to form an unstable complex which decomposes into two molecules of carbon dioxide. A theory based on these two assumptions will now be formulated.

The first question which must be considered is whether or not the excitation results in the formation of positive holes or of excitons. The former possibility will not be considered.

Absorption of light by an oxalate radical $Ox^{=}$, is assumed to produce a "positive-hole" Ox^{-}, which is trapped at some point in the lattice. Receipt of further irradiation by the trapped Ox^{-} causes the production of an unstable 'true' positive-hole Ox, which breaks up into two molecules of carbon dioxide. The decomposition may be formulated as follows:

$h\nu + Ox^{=} \xrightarrow{k_1} Ox^{-}$ 1st Excitation

$n1 \xrightarrow{k_3} Ox^{=}$ Dissociation of trapped Ox^{-}

$Ox^{-} + n \xrightarrow{k_2} n1$ Trapping of Ox^{-}

$n1 + n \underset{k_5}{\overset{k_4}{\rightleftharpoons}} n2$ Reversible formation of unstable Ox

$n2 \xrightarrow{k_6} 2\,CO_2$ Decomposition of unstable complex.

where n = number of empty traps

n_1 = number of trapped Ox^-

n_2 = number of trapped $Ox^=$

k_1 to k_5 ≡ Appropriate rate constants.

I = Intensity of irradiation N = number of $Ox^=$ radicals.

Applying stationary state methods

$$\frac{d}{dt}(Ox^-) = Nk_1I - k_2(Ox^-)\,n = 0$$

$$\frac{d}{dt}n_1 = k_2 Ox^- n - k_3 n_1 - k_4 N_1 I = 0$$

$$\frac{d}{dt}n_2 = k_4 I n_1 - k_6 n_2 - k_5 n_2$$

$$\frac{d}{dt}co_2 = \text{Rate}, R_3 = k_6 n_2$$

$$\text{Solving } R = \frac{k_1 k_4 k_6 I^2}{(k_3 + k_4 I)(k_5 + k_6)}$$

$$\text{Since } R \propto I^2, \quad Ik_4 < k_3$$

$$\text{and hence } R = \frac{k_1 k_4 k_6 I^2}{(k_5 + k_6)k_3}$$

Now k_3, k_5, k_6, refer to rates of thermal dissociation, and hence

$$k_3 = \nu e^{\frac{-E_3}{RT}}$$

$$k_5 = e\,\nu^{\frac{-E_5}{RT}}$$

$$k_6 = \nu e^{\frac{-E_6}{RT}}$$

where E_3, E_5, E_6 are appropriate activation energies

$$\therefore \frac{k_1 k_4 I^2 \omega\, e^{-\frac{E6}{RT}}}{\omega^2 e^{-\frac{E3}{RT}} \left(e^{-\frac{E5}{RT}} + e^{-\frac{E6}{RT}}\right)}$$

If it is assumed that the rate of decomposition of the complex is small compared with the rate of thermal dissociation of the trapped Ox,

$$R = \text{constant} \times e^{-\frac{E6 + (E3 + E5)}{RT}}$$

and hence in order to obtain a positive temperature coefficient, , as found experimentally,

$$E_6 > E_5 + E_3$$

Since E_6 is approximately 900 cal. E_5, E_3, must each be very small. In that event, a high concentration of positive holes would be expected, which is contrary to the photo-conductance results. Thus it does not seem that excitation of the oxalate results in positive-hole formation.

The theory will now be re-formulated on the basis that neutral excitons rather than charged positive holes are produced.

Let $Ox^{\ddagger x}$ = A surface oxalate radical

Ox^{x} = An exciton

Ox^{xx} = Unstable exciton complex

N = Number of oxalate radicals in the surface

n = Number of empty traps

n_1 = Number of trapped O^x

n_2 = Number of Ox complexes

I = Intensity of irradiation

Then

1. $Ox^{=} + h\nu \xrightarrow{k_1} Ox^{x}$ Production of exciton

2. $n + Ox^{x} \xrightarrow[k_2]{} n_1$ Trapping of exciton

3. $n_1 \xrightarrow{k_3} Ox^{=}$ Reversion of exciton to ground state

4. $n_1 + n \underset{k_5}{\overset{k_4}{\rightleftharpoons}} n_2$ Reversible formation of trapped unstable complex Ox^{xx}

5.

6. $n_2 \xrightarrow{k_6} 2CO_2$ Decomposition of complex.

Here k_1, k_4, represent the transition probabilities of excitation to exciton level k_3, k_5, represent the probability of the radical remaining in an excited state $t_3 = \frac{1}{k_3}$, $t_5 = \frac{1}{t_5}$ are identified as the life-times of the trapped exciton and complex respectively. If the complex can receive sufficient thermal energy from the lattice during its life-time it will decompose unimolecularly to form two molecules of carbon dioxide. Since there are several ways in which the complex may lose its excess energy, e.g. by partial return to the ground state, k_5 may be a composite term. This, however, will not affect the subsequent discussion. Without defining the nature of the trapping species, or the structure of the complex Ox^{xx}, a general treatment of the theory will be given, and

some orders of magnitude derived for the different processes.

Applying stationary state method:-

$$\frac{d}{dt}(O\,x^{x}) = 0 = k_1\,NI - k_2\,Ox^{x}\,n$$

$$\frac{dn_1}{dt} = 0 = k_2\,Ox^{x}\,n - k_3\,n_1 - k_4\,n_1\,I$$

$$\frac{dn_2}{dt} = k_4 n_1 I - k_6 n_2 - k_5 n_2 = 0$$

$$\frac{dco_2}{dt} = \text{Rate, } R = k_6\,n_2$$

Solving for n_2

$$R = \frac{k_1\,k_4 k_6\,NI^{2}}{(k_3 + k_4 I)\,(k_5 + k_6)}$$

In order to attain the experimental condition that $R \propto I^{2}$, it is required that $k_4 I < k_3$, i.e. that the probability of loss of an exciton from a trap be much greater than the probability of performing the second excitation process. This latter entails the exciting of an electron from a resultant strongly positive field, and hence this condition appears reasonable. In the previous theory of the decomposition of silver oxalate, a dependence of R on I to a power between 1.67 and 2 was found. If the applied intensity in this work were sufficiently large, then the term ($k_4 I$) might not have been completely negligible in comparison with k_3. Thus the present

mechanism could still be operative.

However, for the present discussion, it is required that

$$R = \frac{k_1 k_4 k_6 NI^2}{k_3(k_5 + k_6)}$$

The final process, (6), is a thermal decomposition, and the rate, R, may, therefore, be expressed, using conventional symbols, by

$$R = k_6 n_2 = s \sim e^{\frac{-E}{RT}}$$

For a unimolecular decomposition the steric factor $\sim$ unity; $\sim = 5 \times 10^{12}$; the values in the exponential term are all known, and at 300°K, exp. $\sim .5$

$$\therefore k_6 \sim 2 \times 10^{12}$$

The quantum efficiency, η, as previously defined, is given by

$$\eta = 7.6 \times 10^{-2} = \frac{CO_2 \text{ evolved per second}}{\text{Radiation absorbed/cm}^2}$$

$$= \frac{k_6 n_2}{k_1 NI}$$

$$n_2 = \frac{k_1 k_4 NI^2}{(k_4 I + k_3)(k_5 + k_6)}$$

writing the exact expression, i.e. not neglecting $(k_4 I)$

$$\therefore \eta = 6.6 \times 10^{-2} = \frac{k_1 k_4 NI^2 k_6}{(k_4 I + k_3)(k_5 + k_6) k_1 NI}$$

$$= \frac{k_4 I \, k_6}{(k_5 + k_6)(k_4 I + k_3)}$$

$t_3 = \frac{1}{k_3}$, $t_5 = \frac{1}{k_5}$, are the life-times of the trapped excitons. Calculations by Jacobs and Tompkins (63) by two different methods have shown that in potassium azide $t_3 = t_5 \sim 2 \times 10^{-11}$s. It is reasonable to suppose a similar order of magnitude here. Writing $k_5 = k_3, \sim 5 \times 10^{10}$ s^{-1} and $k_6 \sim 2 \times 10^{12}$s^{-1}

$$6.6 \times 10^{-2} = \frac{k_4 I \times 2 \times 10^{12}}{2.05 \times 10^{12} (5 \times 10^{10} + k_4 I)}$$

$$3.3 \times 10^{9} + 6.6\ 10^{-2}\ k_4 K = k_4 I$$

$$\therefore\ \underline{k_4 I \sim 3.5 \times 10^{9}}$$

It has previously been shown that in order to obtain the experimental relationship $R \propto I^2$ it is necessary that $k_4 I < k_3$, which is now found to be in agreement with the calculated result $3.5 \times 10^9 < 5 \times 10^{10}$. Moreover, the value calculated for the quantum efficiency probably represents a maximum value, since it has been shown (40) that η decreases with increasing exposure. Hence the approximation does seem to be consistent with the orders of magnitude expected on the present theory.

The number of (Ox^{xx}) formed is thus of the order of 3.5×10^9, whereas from the conductance measurements a maximum number of $\sim 1.5 \times 10^5$ traps was calculated. This discrepancy is not surprising in view of several factors

which have not yet been considered. In the first place, it was assumed that the number of defects in the bulk of the crystal could be converted to the number of defects in the surface by the simple relationship $(n\ \text{Bulk})^{2/3} = n(\text{surface})$. This could only lead to a minimum value since a) The number of defects on the surface is expected to be higher than the number in the bulk, due to "surface" absorption, and b) The surface is not expected to be plane. In actual fact, since silver oxalate is composed of micro-crystals a much larger surface area is expected in the photolysis experiments than in the conductance measurements, where a compressed pellet was used. It is frequently observed that in irradiation of fresh samples of silver oxalate a short initial acceleration appears, before the normal constant rate is established. This may be due to the creation of defects. Since the conductance measurements were performed in dark-room conditions, this effect would not appear, and hence once again a minimum number of defects would be measured.

In order that a photo-decomposition will predominate in process four, it is necessary that the activation energy for an analogous thermal reaction be very high. If thermal reaction could take place, then in the present mechanism a dependence of Rate on $I^{1.0}$ would be expected.

An estimate of the thermal energy can be made as follows:

Writing process four as a thermal process

$$k_4 = e^{\frac{-E}{RT}} \quad \text{(thermal)}$$

k_4 has been calculated to be $\sim 10^{-6}$, and $\nu = 5 \times 10^{12}$. $R = 4.57$, $T = 300^{\circ}K$, and writing a value of 10^2 for the inequality factor

$$10^{-8} = 5 \times 10^{12} \; e^{\frac{-E}{1,371}}$$

$$\therefore \frac{E}{RT} = 21 - \log 2$$

$\therefore$ E thermal $\sim$ 28 kcal., which represents a minimum value. The expected value would in fact be considerably larger than this, so that no difficulties arise. Since $k_4 I \sim 10^9$, in order to account for the measured rates, it may be assumed either that a higher frequency than the 2357A line is used for the excitation, hence the effective intensity is much less than the applied intensity, or that the I term is correct in order of magnitude, but that few Ox^{xx} complexes are produced. If the second process is $\sim 1\%$ of the first excitation process this would explain the magnitude. Since the lamp is almost monochromatic, very little radiation of higher frequency would be available for decomposition.

It is thus seen that a consistent explanation of the kinetic results can be given in terms of a theory involving

either 1) bimolecular reaction of two adjacent oxalate excitons, or 2) unimolecular decomposition of an unstable complex produced by the double excitation of a single oxalate anion. It is not possible, by kinetic measurements alone, to distinguish between them, but it is considered that the latter is the more likely process. Since an azide ion is univalent, double excitation is not possible, and in order to explain the dependence of rate on I^2, reaction of two separately-excited radicals must be assumed. This is consistent with the fact that decomposition of a single azide radical is energetically unlikely. The oxalate radical is divalent, and as has been pointed out, the exciton radical Ox^x may be expected to possess considerable stability. There is no reason, therefore, to consider process(1) preferable, and in fact, the electrostatic repulsion between two adjacent trapped oxalate 'excitons' renders this process unlikely.

Nature of the Traps

The previous discussion has been independent of the nature of the traps. An attempt will now be made to suggest reasons for identification of the trapping centres. Since an exciton carries no net charge, both vacant anion sites (V.A.S.) and vacant cation sites (V.C.S.), and, in fact, any aperiodicity in the lattice can act as trap.

However, the life-time of a trapped exciton is very small, and a distinction must be made between those traps which act as decomposition centres, and those which merely serve as temporary exciton traps. Vacant cation sites will first be considered.

In alkali-halides, a V.C.S. can trap an exciton; reaction of the site and the positive hole, to form a V-centre and a mobile electron follows. This process is not so likely with silver oxalate, since the "positive-hole" still retains a negative charge. A V.C.S. has a net negative charge; immobilisation of the exciton by trapping of an electron from the exciton will be energetically very difficult. The life-time of a trapped exciton at a V.C.S. is expected to be very short and receipt of further photo-energy is more likely to result in further excitation of the same electron rather than cause production of an unstable complex. It is not expected, therefore, that V.C.S. function as effective exciton traps.

Capture of an exciton by a V.A.S. will now be considered. Since the V.A.S. bears a net positive charge, the transition probability of an electron tunneling through to the site is high. In alkali halides, therefore, trapping of an exciton by a V.A.S. results in the formation of an F-centre and a positive hole, which

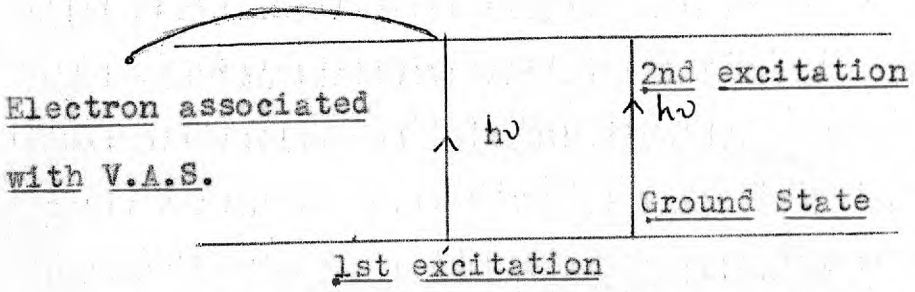
diffuses away. In silver oxalate this is unlikely since a), there is no reason to assume mobility of the 'positive-hole', and b), the radical will have lost only one valency electron. It is, therefore, assumed that trapping of an oxalate exciton at a V.A.S. will result in the formation of an $F^{\ominus}$-centre-$Ox^{\ominus}$ complex, with an electron existing in a resonance state between V.A.S. and the parent exciton. The first excitation and trapping process may be represented as follows:-

$$Ox^{=} + h\nu \longrightarrow Ox^{x}$$

$$Ox^{x} + \square \longrightarrow \underset{F\text{-centre}}{\ominus[\square \,.\, Ox^{\ominus}]} \quad \text{complex}$$

where $\square \equiv$ a V.A.S.
and $. \equiv$ an electron.

The term $F^{\ominus}$- centre is used only for convenience, and it is not implied that capture of the electron by the site is complete. The electron functions as a covalent bond between the F -centre and the remaining radical. Since the Ox radical is expected to be chemically stable, further irradiation is necessary to cause decomposition. The second irradiation is supposed to raise a second electron into the exciton band. An energetic diagram is shown overleaf.



When this occurs, the $(COO)_2$ remaining breaks up into two molecules of carbon dioxide. The second valency electron can jump into the V.A.S. with formation of a true F-centre, i.e. two electrons trapped at a divalent anion site. This is presumed to remain associated with the two Ag^+ ions left by the decomposition, the association being of a character precisely analogous to that envisaged for the first excitation complex.

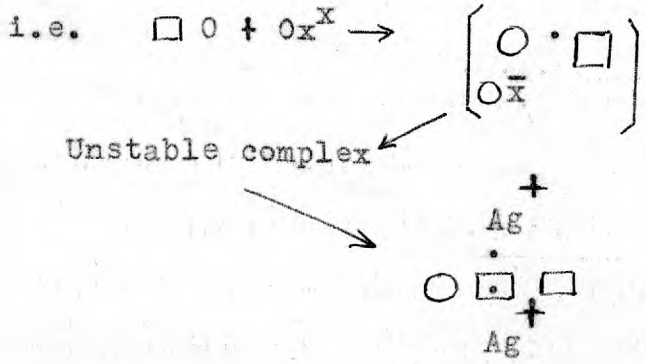
i.e. $\{Ag^+ \bullet \square \bullet Ag^+\}$

As these sites accumulate, eventual collapse from the lattice matrix to form silver atoms and vacant sites will probably occur. In this mechanism each decomposition will release a vacant anion site (from the decomposed $(COO)_2$) and hence the trapping centre is regenerated. Thus the constant rate of photolysis is explained.

The ionic conductance of silver oxalate is very low, less than that of Ag Br by a factor of about 10^8. An obvious explanation of this is that the low conductance is due to the formation of associated V.A.S.-e^2 V.C.S.

to form 'pairs' which do not participate in ion movement. The above theory may be applied to such pairs considered as trapping centres. The first excitation complex will consist of an $F^{\ominus}$-centre-V centre complex, the "positive hole" being assumed to be linked to the V.C.S. in the same sense as applied to the bond between the V.A.S. and the electron. As before, further irradiation results in the formation of an unstable complex which decomposes unimolecularly. Here the net product will involve an F-centre, 2 Ag^{+}, a V.C.S., and a V.A.S.

Let O ≡ V.C.S.



In order to account for the formation of associated pairs, mobility of V.C.S. must be assumed. Hence either Ag^{+} in the product can interchange positions with the vacant cation site, which will then be in a position to form an associated pair with the V.A.S. formed from the decomposition of the $(COO)_2$ radical. Once again, therefore, the trapping centre is regenerated, and a constant

rate predicted. Thus the present theory is applicable to trapping either by a V.A.S. or by an associated complex.

This theory differs from the previous theory since the negative photo-conductance evidence has indicated that formation of 'mobile' electrons or positive holes in sufficient numbers to account for the measured rates of reaction is impossible. An explanation of the measured small temperature coefficient was that the experimental E was a true value, i.e. not a difference term, but was insufficient to produce the photo-reduction without further energy. It was suggested that the extra energy was derived from lattice vibrations, e.g. that associated with the escape of the CO_2 from within the lattice. Here it is also assumed that the small E is a true activation energy, but it is now identified as the energy needed to cause the decomposition of the complex.

The Photolysis of Lead and Mercuric Oxalates

It was decided to investigate the photolysis of lead and mercuric oxalates in order to see whether the theory developed for silver oxalate could be applied to these compounds. Neither compound decomposes simply into metal plus carbon dioxide, and, by analogy with the thermal decompositions, the reaction is not expected to be stoicheiometric, as is the decomposition of silver oxalate. Nevertheless, it is possible to compare the kinetics of the overall decompositions in the three systems. This will now be done, the lead and mercuric compounds being treated together.

Both mercury and lead oxalates evolve gas immediately on irradiation, and the evolution ceases simultaneously with cessation of irradiation. The rate of decomposition is slow, the rate decreasing in the order $Ag^{+} > Hg^{++} > Pb^{++}$. Both compounds change colour, from pure white to brown, as reaction proceeds, and at no stage are discrete nuclei observable, i.e. as with silver oxalate it appears that the rate of formation of nuclei is greater than their rate of growth. However, the colour of the irradiated salt suggests that the products do not consist solely of mercury metal and lead metal respectively, but probably

include oxides. This is expected by analogy with the thermal reactions, which have been formulated.

$$Hg(COO)_2 = HgO + Hg + CO + CO_2$$

and $$Pb(COO)_2 = Pb + PbO + CO + CO_2$$

The temperature coefficient of both decompositions is small. That for mercuric oxalate is ~ 1500 cal. (cf. $Ag(COO)_2$ where E~900). The energy of activation of lead oxalate was not measured, owing to the low rates in the available temperature range (-70° to $+40^{\circ}C$), but on the evidence of some few measurements is not expected to show an anomalous value.

Irradiation of mercuric oxalate gave rise to linear p-t curves, which like those obtained with silver oxalate, were strictly reproducible, and it was found that the rate of reaction at constant temperature varied as the square of the intensity.

Irradiation of lead oxalate, however, showed some features which were not observed in the other compounds. The rate of evolution of gas was found to decrease progressively with time, in a manner which was experimentally separable into two effects. In the first place, a decrease in rate was noticed after ca. 30 minutes irradiation. The onset of the reduced rate was not reproducible, nor was the 'new' rate constant. It was

found that if irradiation was stopped, and the sample pumped for some hours, then, on re-irradiation, the original constant rate was reproduced. Hence it is evident that the slowing of the rate is due to some surface recovery process. In addition to the recovery process, however, it was noticed that the rate continued to decrease, and after prolonged photolysis the rate of reaction dropped to a very low value. This effect was permanent and irreversible, i.e. a saturation stage had been reached, when further illumination had no effect. Photolysis generally is recognised to be a surface process, and consequently a similar stage when further irradiation has no effect is reached in all compounds. In lead oxalate, however, the appearance of this effect is very much sooner than in the other oxalates. By performing runs on samples during the time-range when this process is not significant, it was possible to investigate the rate-intensity relationship. As before, the rate was found to vary as the square of the intensity.

Hence the general features of the silver oxalate photo-decomposition are shown by the two other compounds. The kinetics of the Ag and Hg oxalates are very similar, although the rates of reaction and nature of the product differ. It is suggested, therefore, that the theory

developed for silver oxalate can be applied to mercuric oxalate. Receipt of irradiation is expected to raise an oxalate molecule into an excited state. The energy, in the form of an exciton, is trapped at a vacant anion site, where an electron is shared between the site and the oxalate (Ox^-) radical. Further irradiation results in the formation of an unstable exciton complex, which by co-operation with thermal (lattice) energy, decomposes. It has already been stated that it is probable that some oxide is formed as reaction product. If the decomposition of the complex were formulated as for silver oxalate, then Hg + CO_2 would be formed.

i.e. $$Hg\begin{matrix}OOC\\OOC\end{matrix} = Hg + 2\ CO_2$$

It now appears that this reaction is not a complete representation of the final process. Since the decomposition temperatures of Ag_2O and HgO are 290° and 400°C respectively, it is evident that the Hg-O bond has greater stability than the Ag_2-O bond. This is a qualitative explanation of the different nature of product in the two salts. In mercuric oxalate, the Hg-O bond is sufficiently stable for the reaction

$$Hg\begin{matrix}OOC\\OOC\end{matrix} \longrightarrow Hg - O + CO_2 + CO$$

to occur, whereas in silver oxalate the production of Ag

and carbon dioxide is energetically preferable. Alternatively, it may be that the crystal structure of mercuric oxalate is such that a particular mode of decomposition will be favoured. An analogous reaction is the dehydration of copper sulphate pentahydrate, where the removal of the final water-molecule is much more difficult than the removal of the first four molecules. No information regarding the structure of mercuric oxalate is available, but by analogy with the cyanide and chloride, it is expected to posses a layer lattice. The conductance at 0°C of mercuric oxalate is less than that of silver oxalate by a factor of about 10^3. This may mean that there are fewer vacant sites, which would account for the lower rates of reaction.

In a previous investigation of the decomposition of mercuric oxalate (38) the effect of u.v. pre-irradiation, followed by subsequent thermal decomposition, was also studied. Here, however, irradiation took place in a larger apparatus designed for thermal decompositions, which were followed by measurement of gas pressure on a McCleod gauge. Under these conditions detection of the small pressure of gas evolved in photolytic decompositions would be unlikely, in agreement with the reported result that absorption of irradiation appeared to take

place without evolution of gas. It was, therefore, suggested that the production of mercurous oxalate, by transfer of an excited electron from a surface molecule, might occur. This possibility has not been considered in the present discussion although the excited complex might in fact correspond in bond distribution to a "mercurous" compound. Moreover, it is expected that any thermal effect of decomposing mercurous salt would be completely masked by the photo-process. Moreover, there are insufficient available data for this matter to be considered further.

The kinetics of the lead oxalate photolysis are also analogous to those exhibited by silver oxalate. In addition, however, there occur two phenomena, a recovery process and a (comparitively) rapid attainment of a saturation stage, which are not shown either by mercuric or silver oxalate, and the rates of reaction are slower. The general theory proposed for silver and mercuric oxalates is expected to apply to lead oxalate.

Thus irradiation produces an unstable complex which decomposes unimolecularly, with interaction of a small amount of thermal energy derived from the lattice. By analogy with the silver oxalate decomposition, the final stage of the reaction is assumed to produce one Pb^{+}

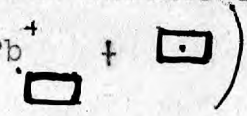
ion, one vacant anion site containing two electrons, and a V.A.S. produced from the decomposing $(COO)_2$ radical. In silver oxalate it was shown that if the electrons were shared between the Ag^{+} ions, and the original trapping centre as Ag^{+} □ Ag^{+}, then one V.A.S. would be left to function as a new trap. Thus a net regeneration of the original trap had occurred, and hence the constant rate of photolysis was explained. In the present case it is suggested that a reversible electron 'transfer' occurs viz:



The forward process represents the first decay process noticed in short-time photolysis. The back-reaction, which is a trap-regenerating process, is identified as the vacancy process. The complex of Pb and 2 vacant anion sites plus electrons whether formulated as



or as



is not believed to act as trap. Only V.A.S. can act as traps, and hence the constant rate depends on the regeneration of these sites. Since PbO is stable at high temperatures, it is expected that the product of irradiation will contain this compound in high propertion. If this

happens, then regeneration of traps becomes impossible, since one V.A.S. will be occupied by two electrons, and the other by Pb-O. i.e. no V.A.S. will have been produced by decomposition of $(COO)_2$ to replace the original trap. An irreversible decrease of rate with time is, therefore, expected. The saturation stage is thus envisaged as that wherein all effective trapping-centres have been destroyed.

The Thermal Decomposition of Silver Oxalate

Before discussion their interpretation, the experimental results obtained will be summarised.

The thermal decompositions were carried out at temperatures in the range 105° to 120°C, since at these temperatures it has been shown (33c) that errors due to self-heating are negligible. A small, constant weight of oxalate was used, and all mounting operations were performed in a standard manner in dark-room conditions. It was found that the p-t curves were exponential in character. Attempts to fit the curves to expressions of the Power-Law type, i.e. $p = Ct^x$ were made. These were unsuccessful, even with attempted corrections to the p term, (44), or to the t term, i.e. the expression $(p - p_o) = C (t-t_o)^x$ did not adequately represent the experimental results. It was found that after a short initial period of about five minutes, the graph of log p-t gave a good straight line up to the point of highest decomposition (about 30%). The equation $P = Ce^{kt}$ was found to hold in all decompositions studied. The pre-exponential factor C was independent of temperature, in distinction to MacDonald, (33a) who found that in the "second" (exponential) process the analogous term increased with increasing temperature. In the present investigation

C is identified as the number of decomposition centres in the crystal. Reasons for this will be discussed later. The constant k was found to increase progressively with increasing temperature, and was, therefore, interpreted as a rate-constant. Values of the activation energy E for the process were obtained from graphs of log k — $\frac{1}{T}$, where T = temperature in degrees K. The effect of pre-irradiation with ultra-violet light on the subsequent thermal rate was studied quantitatively by systematic variation both of the time (t_i) and intensity (I) of illumination. As expected, the rate of reaction was increased by the pre-treatment and it was found that

$$\log (C - C_u) = 1.1 \log (I^2 t_i)$$

$$\therefore (C - C_u) = I^2 t_i.$$

where C_u = value of C for unirradiated salt.

The value of k remained unaltered during a series of runs carried out on samples which had been subjected to varying amounts of pre-treatment. The variation in rate of reaction was, therefore, entirely controlled by the change of the pre-exponential factor.

Runs on samples prepared under different experimental conditions were performed. It was confirmed that samples prepared with an excess of oxalate ion were less stable than those prepared under stoicheiometric conditions.

Conversely, specimens precipitated from solutions containing excess silver ion were more stable than stoicheiometric samples. Surprisingly, such treatment did not affect the value of C, the variation in the rate constant k determining the new rates of reaction. The p-t results were still fitted by the equation $p = Ce^{kt}$; similar results were obtained by MacDonald who found that the shape of the p-t curve was unaltered by different methods of preparation. Further evidence that the mode of decomposition was not altered is derived from the fact that values of activation energy calculated for such samples were, within experimental error, equal to that obtained for the stoicheiometric salt.

The thermal decomposition of silver oxalate has been studied by many workers, notably MacDonald, Benton and Cunningham, and Tompkins. In general, the results obtained by different workers have not been consistent, and frequently it has not been found possible to obtain agreement between runs performed by one worker on samples of silver oxalate from the same preparation. Benton and Cunningham used varying weights of approximately 1 g. of sample, and although many of their curves were fitted by the equation $p = Ct^x$ it appears that for some runs the plot of log p-log t showed considerable deviation

from a straight line. Similarly, MacDonald reported variations of up to 20% in rate between specimens of equal weight decomposed in identical manners. After a systematic investigation of possible causes or irreproducibility, MacDonald concluded that only by standardisation of the method of preparation could consistency by obtained. This was confirmed by Tompkins, who prepared "stoicheiometric" specimens in solutions of high dilution under dark-room conditions, and obtained p-t curves which were indistinguishable after the first 4% of reaction. In the present work, this method of preparation was duplicated as far as possible, and the conditions of mounting and decomposition standardised. Values of k were reproducible to within $\pm$ 2%; the value of C was small, and did not vary much in absence of irradiation. Reproducible results were, therefore, obtained.

The mean features of the thermal decomposition of silver oxalate are in general agreement amongst different workers. The essential difference lies in the different expressions which have been used to represent the experimental curves. From an analysis of the previous work, and also the present investigation, it is concluded that two general conclusions may be made. (1) That nuclei are produced and grow in three dimensions, though not

necessarily at the same rate in each direction or, (2), That nuclei grow in two-dimensions, and, at certain points in the lattice, branching occurs, i.e. the plane of reaction divides and moves into the crystal, along, for example, other lattice planes. Formal mathematical expressions for these two processes have been made and will now be discussed.

1. Growth Equation

It is assumed that the rate of formation of nuclei is given by $\frac{dn}{dt} = k_1 (N - n)$

where n = number of nuclei

N = Number of centres where a nucleus may form. For silver oxalate, N is expected to equal the total number of oxalate radicals in the crystal.

$$\therefore n = N (1 - e^{-k_1 t})$$

Hence the volume V of nuclei formed in time t is given by

$$V = \int_{\tau=0}^{\tau=t} k_2 \bar{v}^3 (t-\tau)^3 N(1-e^{-k_1\tau}) \, d\tau \qquad \text{I}$$

where τ = time at which a nucleus came into existence.

$\bar{v}$ = Average rate of linear growth in three dimensions.

For small values of t, $N \gg n$, and $N(1-e^{-k_1 t}) \rightarrow N$.

On integration, the result is the power law equation $P = Ct^x$ where $x = 4$, which is the equation used by Benton and Cunningham and Tompkins to describe their results. In this equation, the term k_2 is a rate-constant associated with the growth of nuclei in three dimensions. Values of activation energy derived from this expression, therefore, refer to growth, and the values obtained by both workers, viz. 25.4 and 24.6 kcal. respectively, agree well. In the "first process" of MacDonald, which he identified as two-dimensional growth of nuclei from the surface, an activation energy of 31.6 kcal. was obtained. This is surprising, since it is expected that the latter process would have been energetically easier. In general, the crystals used by MacDonald were prepared with an excess of either component. Such crystals are known to be smaller and of more regular shape than 'normal' crystals, and this may explain the higher activation energy. However, in MacDonald's second paper, where three-dimensional growth is assumed, the reported value of E, calculated from a temperature coefficient of 2.48/10° is 24.3 kcal. in fair agreement with the above values.

2. Using similar nomenclature, the second mechanism may be formulated as

$$V = \int_{\tau=0}^{\tau=t} k' uv(t-\tau)^2 \; wN(1-e^{-k_1 t} e^{-kt}) \, d\tau$$

where the first term refers to a two-dimensional plane of nuclei, growing with velocities u,v. The contribution due to branching is given by the second term, w being the velocity of propogation of the new plane, and k here is the probability that branching will occur. When the probability of branching is small, $k \ll k_1$ and the equation reduces to a form similar to equation I. Conversely, where the branching process predominates, the exponential term determines the shape of the curve, and an exponential rise in pressure is expected. In this case, the constant k is a branching coefficient, and measured energies of activation will refer to the energy necessary for branching and not for growth. The mean value for E obtained in the present investigation, neglecting one alamolously high value, is 27.3 kcal. Comparison of this value with the values obtained by Benton and Cunningham, and by Tompkins, is not possible, since, as shown by Mott, different equations were used. However, the closeness of the figures seems to indicate that

$$E_{branching} \fallingdotseq E_{growth}$$

The value of E branching is expected to vary with

extent of decomposition, due to formation of new planes along which nuclei can grow. The 'second process' found by MacDonald gave the experimental relationship

$$\frac{dp}{dt} = ae^{bt} \text{ where b,a, are constants}$$

Assuming the mechanism postulated above - two-dimensional growth and branching - the theoretical equation

$$\frac{dn}{dt} = \frac{\pi K^2 n}{2b}\left(e^{\frac{bt}{c-1}} - 1\right)$$

was deduced, where b = number of times a plane divides per second. When branching predominates, the term

$$\frac{\pi K^2 n}{2b} \rightarrow a.$$

Both a and b were found to be temperature dependent and MacDonald found values of the respective temperature coefficients to be 3.1 and 2.9 per 10°. These correspond to activation energies of 30.7 to 28.4 kcal. The latter value is in fair agreement with the value of 27.3 kcal. reported for the branching activation energy in the present investigation.

The effect of pre-irradiation on the subsequent thermal rate will now be considered. From the photolysis results, it was found that

$$\frac{dp}{dt} \propto I^2 \qquad \therefore p \propto I^2 t_i$$

where t_i = time of irradiation. Since the thermal rate is

negligible at the temperatures at which photolysis was conducted, the pressure is proportional solely to the number of decomposition centres produced by irradiation

$\therefore$ number of centres $\propto I^2 t_i$

Now the result of the pre-irradiation investigation was that

$$C - C_u \propto (I^2 t_i)$$

where t_i = time of pre-irradiation, and hence $(C-C_u)$ is identified as the number of decomposition centres produced during illumination. Since these are assumed to be vacant anion sites, C_u = number of vacant sites present in the crystal before illumination. The pre-exponential factor in the equation used to describe the experimental p-t curves, viz. $p = Ce^{kt}$ is, therefore, presumed to represent the total number of vacant anion sites present at time t. This is quite consistent with the results obtained for barium azide, where it was found that the corresponding "C factor" varied as (It_i). Since the oxalate radical is presumed to require two excitations, whereas the uni-valent azide radical requires only one, an additional I term is needed. Thus an analogous "reciprocity" law is obtained. The effect of pre-irradiation is thus to increase the number of positions from which reaction can take place, the rate constant k remaining unaffected.

It was hoped that an investigation of the decomposition of samples prepared under different experimental conditions might give added data. It was found, however, that the shape of the p-t curves remained unaltered. The value of the pre-exponential factor remained unchanged. Thus it appears that the number of vacant sites is not materially affected by the different methods of precipitation. Since the process of decomposition in the present case seems to involve production of two-dimensional planes of nuclei which later branch, it was expected that surface absorption of excess ions would result in the production of vacancies which would act as centres for new planes. An increase in vacancies would be reflected in an increase in C, and so it is assumed that some other reason is responsible for the altered rates of reaction. The general features of reaction are the same for all preparations, i.e. the expression $P = Ce^{kt}$ fits the experimental results and the altered rate is determined solely by the variation in the value of k. The activation energy of the process is, within experimental error, equal to the value obtained for the stoicheiometric salt, and so no change in mechanism is indicated. A rate constant k may be written, using conventional symbols as

$$k = \nu e^{-\frac{\Delta H^*}{RT}} \quad \Delta S^* \quad \text{---3}$$

In the present case, the value of k varies, whilst that of the energy of activation remains constant. This can only be accounted for by compensating changes in the entropy term in equation 3. A somewhat analogous case is the denaturing of proteins and de-activation of some enzymes (65). The activation energies of these processes are very large, of the order of 100 kcal., but the reactions occur with appreciable velocities at normal temperatures. The heat of activation is found to vary greatly, e.g. from 52 to 110 kcal for the invertase reaction, whilst the free energy of activation remains almost constant. It is, therefore, concluded that changes in the value of $\Delta S^{\ddagger}$ are responsible for the experimental results. The high entropies of activation are explained as a result of the breaking of some of the salt bridges in the original protein, the resultant 'loosening' of the structure being accompanied by a large increase in entropy. It is assumed that all bridges are not equally important in this respect, and that the process of activation consists in the breaking of those bridges which are not accompanied by a large increase in entropy. Those bridges which are significant break spontaneously. Similar considerations may apply to "oxalate-excess" silver oxalate. An excess oxalate

radical is large, and may be "shared" by several ions. Removal of such a "bridge" radical by decomposition may, therefore, lead to a considerable change in structure, which, if accompanied by a large positive change in $\Delta s^{\ddagger}$ can result in the formation of new points from which decomposition may subsequently proceed. That the process is not due to vacancies is further indicated by the fact that addition of Ag^{+} reduces the rate. Since this is normally presumed to be accompanied by the production of a corresponding number of vacant anion sites, which could act as nuclei, an increased rate would have been expected. It has been noted by MacDonald that addition of sulphate ion during preparation results in an even more marked decrease in rate than does silver ions. Since the occlusion into the lattice by the sulphate ion will presumably be less than that of the (common) nitrate ion it is suggested that in this case the effect is associated with the double-charge on the anion. The effect is clearly quite different from that operative when the oxalate anion is present in excess, in which case the rate is increased. Moreover, the sulphate radical is quite stable, and hence removal of the excess ion by decomposition is not here possible.

The reason for the two modes of decomposition

apparently found by different workers is still in doubt. Since in the present investigation the method of preparation corresponded as nearly as possible with that employed by Tompkins, this factor does not appear to be significant. Similarly, the various forms of pre-treatment which have been studied do not seem to favour particular mechanisms. A possible cause which has not as yet been the subject of investigation, may be that due to ageing of the sample. This is known to be of considerable importance in other compounds. Thus it has been found for barium azide (35), that the exponent in the equation $p = ct^x$ falls from 6 to 2 with increasing age of the sample. This indicates quite clearly that a different mechanism is operative. Similarly, the ageing of silver bromide (66) results in a decrease of surface area, and a parallel lowering of the ionic conductance. The rate of exchange with radio-bromine is also considerably reduced. Unfortunately it has not been realised that this effect might be of interest in silver oxalate, and no comparison can be made with other workers.

At present, the cause of reaction appears to be governed by the relative importance of three dimensional growth of nuclei, or two-dimensional growth followed by branching. Since silver oxalate has a molecular layer

lattice, the latter possibility does seem to be the more probable. The low conductivity, and size of the Ag^{+} ion, suggest that cation mobility is not large, and Tompkins has suggested that growth is due to deformation within the lattice, rather than to the mobility of Ag atoms. It is suggested that 'growth decomposition' would be relatively slower than 'branching decomposition', but unfortunately it is not possible to compare the actual rates found by various workers.

The detailed mechanism is presumed to be an extension of the photolysis-mechanism, the excitation energy being derived from thermal lattice vibrations. Two differences may be emphasized. In the photolysis process it was tacitly assumed that no growth occurred. Each radical decomposed separately, and ultimate production of particles of silver was due to collapse of silver atoms and vacant anion sites. Secondly, photolysis is predominantly a surface process. The thermal process is expected to be initiated by planes originating in the surface, and which travel into the bulk of the crystal. The branching mechanism merely presumes that at certain points in the lattice a decomposing radical can initiate the decomposition of more than one neighbouring radical, a new plane of decomposition travelling along an energetically-favoured path.

It may be noted that silver oxalate is intermediate in structure between truly ionic compounds such as barium and potassium azide, and compounds such as mercuric oxalate, which possess a molecular-layer lattice, and, by analogy with similar compounds, are expected to be largely co-valent in character. The mode of decomposition is, therefore, expected to show similarity to both these compounds, as is found. In such a case the state of the crystal lattice will be of importance in deciding the degree of approximation to which the reaction will be represented by different mechanisms associated with the two types of compound.

ABSTRACT

This research is concerned with the solid-phase decomposition of metallic oxalates. Emphasis has been concentrated on silver oxalate since a) the reaction is known to stoicheiometric and b) although a considerable amount of experimental work on the thermal decomposition has been published, different conclusions have been reached by different workers. Furthermore, since from previous investigations the photolysis appeared to be different from that of similar compounds (especially barium and potassium azides) it was hoped that a study of this compound might prove of considerable value in increasing the understanding of the "mechanism of decomposition". The investigation was divided into three parts.

1. Measurement of Ionic Conductance

The ionic conductance of compressed pellets of silver, lead, mercuric, thallous and barium oxalates were measured in the region of structure-sensitivity. By analogy with barium azide the results indicate that the theory of nucleus growth proposed by Mott for the thermal decomposition of barium azide is not applicable to silver oxalates. It was also shown that it was not possible to detect a photo-current as large as 10^{-12} amp.

when silver oxalate was irradiated with ultra-violet light. From this observation it is shown that it is unlikely that receipt of irradiation results in the production of electrons in the conduction band; it is hence thought that excitons are created during illumination. No change in conductance in specimens of thallous oxalate prepared in the presence of barium ions could be detected. It is, therefore, concluded that introduction of a significant number of foreign ions into a lattice by this method is not possible.

2. Photolysis of Metallic Oxalates

The photolysis of silver, lead, and mercuric oxalates was followed by noting the increase in pressure of evolved gas in a vacuum system. The dependence of rate of reaction on time of irradiation, intensity of irradiation and on temperature was investigated. In each case, it was found that the rate of reaction varied as the square of the applied illumination; the temperature coefficient of photolysis was small, of the order of 1 kcal. The general features of the silver oxalate photolysis showed similarity to the corresponding barium azide decomposition, and it is shown that the mechanism postulated for this compound can be formally applied to silver oxalate. However, an alternative theory, in

principle similar to the azide mechanism, has been developed, and reasons are given for preferring this latter theory. It is shown that with slight modification this theory can explain the photolysis of both lead and mercuric oxalates.

3. The Thermal Decomposition of Silver Oxalate

Previous work had indicated that the thermal decomposition was associated either with three-dimensional growth of nuclei or with nuclei which grow in two dimensions and later branched. The results of the present investigation favour the latter alternative, but it has not been found possible to reconcile the two apparent mechanisms. The p-t curves are well represented by the expression $p = Ce^{kt}$, k is identified as a rate-constant for branching, and C as the number of decomposition centres in the crystal. By analogy with the photolysis experiments, these are presumed to be vacant anion sites, and the mechanism for thermal decomposition can now be explained as an extension of the photolysis mechanism. The decomposition of samples prepared in presence of an excess of either constituent has been studied. As noted by previous workers, the rates of reaction were markedly affected, but the value of the pre-exponential constant, i.e. the number of vacant anion sites, and of the measured

energy of activation, did not vary with preparation of the sample. The changes in rate were determined by the variation of the value of k, and it is suggested that the new rates were associated with a change in the free energy of the reaction due to changes in an entropy factor.

The present investigation, then, supports the 'branching-theory' of decomposition of silver oxalate. It is believed that the apparent finding of two different mechanisms is due to ageing of the silver oxalate crystals, the different modes of decomposition being associated with different crystal "structures". This effect has been shown to be independent of the method of preparation, and is operative during the period between precipitation and actual decomposition.

BIBLIOGRAPHY

A. For a recent review of Ionic Conductance in Solid Salts see Tompkins and Jacobs, Quarterly Rev., Vol Vi, No. 3, p.238.

B. The electronic circuits used in the measurement of ionic conductance were designed by Dr. P.W.M. Jacobs. Full details of construction and use are given in references (40) and (55).

1. Birge: Rep. Prog. Phys. 1941 8 90.
2. Mott and Gurney: "Electronic Processes in Ionic Crystals" 2nd edition o.u.p. p.31.
3. Koch and Wagner: Z. Phys. Chem. 1937 38 295.
4. Kanzaki; quoted by Mott and Gurney, ihid p.48.
5. Breckenbridge: J. Chem. Phys. 1948 16 959; 1950 18 913
6. Joffe and Rontgen: Ann. Phys. 1913 41 449.
7. Phipps and Partridge: J.A.C.S. 1929 51 1331.
8. Phipps and Ginnings : ibid 1930 1342.
9. Joffe: Ann. Phys. 1923 72 401.
10. Gothuls: Rec. Trav. Chem. 1930 49 357.
11. von Hevesy: Z. Phyz. 1922 10 80.
12. Tamman and Vezzi: Z. Anorg. Chem. 1926 150 355.
13. Phipps Lansing and Cooke: J.A.C.S. 1926 112 48.
14. Lehpelat: Z. Phyz. 1933 85 717.

15. Bronnecke: J. Appl. Phys. 1940 11 202.

16. Tubandt and Eggert: Z. Anorg.all.Chem. 1920 110 146

17. Tubandt: ihid 1921 117 1.

18. Tubandt and Schiebt: ihid 1921 117 5.

19. Rasch and Hendrikson: Z. Electrochemie 1908 14 4.

20. Smekal: Z. Elect. 1928 34 422.

21. Joffe and Zechmeister: Z. Phys. Chem. B.1926 35 447.

22. Jost: ihid B. 1929 688.

23. Frenkel: Z. Phyz.Chem. 1926 35 652.

24. Wagner and Schottky: 1930. 11 1630.

25. Seitz: "Modern Theory of Solids" McGraw-Hill 1940 p.495.

26. Jost and Neklop: Z. Phys. Chem. 1936 (B) 34 368.

27. Mapother, Crooks and Maurer: J.Chem.Phys. 1950 18 1231.

28. Pohl: Proc. Phys. Soc. 1937 49 3.

29. Mollwo: Ann. Phys. 1937 29 394.

30. Seitz: Rev. Mop. Phys. 46 18 384.

31. Mitchell: Phil. Mag. 1949 40 249.

32. Tompkins: Trans. Far. Soc. 1948 44 206.

33. MacDonald: (a) J.C.S. 1925 2764; (b) 1936 832.

34. Wischin: Proc. Roy. Soc. A. 1939 172 314.

35. Thomas and Tompkins: Proc. Roy. Soc. 1951 209 550.

36. Avrami: J.Chem.Phys. 1939, 7, 1103; 1940, 8, 212;
1943, 11 499.

37. Garner and Hailes: Proc.Roy.Soc. A 1933 139 576.

38. Prout and Tompkins: Trans. Fara. Soc. 1947 43 148.

39. Mott: Proc. Roy. Soc. A. 1939 182.

40. Jacobs: Ph.D. thesis London University, 1952.

41. Thomas and Tompkins: Proc.Roy.Soc. A. 1951 210 111.

42. Colvin and Hume: Proc. Roy. Soc. A.1931 132 548.

43. Bradley, Colvin and Hume: Proc.Roy.Soc. A.137 531 1932.

44. Eyring and Sterne: Chem. Rev. 1939 24 253.

45. Garner: Nature, 1939 144 287.

46. Prout and Tompkins: T.F.S. 1947 43 148.

47. Colvin and Hume: Proc.Roy.Soc. A. 1939 127 635.

48. Lennard-Jones and Dent: Proc.Roy.Soc. A 1928, 131 24.

49. Mott and Gurney: Proc.Roy.Soc. A 164 157 1938.

50. Mitchell: "Photographic Sensitivity" Butterworths" 1951 p.242.

51. Garner and Maggs: Proc.Roy.Soc.A 1939 172 299.
MacDonald and Sandison: Trans.Far.Soc. 1938 592.

52. Benton and Cunningham: J.A.C.S. 1935 57 2227.

53. Griffiths: J.Chem.Phys. 1946 14 403.

54. Bircumshaw and Harris: J.C.S. 1948 1898.

55. P. Jacobs: Journal of Scientific Instruments 1953 30 204.

56. Phipps and Partridge: J.A.C.S. 1929 51 1331.

57. A. Smekal: Handbuck d.Physik 24/2 881 1933.

58. Wagner and Hantelmann: J.Chem.Phys. 16 72 1950.

59. Wagner and Ronge: J.Chem.Phys. 18 72 76.

60. Koch and Wagner: Z.f.Phys.Chem. (B) 38 295 1937.

61. Thomas and Tompkins: J.Chem. Phip. 1952 20 662.

63. P. Jacobs: Proc. Roy. Soc. 215 A 1952 254.

64. Garner and Haycock: Proc. Roy. Soc. 1952 A 211 335.

65. The Theory of Rate Processes: Glasstone, Laidler and Eyring. McGraw-Hill, 1941 p.442.

66. Kølthoff, et al., J.A.C.S., 1939 61 3414 ibid Z 401.